

**Technical Report**

**TR-07-03**

**Äspö Task Force on modelling  
of groundwater flow and transport  
of solutes**

**Review of Tasks 6D, 6E, 6F and 6F2**

David Hodgkinson, Quintessa

September 2007

**Svensk Kärnbränslehantering AB**

Swedish Nuclear Fuel  
and Waste Management Co  
Box 5864

SE-102 40 Stockholm Sweden

Tel 08-459 84 00

+46 8 459 84 00

Fax 08-661 57 19

+46 8 661 57 19



# **Äspö Task Force on modelling of groundwater flow and transport of solutes**

## **Review of Tasks 6D, 6E, 6F and 6F2**

David Hodgkinson, Quintessa

September 2007

This report concerns a study which was conducted for SKB. The conclusions and viewpoints presented in the report are those of the author and do not necessarily coincide with those of the client.

A pdf version of this document can be downloaded from [www.skb.se](http://www.skb.se).

# Abstract

This report forms part of an independent review of the specifications, execution and results of Task 6 of the Äspö Task Force on Modelling of Groundwater Flow and Transport of Solutes, which is seeking to provide a bridge between site characterization and performance assessment approaches to modelling solute transport in fractured rock.

The objectives of Task 6 are:

- To assess simplifications used in Performance Assessment (PA) models.
- To determine how, and to what extent, experimental tracer and flow experiments can constrain the range of parameters used in PA models.
- To support the design of Site Characterisation (SC) programmes to ensure that the results have optimal value for performance assessment calculations.
- To improve the understanding of site-specific flow and transport behaviour at different scales using site characterisation models.

The present report is concerned with Tasks 6D, 6E, 6F and 6F2. It follows on from two previous reviews of Tasks 6A, 6B and 6B2, and Task 6C.

In Task 6D the transport of tracers through a fracture network is modelled using the conditions of the C2 TRUE-Block Scale tracer test, based on the synthetic structural model developed in Task 6C. Task 6E extends the Task 6D transport calculations to a reference set of PA time scales and boundary conditions. Task 6F consists of a series of ‘benchmark’ studies on single features from the Task 6C hydrostructural model in order to improve the understanding of differences between the participating models. Task 6F2 utilises models set up for Tasks 6E and 6F to perform additional sensitivity studies with the aim of increasing the understanding of how models behave, the reason for differences in modelling results, and the sensitivity of models to various assumptions and parameter values.

Eight modelling teams representing five organisations participated in this exercise using Discrete Fracture Network (DFN), continuum and channel network concepts implemented in a range of different codes and applied using a variety of methodologies.

This report: summarises and reviews the Task 6D, 6E, 6F and 6F2 objectives and specifications; summarises and reviews the modelling team reports; compares the modelling team results; and discusses issues raised by the study.

# Executive summary

This report forms part of an independent review of the specifications, execution and results of Task 6 of the Äspö Task Force on Modelling of Groundwater Flow and Transport of Solutes, which is seeking to provide a bridge between site characterization and performance assessment approaches to modelling solute transport in fractured rock.

The objectives of Task 6 are:

- To assess simplifications used in Performance Assessment (PA) models.
- To determine how, and to what extent, experimental tracer and flow experiments can constrain the range of parameters used in PA models.
- To support the design of Site Characterisation (SC) programmes to ensure that the results have optimal value for performance assessment calculations.
- To improve the understanding of site-specific flow and transport behaviour at different scales using site characterisation models.

The present report is concerned with Tasks 6D, 6E, 6F and 6F2. It follows on from two previous reviews of Tasks 6A, 6B and 6B2, and Task 6C.

In Task 6D the transport of tracers through a fracture network is modelled using the conditions of the C2 TRUE-Block Scale tracer test, based on the synthetic structural model developed in Task 6C. Task 6E extends the Task 6D transport calculations to a reference set of PA time scales and boundary conditions. Task 6F consists of a series of ‘benchmark’ studies on single features from the Task 6C hydrostructural model in order to improve the understanding of differences between the participating models. Task 6F2 utilises models set up for Tasks 6E and 6F to perform additional sensitivity studies with the aim of increasing the understanding of how models behave, the reason for differences in modelling results, and the sensitivity of models to various assumptions and parameter values.

Eight modelling teams representing five organisations participated in this exercise using Discrete Fracture Network (DFN), continuum and channel network concepts implemented in a range of different codes and applied using a variety of methodologies.

This report: summarises and reviews the Task 6D, 6E, 6F and 6F2 objectives and specifications; summarises and reviews the modelling team reports; compares the modelling team results; and discusses issues raised by the study. The main findings are summarised below.

## ***Task specification and implementation***

### **Philosophy of basing Tasks 6D and 6E on a hydrostructural model**

The Task 6D and 6E specifications assume that the Task 6C hydrostructural model is a true representation of the TRUE Block Scale site in order to eliminate Site Characterisation uncertainty, and thereby investigate how well Performance Assessment can be carried out on a perfectly characterised site. This specification was followed by some teams but others calibrated their Task 6D model to the C2 tracer tests results with the consequence that the models used in Task 6E differed between the groups.

### **Apertures**

It appears from this review that in general the Task specifications were sufficiently clear and detailed that they could be implemented by all of the modelling teams. One exception to this rule was an ambiguity regarding the ratio of transport to hydraulic aperture value for Task 6F. Most modelling teams assumed that the hydraulic and transport apertures were equal, even though the features were taken from the Task 6C model where the ratio was defined to be 0.125.

### **Additional performance measures and report structure**

With the benefit of hindsight it would have been preferable to have defined additional performance measures for Task 6D, namely the characteristics of the flow paths followed by the tracers, and the outlet tracer concentration. Also, for Task 6E it would have been useful to have included a sensitivity study in which the source region is located in background fractures, in order to draw inferences about the extent of retention in background fractures close to waste canisters. The report structure recommended by the Task Force secretariat improved the clarity of the modelling team reports.

### **Was the C2 test sufficiently representative?**

The locations and flow rates for the 'C' tracer tests were chosen in order to maximise the tracer recovery and were performed with forced injection at the source location, which could have created additional connected pathways and led to additional dispersion. They were therefore not particularly representative of transport from waste canisters in averagely fractured rock. The C2 test was analysed in detail because it had the largest recovery. It is noted that tracer tests with little or no recovery can provide useful information about the connectivity of the fracture system.

### **Flow modelling**

As expected the Task 6C model, which was defined using a Discrete Fracture Network (DFN) code, was most accurately implemented using such codes rather than continuum or channel network codes.

### **Geological structure type**

The definition and specification of a geological structure type (GST) for each structure was a major innovation of the present exercise, and allowed the effects of realistic features to be studied. On SC timescales the GST has a major impact on retention whereas on PA timescales it is not generally important because diffusion and sorption are dominated by intact rock away from the fracture surface.

### **Channelling**

Some teams included the effect of channelling within structure planes. There is extensive evidence that this is an important phenomenon at Äspö and similar sites. However, efforts to include it are hampered by a dearth of relevant information. It remains an important issue for future research.

### **Complexity factor**

The second innovation of the Task 6C hydrostructural model was the specification of a complexity factor for each structure. While in principle this concept could be implemented in a number of ways, in general the modelling teams included it by increasing the flow wetted surface area of structures. This implementation is reasonable for experimental timescales when the diffusion penetration depth is less than the separation between individual fractures of the complex structures. However, for PA timescales this implementation leads to double counting. A further issue is that most modelling teams implicitly assumed that the sub-fractures are of approximately equal transmissivity and the flow and transport is thereby shared equally. In fact it is more likely that there is an approximately log-normal distribution of sub-fracture transmissivities. As shown in the Task 6F2 sensitivity study by Poteri, if the transmissivity of one parallel fracture is more than twice the others it will dominate the transport. This effect scales non-linearly with flow rate because a higher flow rate implies a lower value of the transport retention parameter group ( $\beta$ , defined by the integral of the ratio of flow wetted surface to water

flux along a flow path) and thus further reduces retention. Consequently in most circumstances where there are parallel fractures with a distribution of transmissivities, a single fracture pathway will be expected to dominate the breakthrough curve.

### **Visual presentation**

The modelling team reports demonstrate the power of visual presentation of quantitative information. A number of teams have presented visualisations of the fracture system and in some cases these have been augmented by superimposed head and flow fields. Moreover, the Posiva-VTT team have developed new visual representations to throw light on the variation of the transport retention parameter group ( $\beta$ ) as a function of path length and the contribution of different geological materials to the overall breakthrough curve. All these visualisations considerably enhance the understanding of the system and the modelling results, and it is hoped that the best practice used by the modelling teams will be widely adopted in the future.

### ***Simplifications for PA modelling***

The following conclusions can be drawn regarding the Task 6 objective on simplifications for PA modelling.

- Diffusion and sorption into intact rock are the primary retention processes on PA timescales.
- Diffusion and sorption into higher porosity near-fracture immobile zones provide secondary retention and can be approximated by a retardation factor on PA timescales.
- Geological Structure Type is a useful concept for classifying features, but does not have a first-order influence on PA.

Important outstanding issues regarding simplifications for PA modelling include:

- Appropriate ways of representing flow path geometry based on SC information, and how to extrapolate and simplify this for PA.
- Quantification of the  $\beta$  factor (transport retention parameter group) under PA conditions.
- The degree of connectivity between flow paths in different features that it is reasonable to assume for PA.
- The relative importance of background fractures, for example in the vicinity of waste canisters, in providing retardation on a PA timescale.
- The PA impact of not assuming linear reversible sorption.
- The weight of evidence, e.g. from natural analogues, for the assumption that diffusion occurs for an unlimited distance into the intact rock.

Underlying all these issues, the development and use of microstructural models has provided a useful bridge between SC and PA modelling, which has improved our understanding of what is important for PA timescales.

### ***Tracer test constraints on PA parameters***

The following conclusions regarding tracer test constraints on PA parameters can be drawn from a range of studies conducted as part of Task 6.

- Immobile zone parameters derived from tracer tests are not first-order contributors to PA retardation.
- However, tracer tests are invaluable for confirming our understanding the dominant transport processes for PA.
- Tracer tests provide useful information for quantifying transport aperture and flow wetted surface.

- All (even null) tracer test results, and also hydraulic (especially cross-hole) test results, can provide useful constraints on hydrostructural models.

Important outstanding issues regarding tracer test constraints on PA parameters include:

- Current hydrostructural models tend to be over-connected. For example, the Task 6C model could not explain the lack of conductivity in some parts of the block.
- In the Task 6C model it is assumed that the background fractures and fracture zones belong to separate distributions. It is an open question as to whether they are both essentially part of a universal distribution. Similarly, an important unresolved issue is the transmissivity – length correlation.

### ***Support to the design of SC programmes for PA***

The following conclusions regarding supporting the design of SC programmes for PA have emerged from a number of studies during Task 6.

- Hydrostructural models are an essential link between SC and PA modelling.
- The Task 6C hydrostructural model is a more comprehensive approach to quantitatively describing a volume of fractured rock than has been achieved hitherto. Work on hydrostructural modelling should continue, especially regarding connectivity and eventually the inclusion of channelling.
- PA requires direct measurements of diffusion and sorption parameters on intact rock samples, and also hydraulic tests on background fractures.

Important outstanding issues regarding supporting the design of SC programmes for PA include:

- A key issue is how to improve the experimental characterisation of the flow and diffusion of solutes within structures. For example, channelling within fractures remains a key issue but there is a dearth of quantitative information. Resin injection experiments can throw light on these processes. An alternative perspective is to focus directly on the dynamical behaviour of water along transport paths rather than investigating flow geometries.
- There are arguments against carrying out tracer tests in URLs, because it is desirable to perform them under natural conditions without large gradients. Thus alternative approaches and experimental designs should be considered, for example carrying out tracer tests from boreholes drilled from the surface.
- There are some additional issues that need to be considered in support of the safety case, which would benefit from SC experiments. These include scenarios involving the penetration of oxygenated water into a repository, and phenomena that can block matrix diffusion.

### ***Improving understanding using SC models***

The following conclusions regarding improving understanding using SC models have emerged from studies during Task 6.

- Task 6 has advanced the understanding of the impact of near-fracture-surface immobile zones on retention. For example, gouge is important for retention on SC timescales.
- In general the Task 6 experience has emphasised the importance of geological information, for example in understanding transport pathways and integrating understanding into a hydrostructural model.
- Three-dimensional hydraulic models of complex features are useful for enhancing confidence and understanding, and for the development of equivalent PA parameters.
- In general, the approach of using parameter groups, such as  $\beta$ , has proved a useful aid to understanding.
- $\beta$  tends to reach a plateau when major flow paths are reached, demonstrating the importance of near-source low-flow features.

- Transport through high complexity factor features is mainly through a single path with the highest water flux.
- Two-dimensional diffusion from channels through gouge and other stagnant zones could effectively increase the surface area between mobile and immobile zones on PA timescales.
- Task 6 has provided a good starting point for new thinking on understanding the dynamics of water flow and tracer transport in fractured rocks, which is being taken forward in Task 7.

### ***The Äspö Task Force experience***

Task 6 of the Äspö Task Force has been a valuable learning experience for all concerned, in particular:

- It has been an excellent forum for exchange of ideas and for the training of researchers entering the field.
- Through participating in Task Force meetings, modellers have come to appreciate the strengths and weaknesses of alternative approaches. It has proved useful to augment presentations of results with interactive discussion sessions.
- There has been a surprisingly wide range of models and approaches, but they have all been based on the same underlying physics and the same data.
- In previous tasks the emphasis was on the use of in-house models and there was unspoken competition among modelling teams. In Task 6 there has been a greater sharing of ideas, openness and transparency.
- The involvement of external review guards against ‘group think’. For Task 6, the reviewers started earlier than for previous tasks, and were more proactive.
- It has proved difficult for the modelling teams to produce reports by the agreed dates. The report format has proved useful in improving the clarity of the modelling team reports.
- There is a need to publish more in the open literature. This has been recognised by the secretariat, and there are plans to submit a suite of articles on Task 6 to a peer-reviewed journal.
- The Task Force is a civilised forum with respect for alternative views, reflecting the character of its Chairman, Gunnar Gustafson.

### ***Outlook***

Tracer test data is not directly applicable to PA but this does not diminish their value for PA, which lies in their confirmation of our understanding of the important flow and transport processes.

An intrinsic theme of Task 6 has been that growing computer power brings SC and PA modelling closer together, and thus in future performance assessments can use more complex representations of the system, although the realism will be limited by the available data.

Advances are being made in reactive-transport modelling, which in the future offers the opportunity of treating retention processes from a more fundamental perspective than instantaneous linear reversible sorption.

Flow and transport within features, in particular channelling and flow wetted surface, remain significantly uncertain. However, resin injection experiments have the potential to provide useful supporting evidence.

An important challenge for radioactive waste disposal organisations is to move from scientific understanding to engineering. This transition recognises that we will never know everything about a disposal system and that to take things forward there is a need to take decisions despite the uncertainties.



# Contents

<b>1</b>	<b>Introduction and objectives</b>	13
1.1	Background	13
1.2	TRUE programme	13
1.3	Scope and objectives of Task 6	14
1.4	Scope and objectives of review	15
<b>2</b>	<b>Task specifications</b>	17
2.1	Semi-synthetic hydrostructural model	17
2.2	C2 tracer test	22
2.3	Task 6D	22
2.3.1	Boundary conditions	24
2.3.2	Tracers	24
2.3.3	Breakthrough curves	24
2.3.4	Additional performance measures	25
2.4	Task 6E	26
2.4.1	Boundary conditions	27
2.4.2	Breakthrough curves	27
2.4.3	Additional performance measures	28
2.5	Task 6F	28
2.5.1	Feature and material properties	29
2.5.2	Boundary conditions	30
2.5.3	Performance measures	30
2.6	Task 6F2	30
2.6.1	The effect of flow on transport in low complexity features	31
2.6.2	The effect of flow on transport in high complexity features	32
2.6.3	The effect of flow on transport in networks	32
2.7	Review of task specifications	32
2.7.1	Semi-synthetic hydrostructural model	32
2.7.2	C2 tracer test	33
2.7.3	Task 6C specification	33
2.7.4	Task 6D specification	34
2.7.5	Task 6E specification	35
2.7.6	Tasks 6F and 6F2 specifications	35
2.7.7	Summary	35
<b>3</b>	<b>Modelling teams</b>	37
3.1	ANDRA-CEA	37
3.1.1	Task 6D	37
3.1.2	Task 6E	39
3.1.3	Task 6F	40
3.1.4	Task 6F2	40
3.1.5	Review	41
3.2	ANDRA-Golder	42
3.2.1	Task 6D	42
3.2.2	Task 6E	44
3.2.3	Task 6F	45
3.2.4	Task 6F2	45
3.2.5	Review	45
3.3	CRIEPI	46
3.3.1	Task 6D	46
3.3.2	Task 6E	47
3.3.3	Task 6F	47

3.3.4	Task 6F2	48
3.3.5	Review	48
3.4	JAEA-Golder	49
3.4.1	Task 6D	50
3.4.2	Task 6E	52
3.4.3	Task 6F	52
3.4.4	Task 6F2	54
3.4.5	Review	56
3.5	Posiva-VTT	57
3.5.1	Task 6D	57
3.5.2	Task 6E	60
3.5.3	Task 6F	61
3.5.4	Task 6F2	61
3.5.5	Review	62
3.6	SKB-CFE-SF	63
3.6.1	Task 6D	64
3.6.2	Task 6E	65
3.6.3	Task 6F	65
3.6.4	Task 6F2	66
3.6.5	Review	67
3.7	SKB-KTH-ChE	67
3.7.1	Task 6D	68
3.7.2	Task 6E	70
3.7.3	Task 6F	71
3.7.4	Task 6F2	71
3.7.5	Review	71
3.8	SKB-KTH-WRE	72
3.8.1	Task 6D	72
3.8.2	Task 6E	74
3.8.3	Task 6F	75
3.8.4	Task 6F2	75
3.8.5	Review	76
<b>4</b>	<b>Inter-comparison of modelling results</b>	<b>79</b>
4.1	Task 6D	79
4.2	Task 6E	83
4.3	Task 6F	85
<b>5</b>	<b>Issues</b>	<b>89</b>
5.1	Task specification and implementation	89
5.1.1	Philosophy of basing Tasks 6D and 6E on a hydrostructural model	89
5.1.2	Apertures	90
5.1.3	Additional performance measures and report structure	90
5.1.4	Was the C2 test sufficiently representative?	91
5.1.5	Flow modelling	91
5.1.6	Geological Structure Type	92
5.1.7	Channelling	92
5.1.8	Complexity Factor	93
5.1.9	Visual presentation	93
5.2	Simplifications for PA modelling	93
5.3	Tracer test constraints on PA parameters	94
5.4	Support to the design of SC programmes for PA	94
5.5	Improving understanding using SC models	95
5.6	The Äspö Task Force experience	96
5.7	Outlook	96
<b>References</b>		<b>99</b>

# 1 Introduction and objectives

## 1.1 Background

The understanding and quantification of the transport of radionuclides in groundwater is a key factor in assessing the safety of radioactive waste disposal in geological formations. For fractured crystalline rocks this endeavour is particularly challenging, because of the spatial variability of fracture systems. In order to address this challenge it is beneficial to share ideas and information through international collaboration, and the Äspö Task Force on modelling of groundwater flow and transport of solutes /SKB 2004/ provides a valuable forum for such activities.

## 1.2 TRUE programme

The overall objectives of the Tracer Retention Understanding Experiments (TRUE) programme /Bäckblom and Olsson 1994/ are to:

- develop the understanding of radionuclide migration and retention in fractured rock,
- evaluate to what extent concepts used in models are based on realistic descriptions of fractured rock and if adequate data can be collected in site characterisation programmes,
- evaluate the usefulness and feasibility of different approaches to modelling radionuclide migration and retention, and
- provide in situ data on radionuclide migration and retention.

A staged approach has been adopted to address these ambitious objectives. The first stage (TRUE-1) was concerned with flow and transport on a detailed (0.5–10 m) scale, which formed the basis for Tasks 6A, 6B and 6B2. The experiments were performed within Feature A, which is a near-planar reactivated mylonite feature with an extent of about 10–20 m and a transmissivity in the range  $0.08 \cdot 10^{-7}$ – $4.0 \cdot 10^{-7}$  m<sup>2</sup>/s.

The second stage relates to work performed during the TRUE Block Scale project, which is summarised below.

The specific objectives of the TRUE Block Scale project /Winberg 1997/ were to:

- increase understanding of tracer transport in a fracture network and improve predictive capabilities,
- assess the importance of tracer retention mechanisms (diffusion and sorption) in a fracture network, and
- assess the link between flow and transport data as a means for predicting transport phenomena.

The achievements of this project are described in a four-volume final report /Andersson et al. 2002ab, Poteri et al. 2002, Winberg et al. 2003/. Characterisation included drilling, core logging, borehole imaging, borehole radar, 3D seismic surveys, hydraulic tests (flow logging, single hole tests, cross-hole interference tests), tracer dilution tests, hydrogeochemical analyses of groundwater samples and various types of mineralogical, geochemical and petrophysical measurements on drill core samples. Drilling and characterisation of each new borehole was followed by analysis and a decision with regards to the location of any subsequent borehole. The main set of tools for determining the conductive geometry and the hydrostructural model was a combination of borehole television (BIPS), high-resolution flow logging, and pressure responses from drilling and cross-hole interference tests.

A hydrostructural model was constructed from a set of deterministic sub-vertical structures mainly oriented northwest. Hydraulic features not part of the deterministic set were included in a stochastic background fracture population. Material properties and boundary conditions were also assigned to the developed model. Characteristics and properties measured in the laboratory were integrated in generalised microstructural models. Hypotheses formulated in relation to defined basic questions were addressed in in situ tracer tests using sorbing radioactive tracers and in the subsequent evaluation using numerical models. The in situ tracer test programme was concluded by injecting a cocktail consisting of 5–7 tracers with different sorption properties in three different source-sink pairs over distances ranging between 15 and 100 m, as integrated along the deterministic structures of the hydrostructural model, defining flow paths of variable complexity.

Numerical modelling using a variety of concepts and codes constituted an important and integrated component of the TRUE Block Scale project. A major accomplishment in this context was the development of a common conceptual basis for transport and retention. The fractured crystalline rock volume was conceptualised as a dual porosity medium (mobile-immobile). Model predictions of the sorbing tracer tests were followed by evaluation modelling where the various modelling results were used for increasing understanding of block scale transport and retention and the relative role of processes.

Diffusion to the immobile pore space, sorption in the immobile pore space and surface sorption on the fracture surfaces along the transport paths were interpreted as being the main retention processes in the prediction and evaluation models. This interpretation was supported both by the characteristics of in situ breakthrough curves and by modelling, where in the latter case the measured residence time distributions were reproduced more accurately with diffusional mass transfer included. Geological information from the site also provided support for the assumption of multiple immobile zones along the investigated flow paths.

### **1.3 Scope and objectives of Task 6**

This review is concerned with the sixth in a series of tasks within the Äspö Task Force (TF) on Modelling of Groundwater Flow and Transport of Solutes. Task 6 seeks to provide a bridge between site characterization (SC) and performance assessment (PA) approaches to solute transport in fractured rock. This is addressed by considering two spatial scales (a single feature and a network scale) and two temporal scales (SC and PA time scales).

In Task 6 both PA and SC models are applied to tracer experiments considering both the experimental boundary conditions and boundary conditions of relevance to PA. The approach is firstly to implement models such that they can reproduce the results from relevant Äspö in situ tracer experiments. Appropriate assumptions for PA modelling are then made, while continuing to honour the in situ tracer experimental results.

The objectives of Task 6 have been set out by /Benabderrahmane et al. 2000/ as follows.

1. To assess simplifications used in PA models including:
  - a. identifying the key assumptions and the less important assumptions for long-term PA predictions,
  - b. identifying the most significant PA model components of a site,
  - c. prioritisation of PA modelling assumptions and demonstration of a rationale for simplification of PA models by parallel application of several PA models of varying degrees of simplification,
  - d. provision of a benchmark for comparison of PA and SC models in terms of PA measures for radionuclide transport at PA temporal and spatial scales, and
  - e. establishment of a methodology for transforming SC models using site characterisation data into PA models in a consistent manner.

2. To determine how, and to what extent, experimental tracer and flow experiments can constrain the range of parameters used in PA models.
3. To support the design of site characterisation programmes to ensure that the results have optimal value for performance assessment calculations.
4. To improve the understanding of site-specific flow and transport behaviour at different scales using site characterisation models.

The scope of Task 6 covers eight sub-tasks as follows.

**Task 6A** models selected TRUE-1 tests in order to provide a common reference platform for all SC and PA modelling to be carried out in subsequent tasks, thereby ensuring a common basis for future comparison.

**Task 6B** models selected PA cases at the TRUE-1 site with PA relevant (long term/base case) boundary conditions and temporal scales. This task serves as a means to understand the differences between the use of SC and PA models, and the influence of various assumptions made for PA calculations for extrapolation in time.

**Task 6B2** is similar to Task 6B except that the boundary conditions are modified to produce flow and transport over a larger area of Feature A. The input boundary is no longer a point source and the tracers are assumed to be collected in a fracture intersecting Feature A.

**Task 6C** is concerned with the specification of a 50–100 m block scale synthesised structural model with a hydraulic parameterisation. A deterministic rather than a stochastic model is specified so that the differences between models result from variations in assumptions, simplifications and implementation rather than from the structural framework.

**Task 6D** is similar in purpose to Task 6A, but is based on the synthetic structural model developed in Task 6C and a 50 to 100 m scale TRUE-Block Scale tracer experiment. This task provides a common reference platform for all SC and PA modelling at the network scale and ensures a common basis for Task 6E.

**Task 6E** extends the Task 6D transport calculations to a reference set of PA time scales and boundary conditions. The first part of Task 6E uses a basic set of PA and SC assumptions and simplifications while in the second part a sensitivity analysis is carried out by investigating the effects of alternative assumptions.

**Task 6F** consists of a series of “benchmark” studies on single features from the Task 6C hydrostructural model in order to improve the understanding of differences between the participating models.

**Task 6F2** utilises models set up for Tasks 6E and 6F to perform additional sensitivity studies for evaluating specific topics of concern for the modelling of transport in fractured rock. The aim is to increase the understanding of how models behave, the reason for differences in modelling results, and the sensitivity of models to various assumptions and parameter values.

## 1.4 Scope and objectives of review

This report forms part of an independent review of the specifications, execution and results of Task 6. The review has been carried out by:

- reviewing background reports on the TRUE programme,
- reviewing the Task 6 specifications, modelling team reports and questionnaire responses,
- participating in Äspö Task Force workshops and meetings, and
- discussions with individual modelling teams.

Previous reviews in this series have been concerned with Tasks 6A, 6B and 6B2 /Hodgkinson and Black 2005/ and Task 6C /Black and Hodgkinson 2005/. The present report reviews Tasks 6D, 6E, 6F and 6F2. In order to avoid too much duplication, general review comments from /Hodgkinson and Black 2005, Black and Hodgkinson 2005/ relating to Task 6 as a whole are not repeated here. However, to produce a self-contained document, this report provides summaries of the tasks and the work of the modelling teams. Also, an evaluation of the modelling team results is included. Thus in essence it is a summary, evaluation and review report.

Section 2 presents a summary of the task specifications followed by review comments on the specifications.

Following an overview of the work of the modelling teams, the sub-sections of Section 3 consider the work of each modelling team in turn. Their approaches and key results are summarised and discussed followed by review comments on the work of each team.

Section 4 presents a preliminary inter-comparison of the currently available modelling team results in order to draw conclusions of relevance to the objectives of Task 6.

Section 5 of this report draws together some important issues arising from this review, drawing on discussions at interactive sessions at the Task Force meetings.

## 2 Task specifications

This section presents an overview of the geoscientific basis for Tasks 6D, 6E, 6F and 6F2 (Sections 2.1 and 2.2) followed by a summary of the specifications for these tasks (Sections 2.3–2.6). Finally, Section 2.7 presents review comments on the task specifications.

### 2.1 Semi-synthetic hydrostructural model

While Tasks 6A, 6B and 6B2 were concerned with transport through a single feature on a 5 m scale, Tasks 6D, 6E, 6F and 6F2 relate to transport through a network of conducting features on a 50 m scale. Clearly this requires much more geoscientific information, which is supplied through the semi-synthetic hydrostructural model developed in Task 6C /Dershowitz et al. 2003/.

This hydrostructural model has been developed on two different scales (200 m and 2,000 m) based on an interpretation of the conditions at the TRUE Block Scale site. Tasks 6D, 6E, 6F and 6F2 are based on information at the 200 m scale. As described by /Dershowitz et al. 2003/ it is a deterministic model developed by integrating the full range of geoscientific information available. In parts of the model where direct data is lacking, statistical techniques were used to infer the existence and characteristics of possible (synthetic) hydraulic structures. The model thereby represents one possible realisation of the hydrogeological conditions at the site, and allows the uncertainties in these conditions to be set aside so that the tasks can focus on the Task 6 objectives (Section 1.3).

/Black and Hodgkinson 2005/ have reviewed the formulation of the Task 6C hydrostructural model, and this is not repeated here. However, in what follows the basic elements of the model are outlined in order to provide sufficient background information for the current review.

At the 200 m scale the model contains 11 deterministic structures, 25 synthetic 100 m scale structures and 5,660 synthetic background fractures (Figures 2-1 and 2-2).

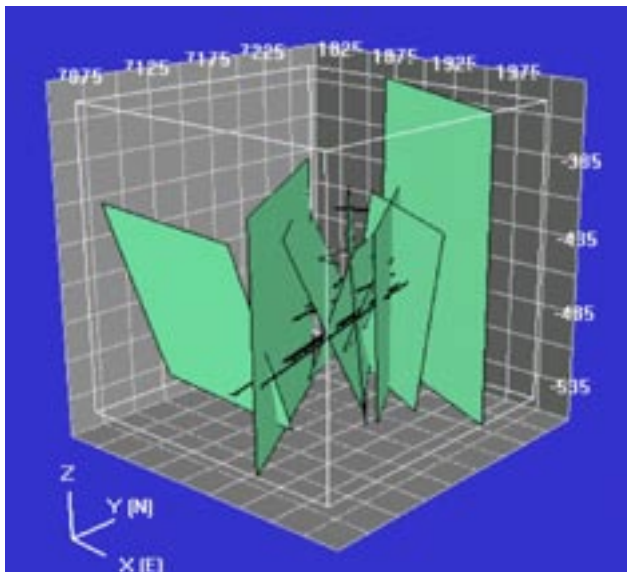


**Figure 2-1.** Deterministic 100 m scale structures in the 200 m block scale model from the Task 6C report /Dershowitz et al. 2003/.



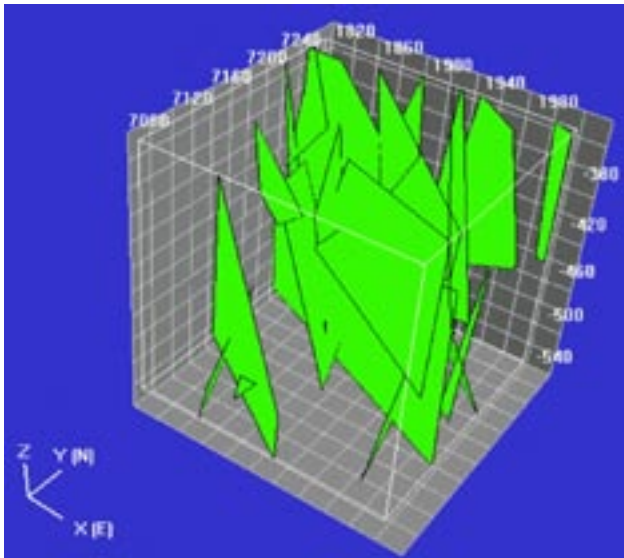


**Figure 2-2.** Synthetic 100 m scale structures in the 200 m block scale model from the Task 6C report /Dershowitz et al. 2003/.

While the properties of the deterministic features are based on measured data, the properties of the synthetic structures are assigned using a procedure depending on their size. Based on experience at Äspö, the geological structures are divided into two basic Geologic Structure Types, Type 1 “Fault” and Type 2 “Non-fault”, as shown in Figures 2-3 and 2-4.

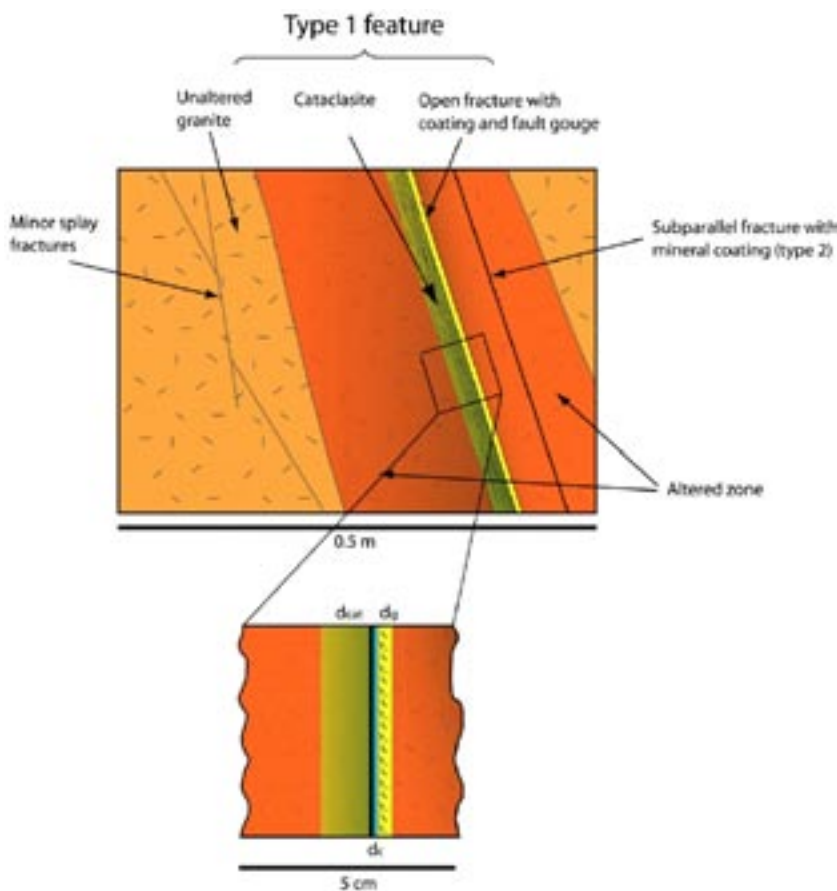


**Figure 2-3.** Illustration of the geological structure type 1 (Fault) from the Task 6C report /Dershowitz et al. 2003/.



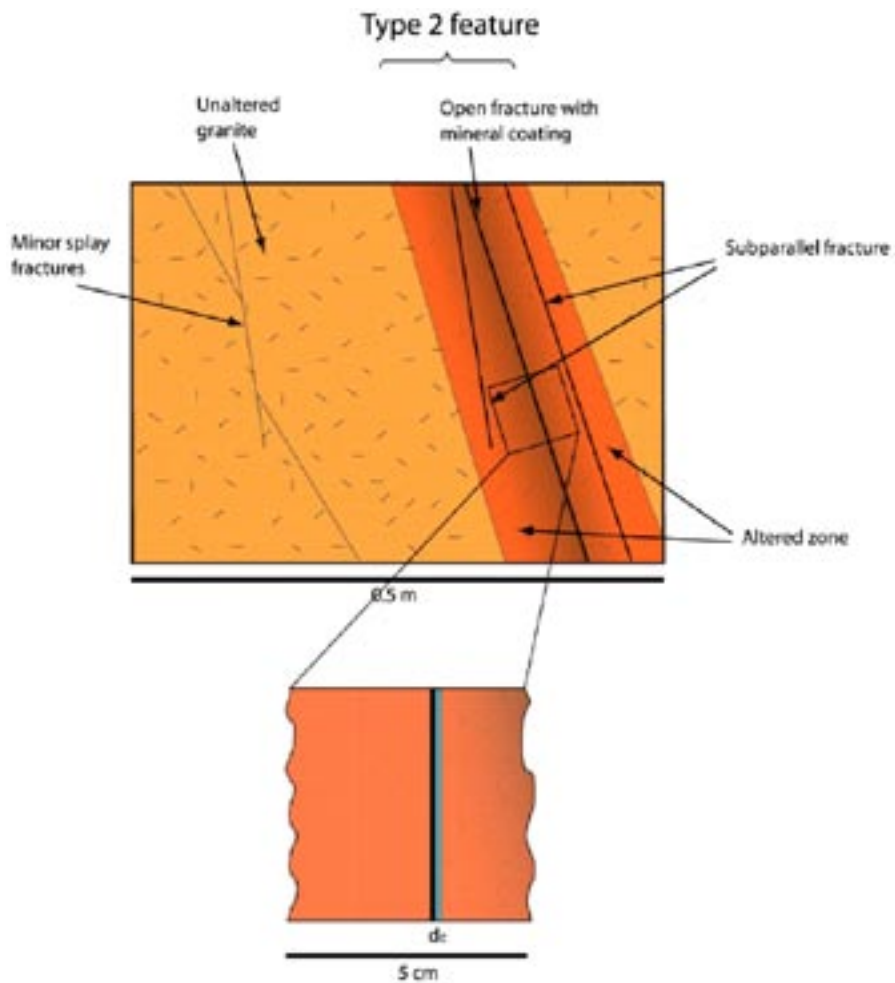


**Figure 2-4.** Illustration of the geological structure type 2 (Non-fault) from the Task 6C report /Dershowitz et al. 2003/.

/Dershowitz et al. 2003/ describe these two types of structure as follows.

- Type 1 is characterised by a significant shear movement along one main fault plane. The structure contains a ductile precursor (mylonite) which has been reactivated forming a brittle fault filled with mineralizations, cataclasite and fault gouge. The host rock around the structure has been altered by hydrothermal solutions. It is often accompanied by sub-parallel fractures in the cataclasite and in the altered zone. Alternative definitions of geological structure type 1 within the spectrum of possible variants include e.g. a) cataclasite + fault gouge, b) fault gouge, c) cataclasite + mylonite, d) mylonite + fault gouge.
- Type 2 is characterised by a fracture without typical shear indicators. The fracture is formed without any plastic precursor and contains fracture mineralisations only. There is a significant zone of alteration around the open fracture plane and it is often accompanied by sub-parallel fractures of the same type.

Moreover, investigations at Äspö have shown that many structures are made up of several conductive features/fractures and the number of sub-parallel features/fractures may vary over the extent of the structure. Thus, a structure may at one location consist of a single fracture of geological structure type 1, while at another location it may consist of two fractures of geological structure type 1 and 2, respectively. Larger scale structures may consist of tens or more of sub-parallel hydraulically conductive features/fractures. In order to incorporate this concept into the model at a level of detail justified by the data, a simplified classification scheme has been introduced by defining a complexity factor ranging from 1 to 5, with the characteristics specified in Table 2-1.

**Table 2-1. Definition of complexity factor assigned to modelled synthetic structures.**

Complexity factor	Number of sub-parallel conductive features/fractures per structure	Percent of primary geological structure type or combination of geological structure types (by area)
1	1	90 to 100%
2	1 to 2	70 to 100%
3	1 to 3	50 to 90%
4	3 to 10	50 to 90%
5	10+	50 to 90%

Based on available data, the distance between near-parallel features/fractures within a single structure was assumed to be 0.2 m.

In addition to the 100 m structures, the model contains background fractures, which are defined as features on a scale of less than approximately 50 m. These features can be of Type 1 or 2 and can consist of one or more discrete features. However, background fractures are generally of Type 2 and are generally made up of one discrete feature. Two sets of background fractures are included in the model, as shown in Figure 2-5.

Transmissivities were assigned to the synthetic structures using Monte Carlo simulation based on fracture length to achieve the trend line and scatter shown in Figure 2-6. Similarly, the relationship shown in Figure 2-7 was used to assign a geological structure type to each of the synthetic 100 m structures and to all of the background fractures. Complexity factors were assigned to the 100 m synthetic structures based on a correlation with size. For the background fractures, 80% were assigned a complexity factor of 1 and 20% were assigned a complexity factor of 2. Finally, some scale dependence of the geometrical parameters included in the microstructural models was assumed to reflect differences in geological and geochemical evolution and conditions affecting fractures of different sizes /Dershowitz et al. 2003/.

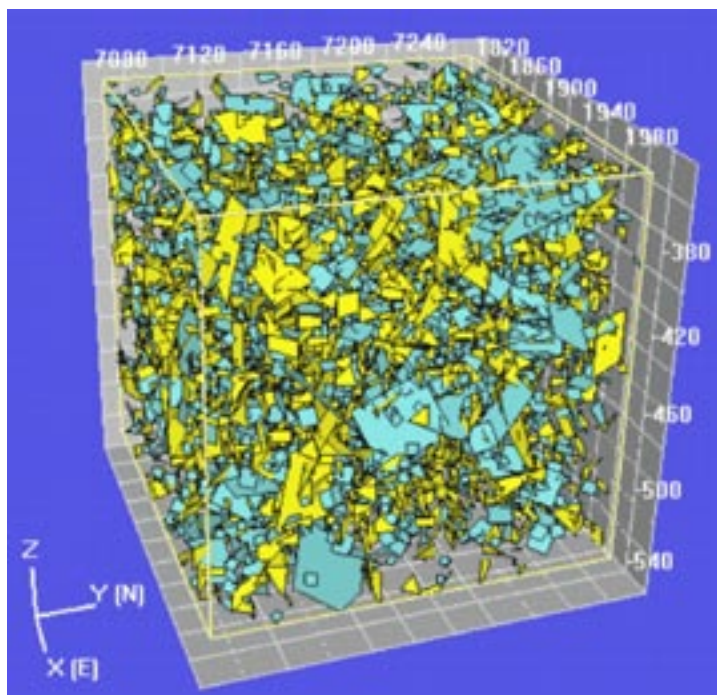


**Figure 2-5.** Background fractures coloured by set: shallow set (blue); NNW (yellow) from /Dershowitz et al. 2003/.

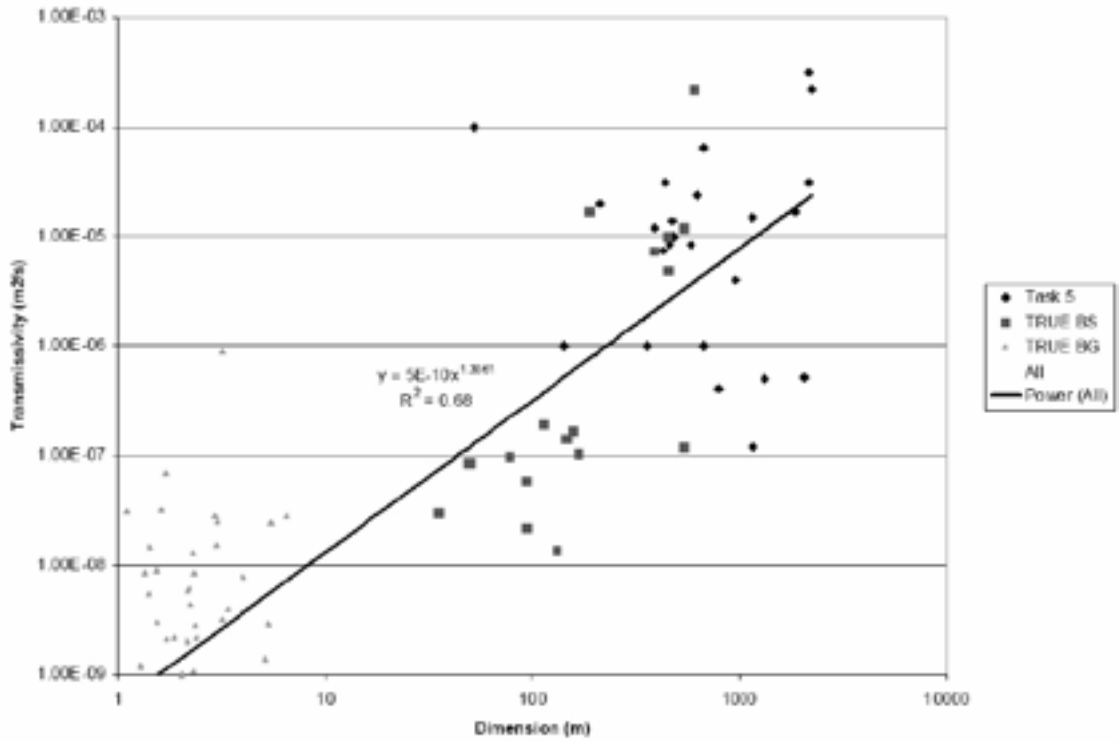


Figure 2-6. Correlation between structure/fracture size and transmissivity /Dershowitz et al. 2003/.

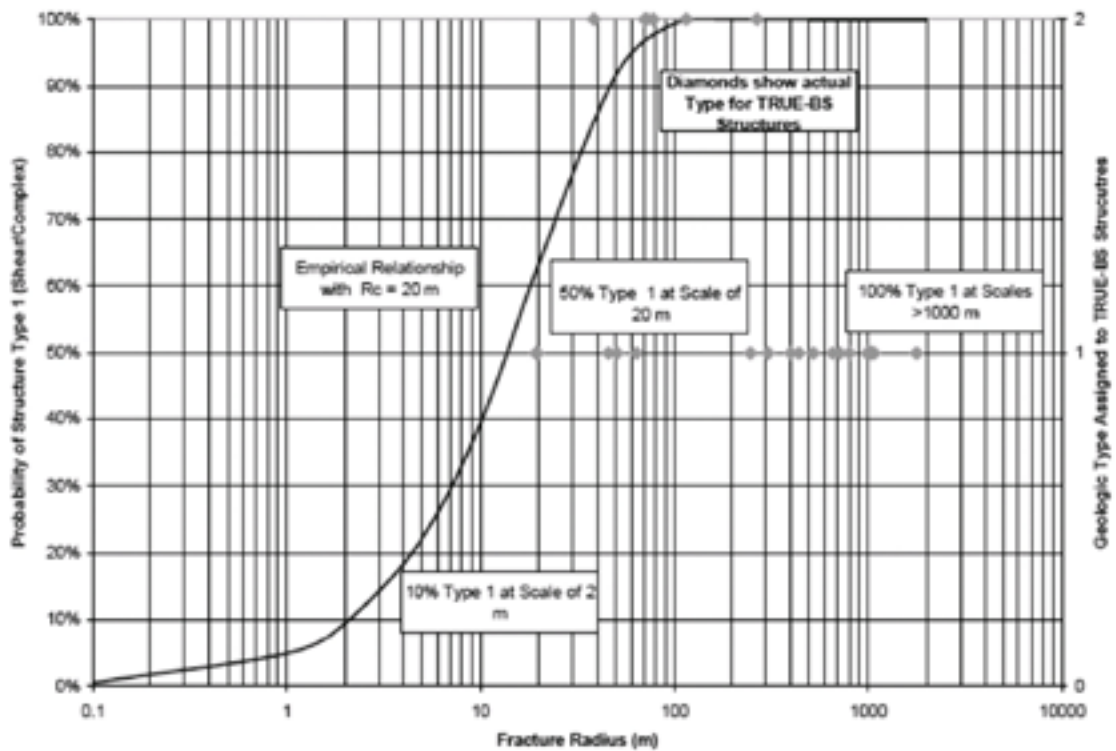


Figure 2-7. Relationship used for assignment of geological structure type to synthetic 100 m structures and background fractures /Dershowitz et al. 2003/.

## 2.2 C2 tracer test

A number of tracer tests have been performed at the TRUE Block Scale site with flow paths varying in length between 10 and 130 m with average travel times varying between 1.5 and > 2,000 hours /Andersson et al. 2002b/.

The main problem faced in these experiments was to select a test geometry that gave a sufficiently high mass recovery within a reasonable time. In contrast with tracer test STT-1B used for Task 6A, it was found that forced injection had to be used to enable detection at the sink location due to strong dilution, and also to avoid problems with artificially induced tailing in the injection signal. The main disadvantage of forced injection is that the convergent flow field is disturbed resulting in the tracer mass being spread out in an uncontrolled way over a larger area around the injection section.

In the final phase (Phase C) radioactive sorbing tracers were injected at three different source locations /Andersson et al. 2001/. Tracer mass recovery was generally rather low (< 60%) for the Phase C tests with the exception of “Path II”, which was investigated using test C2 that forms the basis for Task 6D. Based on the results of previous test phases, the source and sink locations for this test were selected to involve transport along several different deterministic structures (“network flow paths”), namely deterministic structures 23, 22, 20 and 21 as discussed in more detail in Section 3. Table 2-2 details the parameters for tracer test C2.

The tracers used in the C2 test covered a range of sorption properties: non-sorbing (Rhenium-186 as perrhenate), slightly sorbing (Calcium-47), moderately sorbing (Barium-131) and strongly sorbing (Cs-137). The injection functions for these tracers are shown in Figure 2-8, and the breakthrough curves for the tracers with measurable concentrations are shown in Figure 2-9.

## 2.3 Task 6D

The purpose of Task 6D is to model selected tracers using the conditions of the C2 tracer test (Section 2.2) in order to provide a common basis for comparison of later Task 6E modelling. Accordingly Task 6D deals with solute transport over distances of tens of metres and time scales of months through pathways that involve several geological features. The aim is to reproduce the tracer test data and to assess its constraining power. The task was defined so that both PA and SC models could be used.

A key aspect of this and other work of the Åspö Task Force is to encourage the modelling teams to apply alternative models and approaches in order to be able to draw robust conclusions.

**Table 2-2. Data for source and sink sections used in tracer test C2 /Dershowitz et al. 2003/.**

Parameter	Test C2
Source section	K100F03:P7
Sink section	K10023B:P6
Cartesian distance	17 m
Distance along deterministic structures of the TRUE Block Scale Hydrostructural model	97 m
DFN path length	66 m
Structures involved	23, 22, 20, 21
Injection rate	1.5 E-7 m <sup>3</sup> /s
Pumping rate	3.27 E-5 m <sup>3</sup> /s

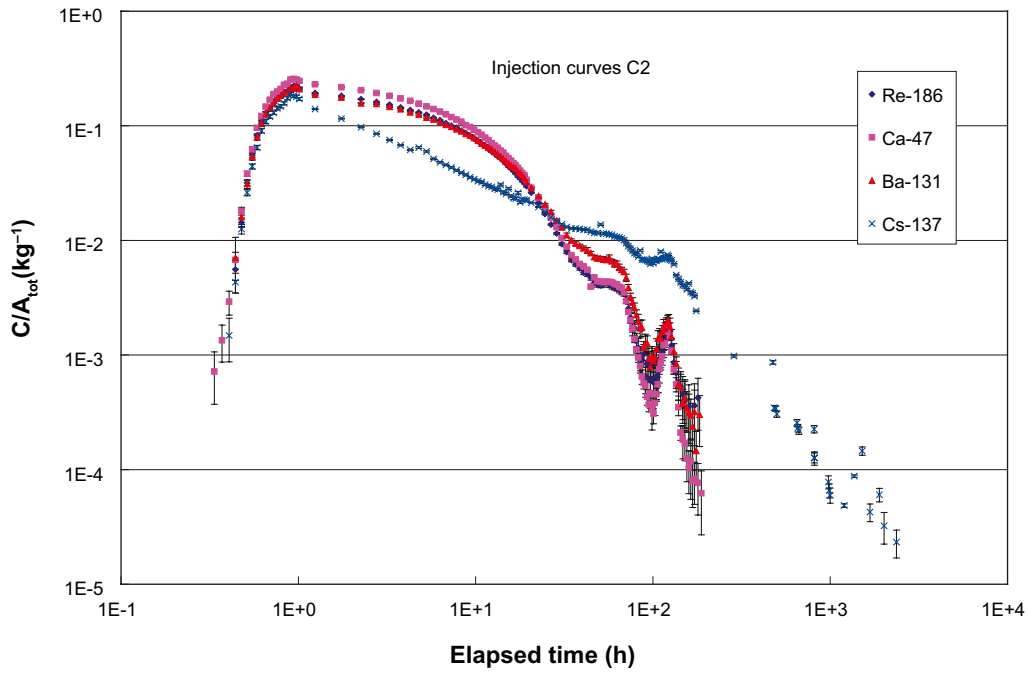


Figure 2-8. Test C2 injection functions for Re-186, Ca-47, Ba-131 and Cs-137 /Dershowitz et al. 2003/.

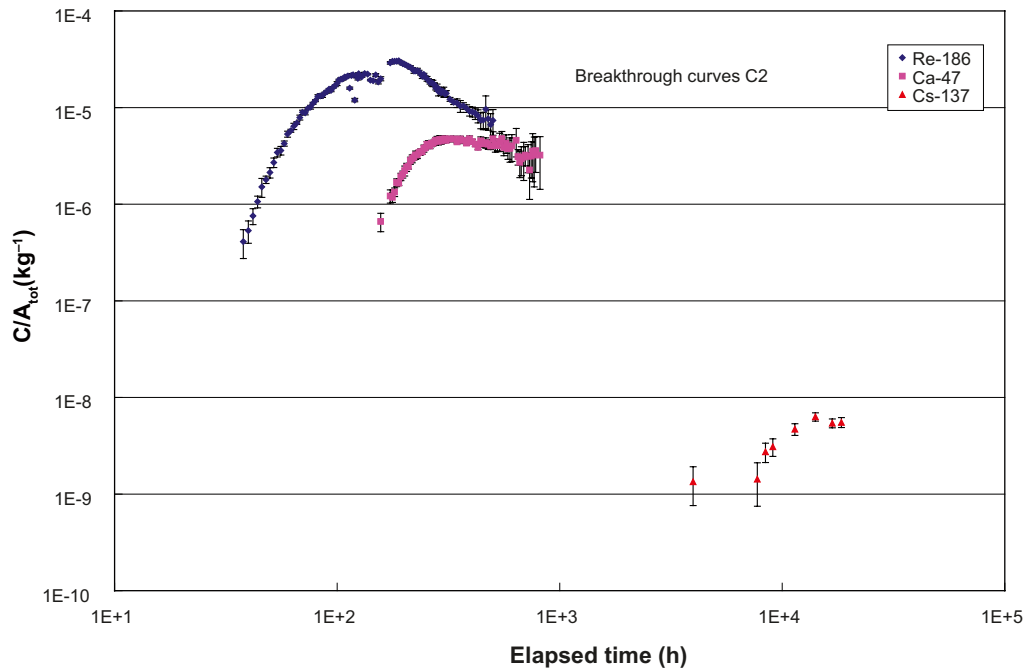


Figure 2-9. C2 tracer test concentrations normalised to total injected activity /Andersson et al. 2002b/.

Task 6D was specified in /Elert and Selroos 2002, 2004a/. For the purposes of Task 6D, the semi-synthetic hydrostructural model outlined in Section 2.1 and described in detail in the Task 6C report /Dershowitz et al. 2003/ is assumed to be a true representation of the site. In addition material properties set out in the Task 6C report were provided as guidance to the modelling teams, with the recommendation that if other values were used the motivation should be documented.

### 2.3.1 Boundary conditions

Head boundary conditions were specified to reflect the experimental conditions as closely as practicable. It was therefore necessary to take into account the underground openings of Äspö HRL. In order to avoid the construction of complex 3D models, boundary conditions that embed the underground openings without including them explicitly in the models were used in Task 6D.

Boundary conditions for the Block Scale model were obtained by interpolation from head measurements in the TRUE Block Scale rock block. These head data were provided to the modelling teams on 10 m scale panels for each of the faces of the TRUE Block Scale rock volume, and are illustrated in Figure 2-10. These head values have to be adjusted further to condition them to the measured head values in boreholes transecting the rock block.

### 2.3.2 Tracers

In Task 6D the breakthroughs of the tracers I-129, Ca-47, Cs-137, Ra-226, Tc-99 and Am-241 were simulated, although not all of these tracers were used in the C2 test. The purpose was to relate to the behaviour of radionuclides relevant for PA, and in the case of Technetium and Americium also to study how the retardation of more strongly sorbing radionuclides can be extrapolated in time.

In the short time perspective of the C2 test the perrhenate anion ( $\text{ReO}_4^-$ ) is expected to be non-sorbing with very similar behaviour to iodide ( $\text{I}^-$ ), e.g. /Byegård et al. 1992, Holmqvist et al. 2000/. The injection time history of I-129 was assumed to be identical to that of Re-186. The simulated results can thereby be compared with the breakthrough of Re-186.

The injection time histories of Ra-226, Tc-99 and Am-241 were assumed to be identical to that of Cs-137. However, in this case no comparison can be made with experimental data.

### 2.3.3 Breakthrough curves

In addition to the drawdown in the injection and pumping boreholes, the basic performance measures relate to the breakthrough curves for the measured injection of tracers I-129, Ca-47, Cs-137, Ra-226, Tc-99 and Am-241, namely:

- Breakthrough curves for each tracer (Bq/kg vs. hour).
- Maximum flux (Bq/hour).

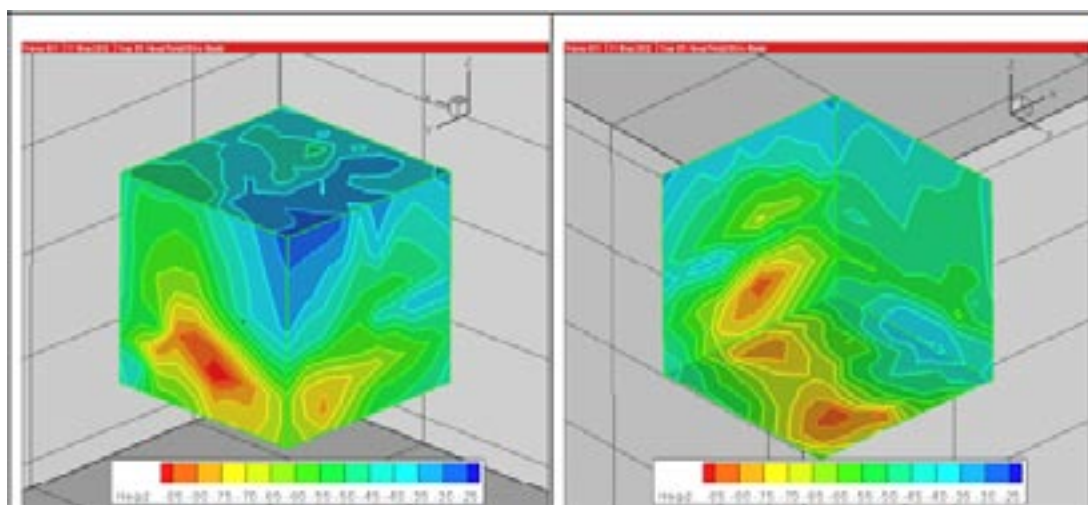


**Figure 2-10.** Boundary conditions on 200 m model block for Task 6D. Note that these are not conditioned to measured hydraulic heads in boreholes /Dershowitz et al. 2003/.



- The breakthrough times (hours) for the recovery of 5, 50 and 95% of the injected mass:  $t_5$ ,  $t_{50}$  and  $t_{95}$ .

Similarly, the following output was specified for a Dirac pulse injection:

- Breakthrough time history for each tracer (1/hour vs. hour).
- Maximum flux (1/hour).
- The breakthrough times for the recovery of 5, 50 and 95% of the injected mass:  $t_5$ ,  $t_{50}$  and  $t_{95}$  (in hours).

In the specification, it was noted that radioactive decay should not be considered in the modelling, and the injection concentrations were corrected for decay. Simulation results were requested for times up to  $10^8$  hours or until a full recovery is obtained for all tracers.

Different combinations of parameters and/or processes could reproduce the same C2 breakthrough curves, but could lead to different responses on PA time scales. Thus the modelling teams were encouraged to seek out alternative combinations of parameters/processes consistent with the C2 data set.

### **2.3.4 Additional performance measures**

A number of additional performance measures were specified aimed at understanding key parameters of relevance to radionuclide transport, as described below.

#### ***Conceptualisation of pore spaces***

The modelling groups were requested to provide a description of how they implemented the Task 6C model, and to supplement this with schematic diagrams, addressing the following questions:

- Were the geological structure types 1 and 2 as defined in the Task 6C report implemented? If not, any deviations should be explained together with the motivation for introducing these.
- How were the rock type properties of the 100 m scale geological structure types as defined in Tables 2-1 and 2-2 of the Task 6C report conceptualised in the model?
- What characteristic thicknesses (extent) of the different types of pore spaces (rock types) were modelled?
- How were the different types of pore spaces (rock types) distributed over the fracture surface (e.g. parallel layers, patches of different rock types)?
- How were the water flow paths distributed over the fracture surfaces? (e.g. entire plane of feature, channelling?)
- Was the distribution of rock types correlated to the location of the flow paths? For example, the presence of gouge or fracture coating?
- Was geological structure type assigned to the individual features strictly according to the specification in the Task 6C report?
- Was the concept of complexity included? If so, how was the complexity factor implemented as to: the number of features making up the structure; the variation in the number of features; and the variation of geological structure type along the feature?

### **Matrix parameter group**

The modelling groups were requested to provide the relevant parameters for the different types of pore space (rock type) needed to define the matrix parameter group:

$$\kappa = \sqrt{D_e (\epsilon + K_d \rho)},$$

where:

$D_e$  is the effective diffusion coefficient in the matrix (m<sup>2</sup>/s),

$\epsilon$  is the porosity of the matrix,

$K_d$  is the matrix sorption coefficient (m<sup>3</sup>/kg), and

$\rho$  is the bulk density of the matrix (kg/m<sup>3</sup>).

### **Water residence time distribution**

The modelling groups were requested to provide the water residence time distribution for the calculated flow path, for example by calculating the breakthrough curve for a tracer neglecting all surface/matrix interactions in the model. The calculation should be performed using a Dirac pulse input (unit input).

### **Transport retention**

The  $\beta$ -factor (also called F-factor) is a parameter group defined by the integral of the ratio of flow wetted surface to water flux along a flow path. This parameter group gives a measure of the surface available to matrix interaction and the time constant for the matrix interaction to occur. A large flow wetted surface increases the area available for matrix interaction and a low water flux increases the time constant for interaction between the flowing water and the fracture surfaces.

The parameterisation of the  $\beta$ -factor can be made in several ways depending on the type of model used and the conceptualisation of the flow paths. The additional specification document /Elert and Selroos 2004a/ gives a wide range of possible ways of defining the  $\beta$ -factor. For example for a channel of length L, width in the plane of the fracture W and water flux Q, the  $\beta$ -factor is defined by  $\beta = 2WL/Q$ . The modelling groups were requested to deliver statistics for the  $\beta$ -factor.

### **Modelling team reports**

Last but by no means least, a template setting out the requested structure, including section headings, for modelling team reports was specified.

## **2.4 Task 6E**

Task 6E /Elert and Selroos 2004b/ extends the Task 6D transport calculations to a reference set of PA time scales and boundary conditions. The constraints imposed on the models by application to Task 6D are thereby propagated to Task 6E so that the constraining power of tracer tests can be evaluated. In the first part of Task 6E, it was recommended that a basic set of PA and SC assumptions and simplifications should be used. The modelling teams were invited to carry out sensitivity analyses for alternative assumptions as an extension to Task 6E.

In moving from SC to PA boundary conditions and time scales the modelling teams were expected to adapt their models in such way that the transport and retention processes are described in a relevant way. The material properties in the Task 6C report were provided as



guidance to the modelling teams, with the recommendation that the motivation for using other values should be documented. Similarly, modelling teams were requested to explain any changes to the modelling assumptions used in Task 6D.

The spatial scale for the simulation is the 200 m block scale summarised in Section 2.1 and detailed in the Task 6C report /Dershowitz et al. 2003/. In contrast with Task 6D, water flow takes place under natural gradient boundary conditions giving water travel times closer to performance assessment time scales, using the boundary conditions discussed below.

## 2.4.1 Boundary conditions

### *Head boundary conditions*

As the simulations of tracer transport in Task 6E are for post-closure conditions, it is not appropriate to take into account the underground openings of Äspö HRL in contrast to Task 6D. The specified boundary conditions are simplified with fixed head boundary conditions at the eastern and western sides of the 200 m block, while the other sides are treated as no-flow boundaries:

- Eastern side (X = 2,000)      Head = 1 m
- Western side (X = 1,800)      Head = 0 m

The boundary conditions give a gradient from east to west with a magnitude of about 0.5%. This corresponds to modelled gradients in the simulations of the Äspö site in SR 97 /Walker and Gylling 1998/. In contrast, the Task 6D gradient was about 1,000% over the Cartesian distance.

### *Tracers*

The tracer source section (Table 2-3) was chosen to be at the injection point of tracer test C2 in the deterministic feature 23D, i.e. at the same location as in Task 6D. This point is located near the centre of the 200 m block. This feature has a size and transmissivity similar to that of Feature A, which was studied in Tasks 6A, 6B and 6B2. For Task 6E the source is assumed to be an intersecting fracture with a linear extent of 3 m, which may be modelled as a line source or as several point sources on a line.

Task 6E simulates the breakthrough of the tracers I-129, Ca-47, Cs-137, Ra-226, Tc-99 and Am-241. The purpose is to relate to the behaviour of radionuclides relevant for PA.

## 2.4.2 Breakthrough curves

The modelling teams were requested to explain how retention was implemented in their model for Task 6E and to point out differences in the conceptualisation assumptions and parameter values relative to Task 6D.

**Table 2-3. Data for Task 6E source section. Coordinates given in the ÄSPÖ96 system.**

Parameter	Source section		
	Endpoint 1	Centre	Endpoint 2
Easting	1,930.758	1,929.741	1,928.724
Northing	7,193.742	7,194.840	7,195.938
Elevation	-476.100	-476.100	-476.100

The primary performance measures relate to the breakthrough curves for an extended pulse injection curve for each of the tracers I-129, Ca-47, Cs-137, Ra-226, Tc-99 and Am-241, as follows:

- Breakthrough curves for each tracer (Bq/year vs. year).
- Maximum flux (Bq/year).
- The breakthrough times for the recovery of 5, 50 and 95% of the injected mass:  $t_5$ ,  $t_{50}$  and  $t_{95}$  (years).

Similarly the following outputs were requested for a Dirac pulse injection:

- Breakthrough time history for each tracer (1/year vs. year).
- Maximum flux (1/year).
- The breakthrough times for the recovery of 5, 50 and 95% of the injected mass:  $t_5$ ,  $t_{50}$  and  $t_{95}$  (years).

The performance measures were requested at the following points:

- At the western boundary of the 200 metre block (Easting (x) = 1800).
- At the intersection with a vertical plane defined by Easting = 1920, i.e. at a Cartesian distance about 10 m from the release point.
- At the intersection with a vertical plane defined by Easting = 1880, i.e. at a Cartesian distance about 50 m from the release point.

As with Task 6D, radioactive decay is not considered in the modelling. Simulations were requested until a full recovery is obtained for all tracers or a maximum of  $10^8$  years.

### **2.4.3 Additional performance measures**

In addition to breakthrough curves, the modelling groups were requested to provide the same additional performance measures as specified for Task 6D /Elert and Selroos 2004a/ summarised in Section 2.3.4, namely:

- Model conceptualisation of pore space.
- Matrix parameter group.
- Water residence time distribution.
- Flow-wetted surface – flow parameter group.

## **2.5 Task 6F**

The background to Task 6F is that it is difficult to compare and analyse modelling team results for Tasks 6D and 6E, because of the high degree of complexity. Thus, Task 6F /Elert and Selroos 2004c/ specifies a series of ‘benchmark’ transport calculations on simplified systems using ‘building blocks’ from the Task 6C model, namely two single features of geological structure Type 1 or Type 2 respectively.

For the purpose of this exercise the feature is assumed to have homogeneous properties. The tracers I-129, Cs-137 and Am-241 are considered, with transport and sorption data as prescribed for Task 6E. I-129 and Cs-137 were chosen because of their relevance to PA, while Am-241 was chosen to study how the retardation of more sorbing radionuclides can be extrapolated in time. The source term is a Dirac pulse from a spatially extended source as in Task 6E. Performance is measured for the breakthrough over a ‘collection line’ at a distance of 20 metres.

The modelling teams were requested to present and explain how retention is implemented in their model for Task 6F and point out differences in assumptions of conceptualisation and parameter values relative to Task 6D and 6E.

### 2.5.1 Feature and material properties

The selected features are:

- Geological Type 1: Synthetic feature 1S.
- Geological Type 2: Synthetic feature 4S.

In the Task 6C model these features have a complexity factor of 2, but for the purposes of Task 6F the complexity factor is taken to be 1. Also, in the Task 6C model these features are truncated at the boundaries of the 200 m box, but for the purpose of this exercise they are not truncated at the box boundaries.

The properties of the selected features as given in the Task 6C database are presented in Table 2-4.

The flow and transport geometry is shown in Figure 2-11.

**Table 2-4. Properties of selected features.**

Feature name	Width and length	Geological type	Complexity factor	Transmissivity (m <sup>2</sup> /s)	Storativity (-)	Aperture (m)
1S	112.44	1	2*	3.14E-07	2.80E-04	2.58E-04
4S	80.55	2	2*	1.90E-07	2.18E-04	2.01E-04

\*For the purpose of this exercise the complexity factor is 1.

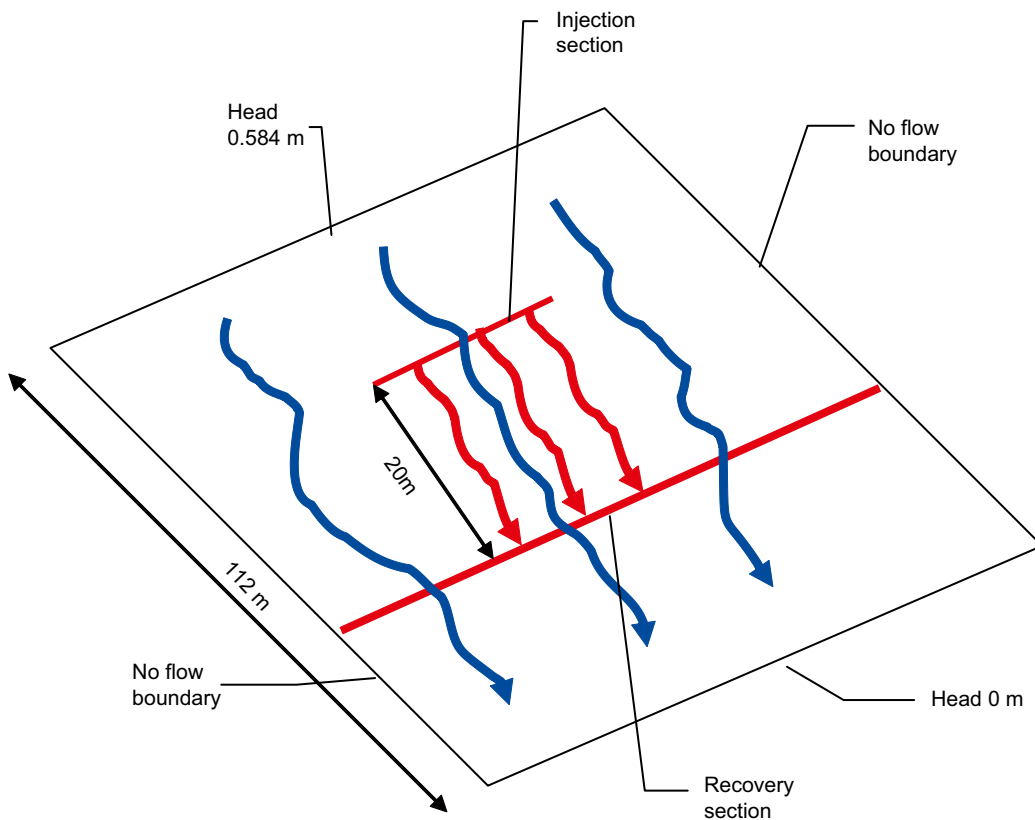


**Figure 2-11. Task 6F geometry and boundary conditions (example for Case A1).**

Transport and sorption properties from the Task 6C report were provided as guidance to the modelling teams, but they were free to choose alternative values provided that the motivation and values were documented.

## 2.5.2 Boundary conditions

The boundary conditions are simplified with fixed head boundary conditions at two opposing boundaries of the selected features, while the other sides are treated as no-flow boundaries, as shown in Figure 2.11. The heads are set in order to have groundwater travel times through the 20-metre section of the features of approximately 0.1, 1 and 10 years. The specified head differences required for this are presented in Table 2-5.

The tracer source section is assumed to be an intersecting fracture with a linear extension of 3 metres, modelled as a line source or as several point sources on a line. The tracer recovery section is assumed to be an intersecting fracture at a distance of 20 metres from the source section. In order to ensure recovery of all tracers the intersecting fracture is assumed to extend over the entire width of the feature.

## 2.5.3 Performance measures

The primary performance measures for each case and each radionuclide are:

- Breakthrough time history for each tracer (1/year vs. year).
- Maximum release rate (1/year).
- The breakthrough times for the recovery of 5, 50 and 95% of the injected mass:  $t_5$ ,  $t_{50}$  and  $t_{95}$  (years).

Also, the modelling groups were requested to provide the same additional performance measures discussed in Section 2.3.4 for Task 6D /Elert and Selroos 2004a/.

## 2.6 Task 6F2

The purpose of the Task 6F2 sensitivity study /Elert and Selroos 2004d/ is to exploit the model setup within Task 6E and 6F to perform additional studies evaluating specific topics of concern for the modelling of transport in fractured rock. The aim is to increase the understanding on how models behave, the reason for differences in modelling results, and the sensitivity of the models to various assumptions and parameter values.

Task 6F2 builds upon Task 6F, which is regarded as ‘Test bench 1’ for which all modelling groups were requested to provide results. The modelling teams were invited to set up studies based on topics described in the following subtasks. Also the modelling teams were invited to propose additional topics to address other issues concerning the effect of flow on transport in fracture systems.

**Table 2-5. Head boundary conditions for different cases.**

Travel time (y)	Feature 1S		Feature 4S	
	Case	Head difference (m)	Case	Head difference (m)
0.1	A1	0.584	A2	0.539
1	B1	0.0584	B2	0.0539
10	C1	0.00584	C2	0.00539

The overall objective of the 6F2 subtasks is to study the importance of flow distribution at different scales and to evaluate how this could be implemented in transport models for site characterisation and performance assessment. The 6F2 subtasks fall into the following categories, illustrated in Figure 2-12:

- The effect of flow on transport in low complexity features (single fracture).
- The effect of flow on transport in high complexity features.
- The effect of flow on transport in networks.

### 2.6.1 The effect of flow on transport in low complexity features

This subtask can be seen as an extension of the Test bench 1 (Task 6F). The purpose is to investigate the effect of various assumptions concerning flow distribution within a feature of low complexity, i.e. a single fracture. Issues to be addressed are:

- the effect on transport of various assumptions about aperture heterogeneity, channel width, fraction of fracture surface area in contact with flowing water, flow distribution between channels, etc,
- the influence of zones with stagnant water,
- possibilities to find limiting values of the ratio of flow wetted surface area and flow rate,
- effects of changes in flow paths over time (e.g. slow continuous change in gradient or cyclic variations due to daily and/or seasonal changes),
- implications for PA modelling.

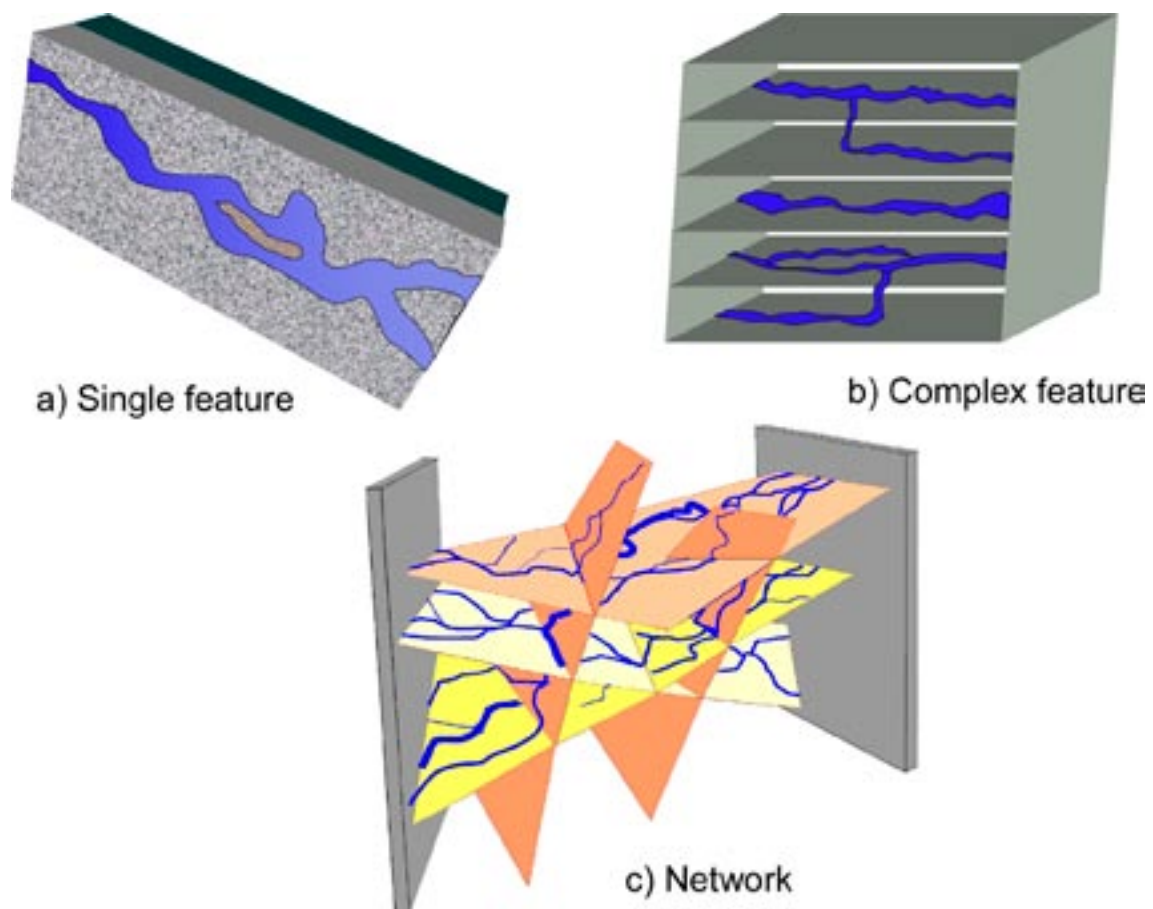


*Figure 2-12. Schematic presentation of flow in fractures /Elert and Selroos 2004d/.*

## **2.6.2 The effect of flow on transport in high complexity features**

This subtask is focused on transport in high complexity features consisting of several sub-parallel conductive features, sometimes of different geological type. These features generally have large dimensions and may be important pathways in the geosphere. The retention effect of these features will depend on how the water flow is distributed between the sub-parallel features. The purpose is to study how transport in complex features is affected by the flow distribution within and between different conductive features and how to implement this in SC and PA modelling. Questions that could be addressed are:

- what geological structure type dominates the transport resistance?
- how sensitive is this to assumptions about flow distribution between parallel conductive features of similar or different geological structure type?
- what is the effect of mixing at intermediate locations?
- what conclusions can be inferred concerning simplifications for PA modelling, for example can complexity be simplified while still retaining 'realistic' results?

## **2.6.3 The effect of flow on transport in networks**

The results from Tasks 6D and 6E show that the flow paths pass through several different deterministic features. To a varying degree also the stochastic background features have been found to be important. In fracture networks, flow paths may be diverging or converging, while in PA transport models often one-dimensional flow paths are assumed. The purpose of this subtask is to study the effect of flow in networks on the transport. The subtask is proposed to address topics such as:

- the effect of varying the properties of stochastic background fractures or excluding them;
- the effect of assumptions about mixing at fracture intersections by using the full fracture network model or by evaluating 'building block' results;
- the effect of assumptions concerning different distributions and correlations in DFN models (e.g. the effect of the assumed fracture length distribution, correlation between fracture length and transmissivity, etc);
- how to implement network transport in PA models, e.g. possible effects of using the 1-D approach in PA.

## **2.7 Review of task specifications**

This section presents review comments on the task specifications, in particular addressing the questions.

- Do the specifications make sense?
- Are the objectives clear?
- Are the tasks well formulated?

### **2.7.1 Semi-synthetic hydrostructural model**

The construction of the semi-synthetic hydrostructural model has been reviewed by /Black and Hodgkinson 2005/ where it was concluded that:

- The Task 6C hydrostructural model is a more comprehensive approach to quantitatively describing a volume of fractured rock than has been achieved hitherto. The idea of including solute retention characteristics as indices attached to individual fractures is efficient, meaning that a whole volume of fractured rock is described by a few spreadsheets.



- It would have been beneficial if the specifications for Task 6C had been more clearly defined as a hierarchy of requirements, and performance measures had been defined and evaluated to allow comparison of alternative approaches.
- The device used to reduce the initially unrealistic connectivity, namely reducing the average size of background fractures, has the effect of producing a final model with an ‘unnatural’ gap in the overall distribution of fracture sizes.
- The hydrostructural model is well defined and provides a useful test bed for Tasks 6D and 6E. However, overall the hydrostructural model seems to be too well connected, with the result that in Tasks 6D and 6E solutes may not have sufficient time to interact with the rock pore spaces.

From the perspective of Tasks 6D and 6E, the model is assumed to represent the truth in order to set aside the hydrostructural uncertainties and focus on other issues. Thus to some extent, it does not matter if the hydrostructural model has some deficiencies.

Of course, if the model is significantly in error within the region of the C2 tracer test then the modelling group interpretations of this experiment in Task 6D would be invalid. However, the location of the C2 test was chosen so that there is a reasonably well connected path along reasonably well characterised deterministic zones, and thus the Task 6C model provides a reasonable basis for Task 6D. It is noted that, this would not have necessarily been the case if other test locations had been chosen. Nevertheless it would have been preferable if the Task 6C model had been fully consistent with all hydrological data.

A key question for Tasks 6D and 6E is whether the hydrostructural model is sufficiently well defined to allow the modelling teams to carry out their analyses unambiguously. From the perspective of this review this generally appears to be the case, as the modelling teams did not experience too many problems in implementing the hydrostructural model.

### **2.7.2 C2 tracer test**

The TRUE Block Scale tracer test programme has been well planned, executed and documented, and the data set provides a valuable resource for understanding transport in fractured rocks.

It is noted that forced injection had to be used in order to get a sufficiently strong signal at the sink location due to strong dilution, and also to avoid problems with artificially induced tailing in the injection signal. It is interesting to speculate on the nature of the dispersion around the injection section that allowed the breakthrough concentration and recovery to increase so markedly when forced injection was used. Possibly this is a reflection of channelling within Structure 23, whereby tracer was forced into a nearby channel that linked up to a connected channel network to the sink location. As always, it would be relevant to know more about the degree of channelling within the planes of the structures, possibly by using resin injection from the injection borehole at the end of the tracer test.

It is clear that the source and sink locations of the C2 tracer test were chosen in order to maximise connectivity and thereby make tracer transport measurements practicable. The fact that we are considering the high end of the transmissivity and connectivity spectra should not be forgotten when drawing conclusions from Tasks 6D and 6E.

### **2.7.3 Task 6C specification**

There appears to be a spectrum of views on the requirements placed on the Task 6C semi-synthetic structural model, concerning the degree to which it should aim to be a realistic representation of the TRUE Block Scale site. The overall specification of the Task 6C model says that a deterministic rather than a stochastic model is used so that the differences between Task 6D and Task 6E models result from variations in assumptions, simplifications and implementation

rather than from the structural framework. This implies that the primary requirement for the Task 6C model is that it is reasonably representative of the type of rock mass found at Äspö such that it provides a useful test bed for the Task 6D and 6E modelling exercises. However, Task 6D compares tracer transport predictions with the results of the C2 tracer test performed at the TRUE Block Scale site. Thus to some extent the Task 6C model must represent that site, in which case it can be argued that it should be fully consistent with all site characterisation data including head boundary conditions.

The dichotomy of view is highlighted by the credence given to the background fractures in Task 6D, which are just one possible realisation of a stochastic distribution. In order to make an in-depth analysis of the C2 tracer test, it would be necessary to consider many discrete fracture realisations and to determine which of these are most consistent with the tracer test. Alternatively, a modelling group might argue that the background fractures should be omitted from Task 6D because they are either not important or too poorly characterised. Moreover, if the Task 6C model were meant to be a realistic representation of the TRUE Block Scale site then it would be reasonable to calibrate transport parameters to the C2 tracer test. However, if the Task 6C model is only meant to be a test bed that is representative of the type of rock mass found at Äspö, then it would not be appropriate to calibrate transport models in Task 6D.

The modelling team reports summarised in Section 3 display a range of philosophical approaches to tackling Task 6D, which indicates that this issue has not been fully resolved within the Task Force.

#### **2.7.4 Task 6D specification**

/Elert and Selroos 2002, 2004a/ set out a clear and comprehensive modelling specification for Task 6D. In particular, reference is made to specific sections of the Task 6C report containing detailed information and to other well-documented supporting reports such as /Andersson et al. 2001, 2002b/.

The use of the Task 6C hydrostructural model provides a well-defined basis for Task 6D that makes the analysis practicable for a number of modelling teams. Without this, many of the modelling teams would not have had the time and resources to participate.

However, as pointed out by /Tanaka 2005/, there was some potential ambiguity regarding the aperture values supplied in the project specification. These are hydraulic apertures ( $e_h$ ) calculated using the formula:

$$e_h = a_h T^b,$$

where  $T$  is the transmissivity. The constant  $b$  is taken to be 0.5 (Tom Doe's law) and the constant  $a_h$  is taken to be 0.46 as given on page 117 of the Task 6C report /Dershowitz et al. 2003/ and not 0.5, as given on pages 64 and 124 of the Task 6C report. The ratio of the transport aperture to the hydraulic aperture should be taken to be 0.125 as given on pages 64 and 124 of the Task 6C report, and not the range 0.135 to 0.300 as given on page 117 of the Task 6C report. Finally, the column labelled 'transport aperture' in Table 4-1 of the Task 6C report is in fact the hydraulic aperture, and has been calculated using  $a_h = 0.46$ , rather than 0.5 as stated in Section 4 of the Task 6C report.

The above ambiguities have not had as large an impact on Tasks 6D and 6E as might have been the case, as a number of modelling groups calibrated an overall scaling factor for the apertures to the C2 tracer test results.

The specification allows flexibility for modelling teams to choose the flow geometry within features (e.g. discrete channelling of flow over the entire surface area). In this way, questions about the possible over-connectivity of the fracture system could be addressed.

It is noted that the Task 6D specification requests predicted breakthrough curves in mass flow units of Bq/hour. A more stringent performance measure would have been the time-dependent



concentration in the sink borehole, as this requires a quantification of the dilution of the tracer by uncontaminated water. Also, it would have been interesting to have specified the tracer recovery as a performance measure together with an analysis of the reasons for limited recovery. In future exercises, it would be valuable to specify these additional performance measures, or equivalent quantities.

The specification of additional quantitative and descriptive performance measures /Elert and Selroos 2004a/ is particularly welcome. These facilitate a more in-depth understanding of the modelling assumptions and results by readers of the modelling team reports, and by the current reviewer in particular. Also, while there is no model-independent definition of the  $\beta$ -factor, the definitions provided by /Elert and Selroos 2004a/ for a range of models, goes a long way to making this important concept understandable to a wider audience.

Similarly the specification of a structure for the modelling team reports was a welcome development that facilitates wider access to the extensive body of work performed in Task 6.

### **2.7.5 Task 6E specification**

As with Task 6D, /Elert and Selroos 2004b/ specify Task 6E clearly and comprehensively, and the additional performance measures and report structure are useful innovations from earlier tasks.

As noted in the last section, the source region for Tasks 6D and 6E is at the high end of the spectrum as regards transmissivity and connectivity. Thus it might have proved interesting to have considered other source regions in less transmissive rock, for example within the background fractured rock. Inferences could then have been drawn about the importance of selecting canister locations within a repository.

### **2.7.6 Tasks 6F and 6F2 specifications**

Logically one might have expected Tasks 6F and 6F2 to have come before Tasks 6D and 6E. Nevertheless, they are valuable additions to meeting the overall goals of Task 6, and are generally well formulated and documented.

The aperture defined in the Task 6F specification (Table 2-4) is ambiguous. In fact it is the hydraulic aperture ( $e_h$ ) from the Task 6C report, where the transport aperture ( $e_t$ ) is defined by  $e_t = 0.125 e_h$ . However, for Task 6F most of the modelling teams have assumed that the hydraulic and transport apertures are both equal to the specified aperture value. Thus in Section 4.3, where the Task 6F results are discussed, it has been assumed that Task 6F has been effectively re-specified with  $e_h = e_t$ .

The questions posed in Task 6F2, concerning the understanding of the effects of flow heterogeneity at different scales, are particularly pertinent. General conclusions drawn from such studies potentially provide valuable evidence in support of the Task 6 goal of building a bridge between SC and PA modelling.

In principle it would have been interesting to have repeated these exercises for background fractures, which are likely to form the primary resistance in the vicinity of waste canisters. However, it is realised that Tasks 6F and 6F2 were afterthoughts in the final stages of Task 6, and there was insufficient time to pursue this line of reasoning.

### **2.7.7 Summary**

Tasks 6D and 6E are based on extensive and well documented hydraulic and tracer data supported by extensive laboratory data. To make these exercises practicable for a number of modelling teams, it was necessary to pre-process much of this information to provide a well-defined description of the likely flow regime. The Task 6C hydrostructural model fulfils this requirement and has proved to be sufficiently well documented to be implemented by the modelling teams.

The location of the C2 test was chosen so that there is a reasonably well-connected path along known deterministic zones, and so any uncertainties in the hydrostructural model should have little impact on the interpretation of the test.

The TRUE Block Scale tracer test programme has been well planned, executed and documented, and the data set provides a valuable resource for understanding transport in fractured rocks.

The forced injection of tracers required for practical realisation of the C2 tracer test could have been instrumental in initiating a well-connected network of channels, and reinforces the desire to learn more about channelling within features, for example by using resin injection.

There appears to be a spectrum of views within the Task Force on the requirements placed on the Task 6C semi-synthetic structural model, concerning the degree to which it should aim to be a realistic representation of the TRUE Block Scale site.

The Task 6D and 6E specification documents are clear and comprehensive and make reference to well-documented supporting reports. The additional performance measures and suggested report structure are useful innovations from earlier tasks.

The source region for Tasks 6D and 6E is at the high end of the transmissivity spectrum. It might have proved interesting to have considered other less transmissive locations in order to draw inferences about the selection of canister locations within a repository.

The aperture defined in the Task 6F specification is ambiguous and has caused confusion. In analysing the Task 6F results it has been assumed that the hydraulic and transport apertures are equal.

The questions posed in Task 6F2, concerning the understanding of the effects of flow heterogeneity at different scales, are particularly pertinent. General conclusions drawn from such studies could potentially provide valuable evidence in support of the Task 6 goal of building a bridge between SC and PA modelling.

## 3 Modelling teams

Eight modelling teams representing five organisations participated in this exercise, as shown in Table 3-1. The information from the teams is summarised in the first two sub-sections of Sections 3.1 to 3.8 for each modelling team in turn.

The final sub-sections of Sections 3.1 to 3.8 present an independent review of the work of each of the modelling teams, in particular addressing the following questions.

- Has the correct system been modelled?
- Has it been modelled correctly?
- What are the implications for the Task 6 objectives?

### 3.1 ANDRA-CEA

#### 3.1.1 Task 6D

##### *Approach*

The purpose of the work of the ANDRA modelling team from the Commissariat à l’Energie Atomique (CEA) was to address the issue of the identification of an optimal deterministic data set of flow and transport parameters associated with the major structures participating in the C2 tracer test /Grenier and Bernard-Michel 2006/.

Based on its work in Tasks 6A, 6B and 6B2 /Grenier 2004/, the ANDRA-CEA team limited the complexity of its models according to the constraining power of the available information, in particular from the C2 tracer test. The earlier work had demonstrated that the level of information available in tracer tests only allows for the identification of the travel time and dispersivity of simple major features together with averaged properties for the immobile zones accessed by diffusion.

Consequently, in Task 6D the geometrical complexity of the model was limited to the basic elements of the system. The following four-stage approach was used.

1. Firstly the Task 6C hydrostructural model was implemented on a 200 m scale by including the 11 deterministic structures constrained by the supplied head boundary conditions and the C2 test source and sink pumping rates. This model used the smeared fracture approach /Fournio et al. 2003/ implemented within the Cast3M continuum code using a Mixed Hybrid Finite Element (MHFE) scheme.

**Table 3-1. Organisations and modelling teams participating in Tasks 6D, 6E, 6F and 6F2.**

Organisation	Modelling team	Task 6D	Task 6E	Task 6F	Task 6F2
ANDRA	CEA	4	4	4	4
ANDRA	Golder	4	4	4	–
CRIEPI	CRIEPI	4	4	4	–
JAEA	Golder	4	4	4	4
POSIVA	VTT	4	4	4	4
SKB	CFE-SF	4	4	4	4
SKB	KTH-ChE	4	4	4	4
SKB	KTH-WRE	4	4	4	4

2. The 200 m scale flow model was used to provide flow boundary conditions for a flow and transport sub-model (Figure 3-1) consisting of truncated representations of structures 20 to 23, which was selected to provide a simple representation of the key features. These were discretised as planar fractures surrounded by a homogeneous matrix zone using 3D finite elements. Fracture segments that do not contain the travel path were not included. The water inputs associated with these segments were accounted for as source terms at the structure intersections obtained from the 200 m model. In addition to flow within the fractures, the model included dispersion in the fractures and diffusive transport in a zone representing near-fracture materials in particular gouge. Linear equilibrium sorption was included on the fracture walls and in the immobile zones. The transport equations were solved using a finite volume transient Eulerian scheme within the Cast3M code.
3. The transport parameters of the 4-structure model (4 fracture transport apertures, matrix zone diffusivity and porosity, and sorption coefficients) were calibrated to the C2 breakthrough curves. A qualitative calibration approach was used, based on visual comparison to the breakthrough curves. Starting from the parameters supplied in the Task 6D specification, the calibration first matched the non-sorbing tracer breakthrough followed by the sorbing tracers.
4. Finally, a sensitivity analysis was carried out for the most sensitive parameter, namely the fracture transport apertures controlling the advection time.

### **Results and discussion**

Good fits to the tracer breakthrough curves were achieved based on minor changes to the parameter values supplied in the Task 6D specification. However, the calibration is not unique. In particular it is difficult to discriminate between the effects of dispersion and matrix diffusion. Similarly, to a certain extent, it is possible to obtain comparable breakthrough curves by reducing the fracture transport porosity or increasing the effect of diffusion into immobile zones.

The most sensitive feature of the system is the mean transport time. For the specified flow system this is governed by the fracture transport aperture, which also changes the  $\beta$ -factor, and the surface sorption coefficients. It follows that these parameters are the most highly constrained. The influence of diffusion into immobile zones is relatively greater here than for Task 6A because of the larger contact time and longer travel path, but does not significantly affect the peak arrival.



*Figure 3-1. ANDRA-CEA detailed flow and transport model for structures 20–23 showing the head field (left) and the Darcy velocity field (right) /Grenier and Bernard-Michel 2006/.*

### 3.1.2 Task 6E

#### **Approach**

In view of the limited constraining power of tracer tests for PA modelling discussed in Section 3.1.1, /Grenier and Bernard-Michel 2006/ chose not to constrain Task 6E using the results of Task 6D. The approach adopted for Task 6E was to model the Task 6C fractures as 2D planes discretised with triangular finite elements, with the fracture intersections represented by 1D elements.

Transport in the fracture network included advection, dispersion, diffusion and linear sorption, with just diffusion and sorption in the matrix blocks. Sorption in altered and non-altered granite were included using a semi-analytical approach based on analytical solutions to the one-dimensional diffusion equation for infinite, limited, and composite media. Based on previous work, the matrix zones in the vicinity of the fracture planes were represented by means of a retardation coefficient. Fracture complexity was fully accounted for in a deterministic manner, with the dominant fracture type applied to each modelled fracture.

A careful study was made of the effect of truncating the number of features from 5,600 included in the specification. The features were selected after: (i) ordering the fractures by decreasing order of size; (ii) retaining minor fractures present in the vicinity of the source term location; (iii) studying connectivity within the fracture network for a sample of 3,000 larger fractures; and (iv) studying the sensitivity of flow and transport properties of the block to the number of fractures included.

Sensitivity analysis was used to assess the quality of the numerical simulations and to address physical modelling issues as follows:

- Numerical studies included convergence of the simulations with regard to mesh size, time step, and sensitivity to the dispersion coefficient.
- Physical modelling issues included sensitivity to: the number of fractures considered; complexity factor; extent and characteristics of altered and intact rock matrix units.

#### **Results and discussion**

Matrix diffusion was found to be a first order effect for transport on PA time scales. The impact on peak arrival time corresponded to a factor of 10 for non-sorbing Iodine to  $5 \cdot 10^5$  for matrix diffusion and sorption of Americium. The maximum flux was reduced by a factor of 50 for Iodine and  $3 \cdot 10^6$  for Americium. Penetration depths of the order of several meters to 10 meters were observed, showing that the primary factor is diffusion into the intact rock and altered diorite rather than near-fracture zones. This contrasts with the experimental time scales of Task 6D where diffusion into near-fracture zones dominated.

The largest features in the semi-synthetic block were found to be responsible for larger scale transfers whereas minor fractures do not increase the connectivity of the system. The main patterns of flow and transport are surprisingly well accounted for by truncated systems of modelled features. The extreme case of 12 features, consisting of the main conductors and minor fractures in the vicinity of the source location, provides a good first-order approximation with predictions within about 10% of the results of more refined calculations. The reasons for the success of this approximation are related to: (i) the connectivity of the system, in particular limited number of smaller connected units; (ii) the boundary conditions imposed to the block; and (iii) the limited volume of the source. The results indicate that the main reason why there is a single dominant travel path is related to the limited connectivity of the fracture network system. The lateral no-flow boundary conditions only play a secondary role in amplifying the importance of fracture paths connecting the input to output (involving features 23D, 1925B, 22D, 21D, 20D, 2292B, 17S and 19D). The 12-fracture system represents a simplified PA model and a good compromise between precision, complexity and numerical efficiency. Further efforts are required to assess the role of minor fractures in the transport properties of the system.

Other characteristics are identified as having a second-order influence on breakthrough curves and transport properties. In addition to the smaller-scale fracturing, dispersion coefficients associated with fractures have minor impact on the breakthrough curves. The spreading of the curves mostly results from the dispersion along the fracture network. Due to the penetration depth of matrix diffusion, a model consisting entirely of intact rock matrix is not distinguishable from one including altered rock. Similarly, simulations considering the dominant fracture type or full Type 1 fractures are roughly comparable.

Further efforts are required to study: (i) the role played by background fracturing, as limited flow and diffusion zones; and (ii) the impact of fracture complexity. The first point could be achieved for instance with a smeared fracture approach since matrix blocks are easily included. However, in view of the low connectivity of the smaller scale fractures in the Task 6C model, it might not be well captured by such a continuum dual porosity approach. Improvements to the treatment of fracture complexity are considered in Task 6F2.

### **3.1.3 Task 6F**

#### ***Approach***

/Grenier and Bernard-Michel 2006/ implemented Task 6F in accordance with the specification using a similar finite-element approach to that used for Tasks 6D and 6E.

#### ***Results and discussion***

As expected, matrix diffusion was the controlling retention mechanism at low velocities both in terms of the peak arrival times and the shape of the breakthrough curves, specifically larger tailing. /Grenier and Bernard-Michel 2006/ complemented the numerical analysis with the use of analytical expressions for the peak arrival time, which are typically accurate to about 10% and give added insight to the dependence on the various parameters.

### **3.1.4 Task 6F2**

#### ***Approach***

/Grenier and Bernard-Michel 2006/ examined the impact of complexity by considering:

- Type 1 and Type 2 features in series and in parallel; and
- dual-porosity and triple-porosity systems for two-dimensional sugar box fracture geometries.

A sugar box geometry was used with flow directed diagonally across the system. Finite-element simulations were performed with and without diffusion in the matrix blocks.

#### ***Results and discussion***

For Type 1 and Type 2 features in series it was demonstrated that the breakthrough curve has a unique peak and can be represented by an equivalent advection-dispersion-matrix diffusion model.

For the case of equal flow rates through Type 1 and Type 2 features in parallel the breakthrough curve has a double peak that cannot be represented by a simple equivalent model.

Illustrative calculations were presented for a non-sorbing tracer in the sugar box system. The study confirmed the importance of matrix diffusion on a PA timescale and provided insight into the effects of fracture geometry in well-connected fracture systems. For example, for the dual porosity system in which only the large matrix blocks were modelled, the breakthrough curve had a long tail. When the second level of fracturing was included, the peak arrival was delayed due to increased porosity, but the breakthrough curve was more symmetrical due to the more rapid rate of exchange with the matrix.



### 3.1.5 Review

#### **Tasks 6D and 6E**

The ANDRA-CEA team has taken an Occam's razor approach to Task 6D by only including features and processes in their model that can be constrained by the experimental data. Thus the synthetic fractures were not included. One consequence of this is that there is a single pathway from source to sink. This provides a useful perspective on Task 6D that is complementary to approaches taken by some other teams.

The work has demonstrated that the C2 tracer test can be understood in terms of a plausible set of parameters for the generally accepted processes. However, because of the visual approach taken to matching the simulated and measured breakthrough curves, it is not clear whether there are other plausible parameter sets that equally match the data. Also, the immobile zone diffusion parameters might be more constrained by focussing on the tails of the distributions rather than on the peak arrival. Focussing on the tails might also help the understanding of whether the single pathway approach is valid or whether the data require more than one route through the system. It would therefore be interesting to extend this work to include a more systematic and quantitative fitting procedure.

The comprehensive analysis of Task 6E by the ANDRA-CEA team has highlighted a number of important issues including:

- Matrix diffusion penetration depths of up to 10 m were calculated for Task 6E. This raises the question of whether such penetration is in accord with natural evidence /Miller et al. 2000, Jacob 2004/.
- The importance of background fractures in linking the source to major features in Task 6E parallels their importance in the repository context and raises the question of whether more focus should be placed on quantifying their role as a transport barrier.
- The rapid travel time in Task 6E of approximately 3 years raises the question of how representative the Task 6C model is of a repository site.

#### **Task 6F**

The ANDRA-CEA team have made a precise implementation of the Task 6F specification that should provide a benchmark for the other teams. Moreover, the analysis of the numerical results and the application of approximate analytical formulae help to make the Task 6F results comprehensible.

#### **Task 6F2**

The sugar cube system combined with finite-element modelling provides a powerful test bed for understanding general features of fracture systems and it would be good to see it more widely investigated.

For the systems and parameters considered in this study, the implications for the Task 6 objectives 1–4 (Section 1.3) include:

- 1. Assess simplifications for PA:** The ANDRA-CEA team have demonstrated that a surface retardation factor, representing near-fracture zones, combined with a single matrix zone representing diffusion into the rock, is adequate for performance assessment. Depending on the connectivity and boundary conditions, only a small fraction of features may contribute to flow and transport.
- 2. Determine constraining power of tracer and flow tests for PA:** The effective fracture transport aperture is reasonably well constrained by tracer tests. However, effective diffusion and sorption parameters determined from short-term tracer tests are not applicable to PA conditions.

3. **Support design of SC programmes for PA:** In view of point 2 above, only non-sorbing tracer tests contribute significantly to SC programmes. More focus needs to be placed on background fractures linking waste canister positions to major flowing features. The diffusive penetration depths observed in natural systems could have a major impact on geosphere performance assessment.
4. **Improve understanding using SC models:** Finite-element approaches have the potential to include the geometrical complexity of immobile zones and intra-structure flows, if such information were to become available.

## 3.2 ANDRA-Golder

The ANDRA modelling team from Golder Associates Oy have used a probabilistic approach to propagate modelling uncertainties remaining after conditioning to the Task 6D data set to the performance assessment conditions of Task 6E /Holmén and Forsman 2005a/. In keeping with the specifications of Tasks 6D and 6E, only one realisation of the hydraulic properties of the system was considered, namely the Task 6C hydrostructural model, in contrast to the ANDRA-Golder methodology for Tasks 6A and B2 where many different realisations were carried through the chain of calculations.

### 3.2.1 Task 6D

#### **Approach**

Flow modelling was carried out using a continuum approach with the finite-difference GEOAN computer code /Holmén 1992, 1997/. The properties of the continuum flow model were based on all the fractures in the Task 6C hydrostructural model, with the conversion based on Oda tensor theory /Oda 1985/, and the 200 m model was discretised into 2 m cubic elements.

Following the calculation of steady-state flow, taking account of the source and sink pumping rates, particle tracking in the advective flow field was used to define a stream tube for the conditions of tracer test C2. Transport modelling was implemented using pipe elements of the GoldSim Radionuclide Transport Module /Goldsim 2004/ to represent the Type 1 and Type 2 features. The path length and the maximum and minimum values for flow-wetted surface were propagated to the transport modelling, and the flow rate was assumed to be constant along the path and equal to the estimated injection flow of  $1.67 \text{ E-}7 \text{ m}^3/\text{s}$ . Thus tracer dilution was not studied in Task 6D. The concept of complexity factor was implemented by considering the four different networks of GoldSim pipes shown in Figure 3-2.

The transport modelling was carried out as a probabilistic sensitivity analysis, with the flow-wetted surface, fracture transport apertures, diffusive zone thicknesses, diffusivities, porosities and  $K_{ds}$  defined by uncorrelated probability distributions based on plausible ranges given in the Task 6D specification and related documents. The constraining power of the tracer tests was quantified by examining those realisations that met a specified criterion for an acceptable fit to the measured breakthrough curves. The set of accepted realisations constitute constrained coupled parameter distributions for use in Task 6E.

#### **Results and discussion**

The flow path from the injection well to the extraction well (Figure 3-3) had a path length of 25.3 m, which is to be compared to the distance along deterministic structures of the TRUE Block Scale hydrostructural model of 97 m, and the DFN path length of 66 m /Dershowitz et al. 2003, Holmén and Forsman 2005a/ attribute this difference primarily to the inclusion of the synthetic background fractures. However, it is possible that the main reason is the homogenising effect of deriving an equivalent permeable medium from the Task 6C model. Based on the particle tracking, two methods were used to estimate the flow wetted surface area for the C2 test.



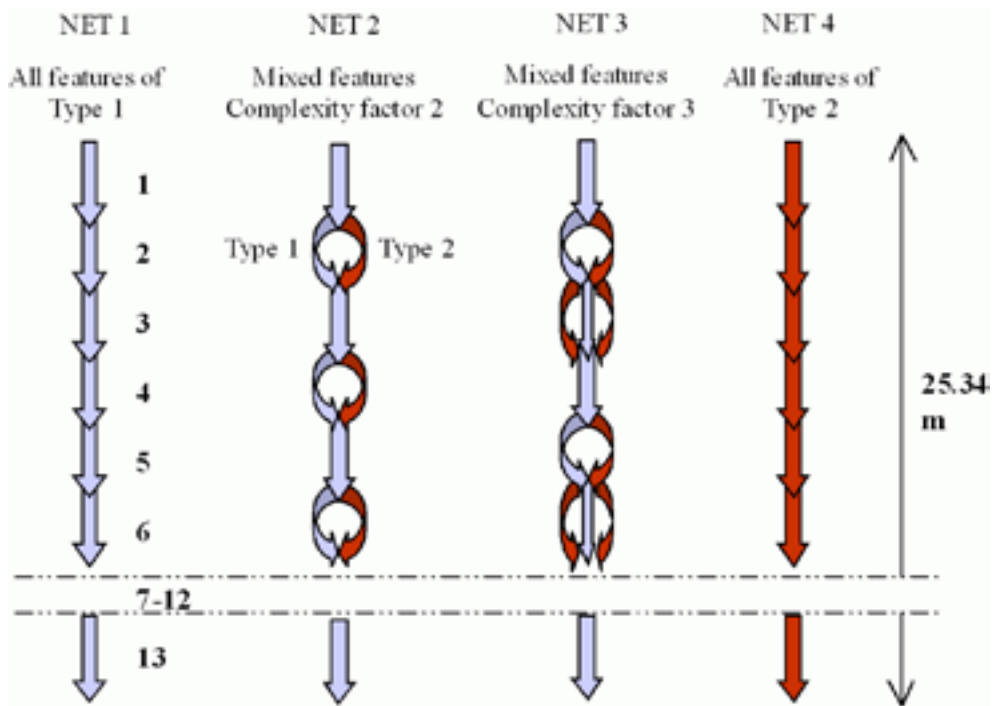


**Figure 3-2.** Schematic view of the four different pipe networks used by the ANDRA-Golder team to represent different complexity factors /Holmén and Forsman 2005a/.

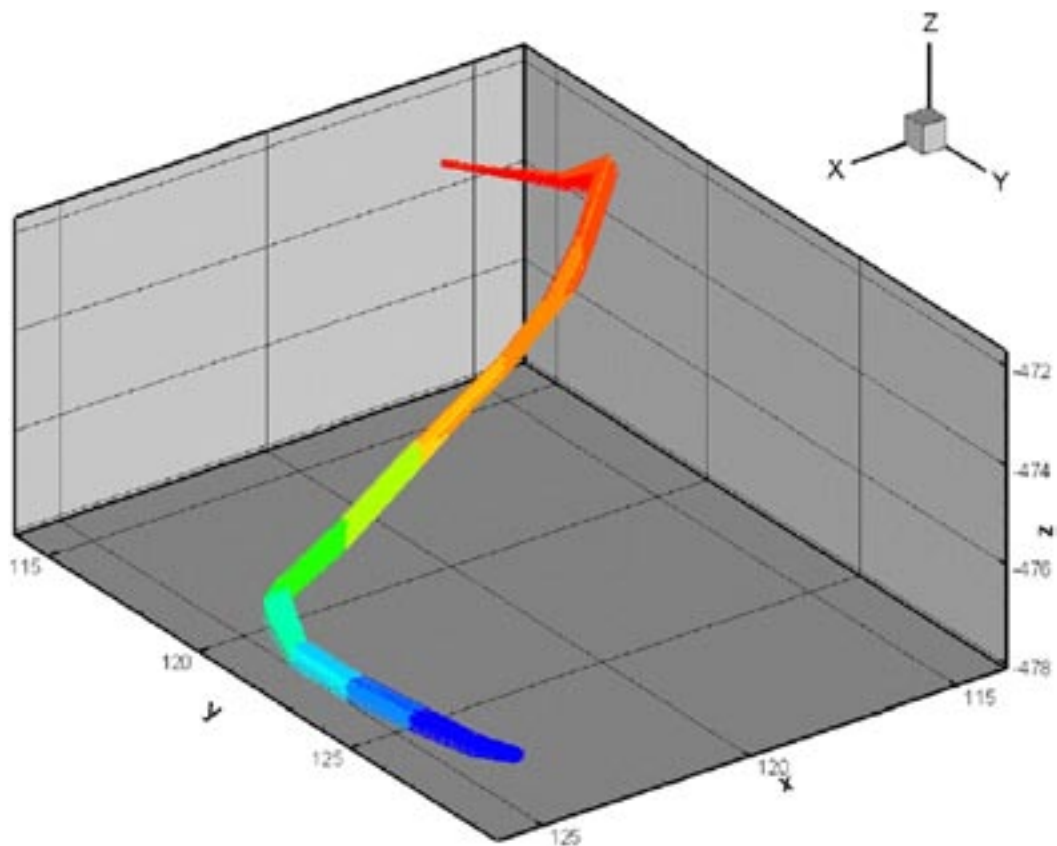


**Figure 3-3.** ANDRA-Golder flow paths from injection well (blue) to extraction well (red). The colour scale corresponds to the breakthrough time at different positions along the plume /Holmén and Forsman 2005a/.

These give values of 70 m<sup>2</sup> and 105 m<sup>2</sup> (and a sensitivity study gave minimum and maximum values of 68 m<sup>2</sup> and 159 m<sup>2</sup>), although it is noted that the concept of flow-wetted surface area is not directly applicable to an equivalent permeable medium.

For the conservative tracer (Re-186) the only parameters that were significantly constrained were the fraction of stagnant zones and the rate at which stagnant and flowing water interact, together with the complexity factor, with pipe networks 3 and 2 (Figure 3-2) strongly favoured. As the flow-wetted surface and  $\beta$ -parameter are correlated to the complexity factor, these were also constrained by the tracer test.

For Ca-47, large constraining power was demonstrated for the sorption coefficients of fault gouge and altered granite. Also, to achieve a good match to the shape of the measured breakthrough curve, it was found necessary to use pipe networks with large complexity factors (networks 3 and 2 in Figure 3-2), and also a dispersivity towards the upper end of the range. The constraining power of the Cs-137 data is highly uncertain because of the low tracer recovery.

### 3.2.2 Task 6E

#### Approach

The continuum flow model was constructed in a similar manner to Task 6D but with the application of the Task 6E boundary conditions. The transport modelling approach used in Task 6E was to construct a large GoldSim pipe network representing the flow routes of contaminated water from the injection section between cells of the continuum model encompassing the flow paths shown in Figure 3-4. The pipes have the following characteristics: connectivity; flow; dilution; length and flow wetted area. In particular, a consistent procedure was used to represent dilution of contaminated water in the pipe network by non-contaminated water from other intersecting pathways. This procedure added water to pipes, starting with those with the shortest breakthrough times, in a way that did not change the length of the flow routes or the breakthrough times inside the pipe network.

The constraining power of the tracer test evaluated in Task 6D was propagated to the Task 6E transport modelling using the constrained coupled parameter distributions /Holmén and Forsman 2005a/.

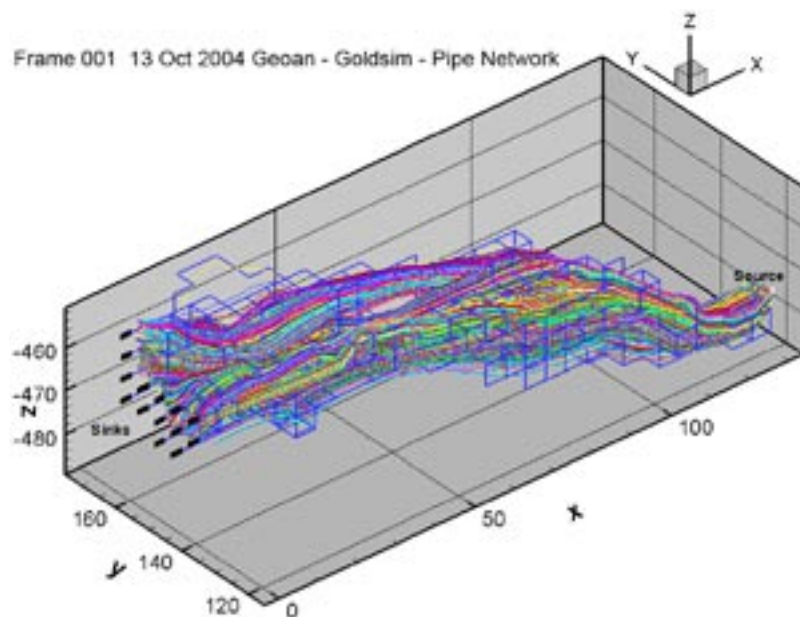


Figure 3-4. ANDRA-Golder Task 6E continuum flow paths and the cells of the pipe network /Holmén and Forsman 2005a/.

## Results and discussion

One thousand realisations of the pipe network were simulated based on the constrained coupled parameter distributions from Task 6D, with a total dilution factor of 10. In addition to the base case, a number of sensitivity studies were carried out to examine: the input parameter distributions; the importance of flow wetted surface compared to water residence time; dilution; and the importance of linking flow wetted surface to flow and dilution. For example the recovery of injected mass with and without dilution for Ca-47 were compared and the arrival times with dilution were found to be approximately 30% of the times without dilution.

### 3.2.3 Task 6F

#### Approach

The same general approach was used for Task 6F /Holmen and Forsman 2005b/ as for Task 6E, although of course the flow regime was much simplified and this allowed the transport to be modelled by a single GoldSim pipe. The constrained coupled parameter distributions were propagated to Task 6F to produce an ensemble of breakthrough curves for each case.

#### Results and discussion

Breakthrough curves were calculated for all specified cases. A typical example, namely for I-129 in feature 1S with a 1-year groundwater travel time (Case B1) is shown in Figure 3-5.

### 3.2.4 Task 6F2

The ANDRA-Golder modelling team did not participate in Task 6F2.

### 3.2.5 Review

The overall probabilistic sensitivity analysis approach allows the Task 6 objective of investigating the constraining power of tracer tests to be analysed comprehensively. /Holmén and Forsman 2005a/ explain this approach carefully and in detail such that it could be understood by a wider audience than the Äspö Task Force.

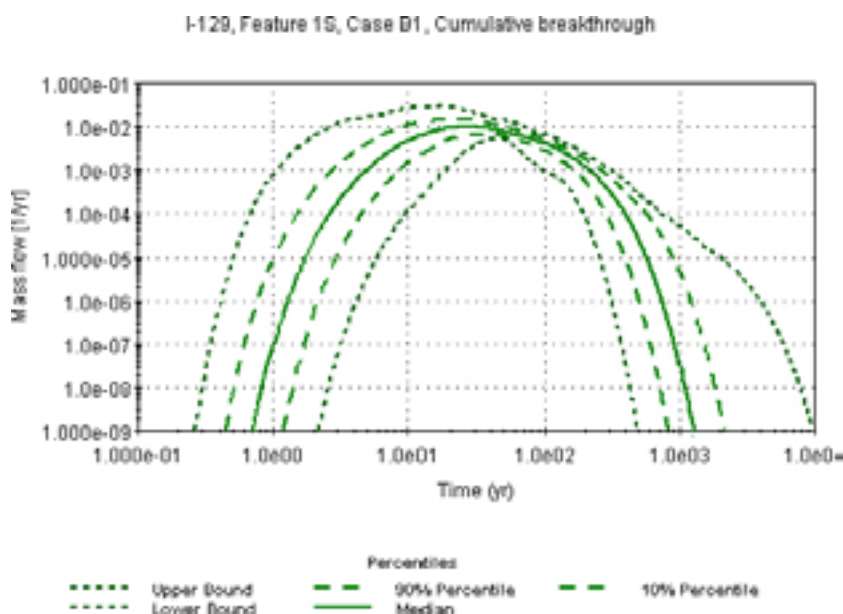


Figure 3-5. ANDRA-Golder breakthrough curves for I-129 in Task 6F Case B1 (Feature 1S, 1 year travel time).

The implementation of the Task 6C flow model in an equivalent permeable medium code with a 2 m discretisation may have resulted in unphysical effects by introducing artificial pathways. An indication of this in Task 6D is that the calculated path length for the C2 tracer test (25.3 m) is significantly closer to the Cartesian distance (17 m) than the two estimated path lengths (66 m and 97 m) through discrete features.

In Task 6D, the implementation of the tracer transport model did not allow for tracer dilution within the vicinity of the sink. However, the authors are to be commended for including dilution in Task 6E. As mentioned elsewhere, the specification of output flux in terms of Bq/hour means that the impact of dilution has not generally been considered in Task 6 analyses.

The degree of complexity of the transport model and fitting procedure used in this work is at the other end of the spectrum from minimalist approach used by the ANDRA-CEA team. Possibly some blending of the approaches, with a more simplified model being used in conjunction with the probabilistic sensitivity analysis technique, could yield useful insights.

For the systems and parameters considered in this study, the implications for the Task 6 objectives 1–4 (Section 1.3) include:

- 1. Assess simplifications for PA:** This was not considered directly, but it is clear that the explicit inclusion of near-fracture diffusive zones such as fault gouge are not required for PA modelling.
- 2. Determine constraining power of tracer and flow tests for PA:** The ANDRA-Golder probabilistic sensitivity analysis approach allows the constraining power of tracer tests to be analysed comprehensively. In particular, for the conservative tracer (Re-186) in Task 6D, the immobile zone parameters and complexity factor were significantly constrained, as were the sorption coefficients of the fault gouge and altered granite for the weakly sorbing tracer (Ca-47). However, with the possible exception of the complexity factor, these parameters are not particularly important for PA.
- 3. Support design of SC programmes for PA:** It is interesting that the complexity factor was constrained by conservative and weakly sorbing tracer tests, but it is not clear that this is of relevance to PA.
- 4. Improve understanding using SC models:** The implementation of the Type 1 and Type 2 features can be considered to be at the level of detail required by site characterisation modelling. However, the pipe flow modelling is more of a simplified PA approach, for example it does not account for channelling within fracture planes or tracer dilution at the sink. Thus overall, the ANDRA-Golder model is not particularly useful for understanding at the SC level of complexity.

### 3.3 CRIEPI

The following summary and review is based on presentations at the 17<sup>th</sup>, 19<sup>th</sup> and 20<sup>th</sup> Task Force meetings /Tanaka 2003, 2004, 2005/. The CRIEPI team applied the finite-element code FEGM to Tasks 6D, 6E and 6F.

#### 3.3.1 Task 6D

##### *Approach*

Groundwater flow in the 200-m rock block was modelled by including the 100-m scale structures explicitly as plane elements in the finite-element model, with the background fractures represented by an equivalent porous medium with a hydraulic conductivity of  $1 \cdot 10^{-9}$  m/s derived from a smeared fracture approach. Flow velocities calculated for structures 20D, 21D, 22D and 23D were used in a transport model that contained these structures and a single immobile

zone for which equivalent transport parameters were derived. Flowing porosity values were calibrated to the conservative tracer breakthrough curve for the C2 tracer test resulting in a value about four times smaller than given in the Task 6C report.

### **Results and discussion**

The results of the CRIEPI team are shown in Figure 3-6. It is seen that the calculated breakthrough time for Ca was somewhat larger than the measured value, but for Cs it was significantly larger demonstrating that retention was overestimated by the model.

### **3.3.2 Task 6E**

#### **Approach**

Based on a preliminary sensitivity analysis, /Tanaka 2004/ selected 42 structures out of the 100-m scale structures and background fractures (Figure 3-7) that have the most influence on groundwater flow for the Task 6E boundary conditions. Advection and dispersion in these structures were modelled using 2D finite elements, and matrix diffusion and sorption were included using 1D elements perpendicular to the structure planes.

### **Results and discussion**

Breakthrough curves were calculated using the Task 6C GST assignments (Model A) and also using a model (Model B) in which diffusion and sorption adjacent to structures 20D, 21D and 17S was modelled as a single immobile zone with effective parameters.

### **3.3.3 Task 6F**

#### **Approach**

Task 6F was modelled by the CRIEPI team using a finite-element grid for a uniform fracture surrounded by 8 m of immobile zones on either side of the structure /Tanaka 2005/. Longitudinal and transverse dispersion were included in the transport model.

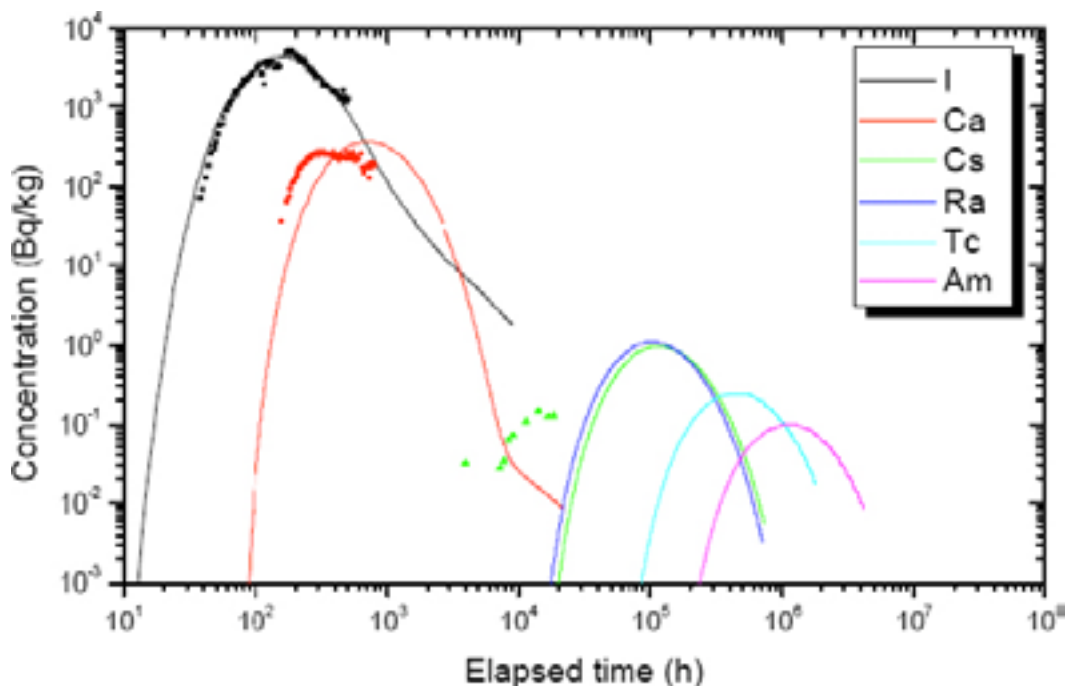


*Figure 3-6. CRIEPI breakthrough curves for Task 6D compared to tracer test results /Tanaka 2003/.*



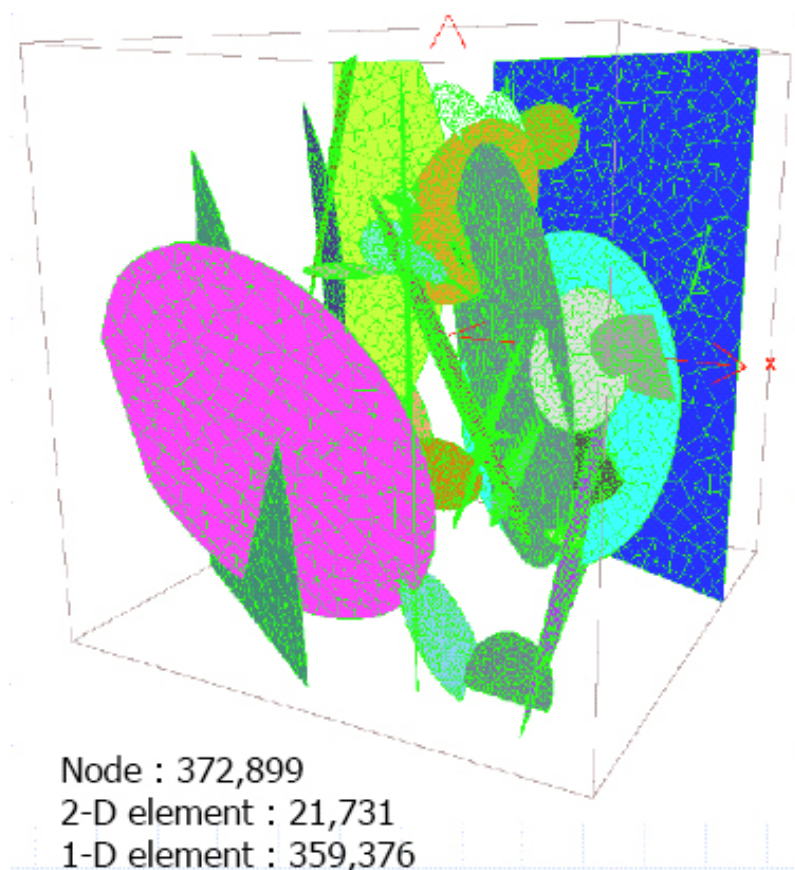


*Figure 3-7. Finite-element mesh for the 42 structures modelled by CRIEPI for Task 6E /Tanaka 2004/.*

### **Results and discussion**

Figure 3-8 shows the results for I-129 transport in Case C1 (10 year travel time, structure 1S), showing both the lateral dispersion in the structure and diffusion into the surrounding rock. In the calculations, an earlier version of the Task 6F specification was used in which the recovery section was 20 m wide, and thus full recovery was not obtained because of transverse dispersion outside this section.

A sensitivity case was evaluated in which matrix diffusion and sorption on the fracture coating was modelled as surface sorption. This did not affect the peak of the breakthrough curve or mass recovery even for the shortest travel time.

#### **3.3.4 Task 6F2**

The CRIEPI team did not participate in Task 6F2.

#### **3.3.5 Review**

The finite-element approach used by the CRIEPI team was able to capture all the essential features of Tasks 6D, 6E and 6F. There are many parallels with the ANDRA-CEA approach, for example the demonstration that a drastically reduced set of structures is able to account for flow with the Task 6E boundary conditions, and the direct solution of the advection-dispersion-diffusion equation. This latter aspect provides a useful complement to the majority of teams who employed a two-step approach based on one-dimensional flow paths determined using particle tracking.

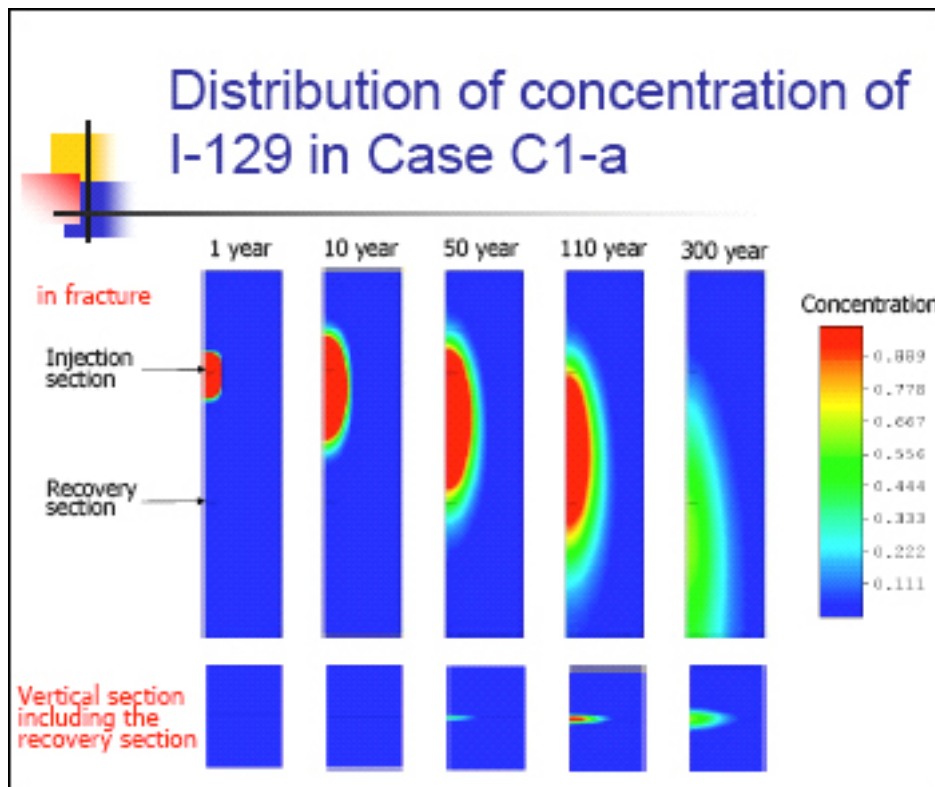


*Figure 3-8. I-129 concentrations in the structure and matrix for Task 6F Case C1 /Tanaka 2005/.*

The CRIEPI team carried out an interesting finite-element analysis of Task 6F. The system was discretised both within the fracture and in the adjacent rock. Because of this they were able to calculate two-dimensional matrix diffusion from a channel, which could have an impact on PA timescales, as discussed in relation to Task 6B2 by /Dershowitz et al. 2004/.

For the systems and parameters considered in this study, the implications for the Task 6 objectives 1–4 (Section 1.3) include:

- 1. Assess simplifications for PA:** It was demonstrated that a single immobile zone with effective parameters is able to provide an accurate representation of Type 1 and Type 2 structures. Also, it was demonstrated that depending on the boundary conditions, only a small fraction of features may contribute to flow and transport.
- 2. Determine constraining power of tracer and flow tests for PA:** Not considered in this work.
- 3. Support design of SC programmes for PA:** Not considered in this work.
- 4. Improve understanding using SC models:** Finite-element approaches have the potential to include the geometrical complexity of immobile zones and intra-structure flows, if such information were to become available.

### 3.4 JAEA-Golder

The JAEA-Golder team /Dershowitz et al. 2006/ carried out all the simulations using channel network (CN) discretisations of the reference 200 m scale discrete fracture network (DFN) model with complexity factors of unity except in some sensitivity cases. A forward modelling strategy was adopted for all tasks. The channel networks were developed using rectangular cross-section pipe elements to connect fracture intersections on fracture planes. Each pipe



element was assigned transport and immobile zone properties corresponding to the Task 6C hydrostructural and microstructural models.

Transport was simulated through the fracture network using the Laplace Transform Galerkin method using the PAWorks/LTG code /Dershowitz et al. 1999/. The processes considered were advection, longitudinal dispersion, diffusion into immobile zones, and equilibrium sorption in immobile zones and the fracture coating.

The pore space included immobile zones for gouge, fracture coating, cataclasite, altered rock and intact rock in parallel, whereas the task specifications assume that only the gouge and fracture coating are in parallel with the remaining zones in series. Thus in the JAEA-Golder simulations diffusion takes place simultaneously into the various immobile zones directly from the channel surface area, thereby potentially overestimating diffusive retention.

The objectives of the JAEA-Golder team were as follows:

- Identify the key assumptions and the less important assumptions for long-term PA modelling.
- Identify the most significant PA model components of the site.
- Prioritize assumptions in PA modelling and demonstrate a rationale for simplifications in PA-models by parallel application of several PA models of varying degrees of simplification.
- Provide a benchmark for comparison of PA and SC models in terms of PA measures for radionuclide transport at PA temporal and spatial scales.
- Establish how to transfer SC models using site characterization data to PA models, i.e., how to simplify SC models into PA models in a consistent manner.

### **3.4.1 Task 6D**

#### ***Approach***

The goal of the JAEA-Golder team in Task 6D was not to determine the single “correct” set of transport pathway properties for the fracture network, but rather to study the relative significance of each of the transport assumptions provided in the hydrostructural model. The strategy used for Task 6D was thus one of forward modelling using the Task 6C hydrostructural model, followed by an analysis of how the results matched in situ observations. This was thus not a calibration exercise but rather a test of how consistent the Task 6C hydrostructural model is with the tracer test measurements.

The JAEA-Golder team implemented the deterministic and synthetic structures in the Task 6C hydrostructural model as specified (Figure 3-9). Given the time scale of interest, the immobile zone for intact rock was not included in the Task 6D simulations.

#### ***Results and discussion***

The breakthrough curves for the base case are shown in Figure 3-10, where they are compared to the measured tracer test data. While the calculated curves are somewhat more retarded than the experimental results, the forward modelling results are nevertheless a reasonably good match indicating the importance of the hydrostructural data. A contributory factor to the over-retarded predictions is likely to be the treatment of immobile zone diffusion as being in parallel rather than in series.

A series of sensitivity studies were carried out to consider different possible implementations of the structure type and complexity factor, and the importance of the background fractures.

Structure type is significant on the experimental timescale because of the importance of immobile zones with the highest porosity and  $K_d$  (fault gouge and cataclasite), which only occur for Type 1 structures. Sensitivity studies were carried out by converting all fractures to either Type 1 or Type 2. The Type 2 case reduces tracer retention and thereby improves the comparison with experimental data.

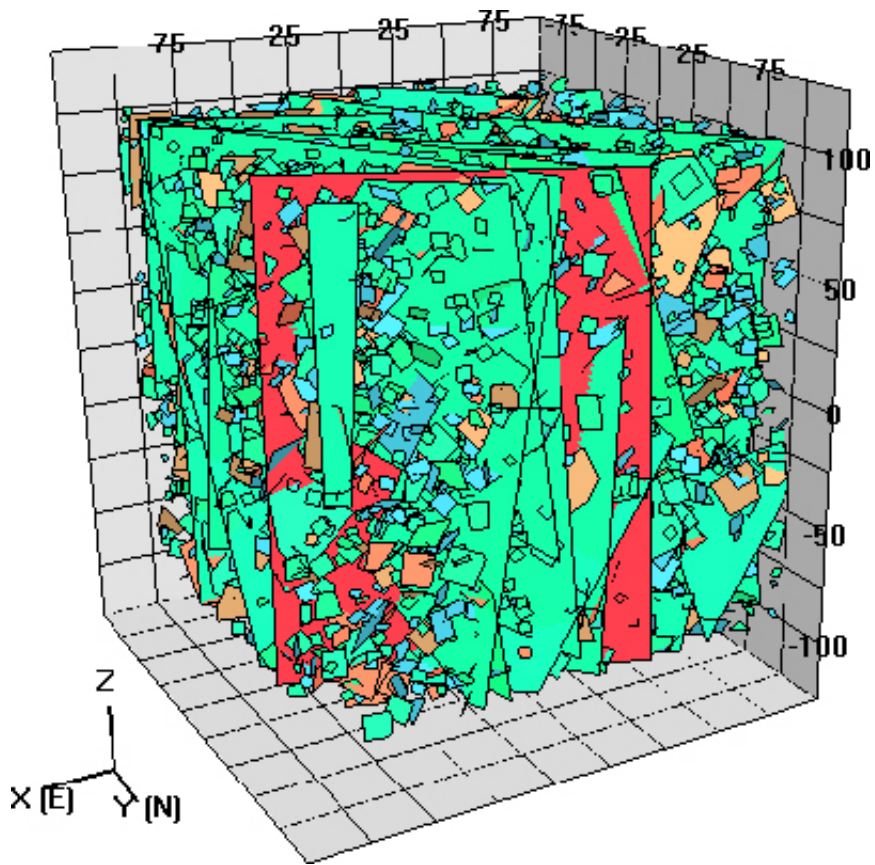


Figure 3-9. Deterministic and background fractures in the 200 m block scale model from the Task 6C report /Dershowitz et al. 2003/.

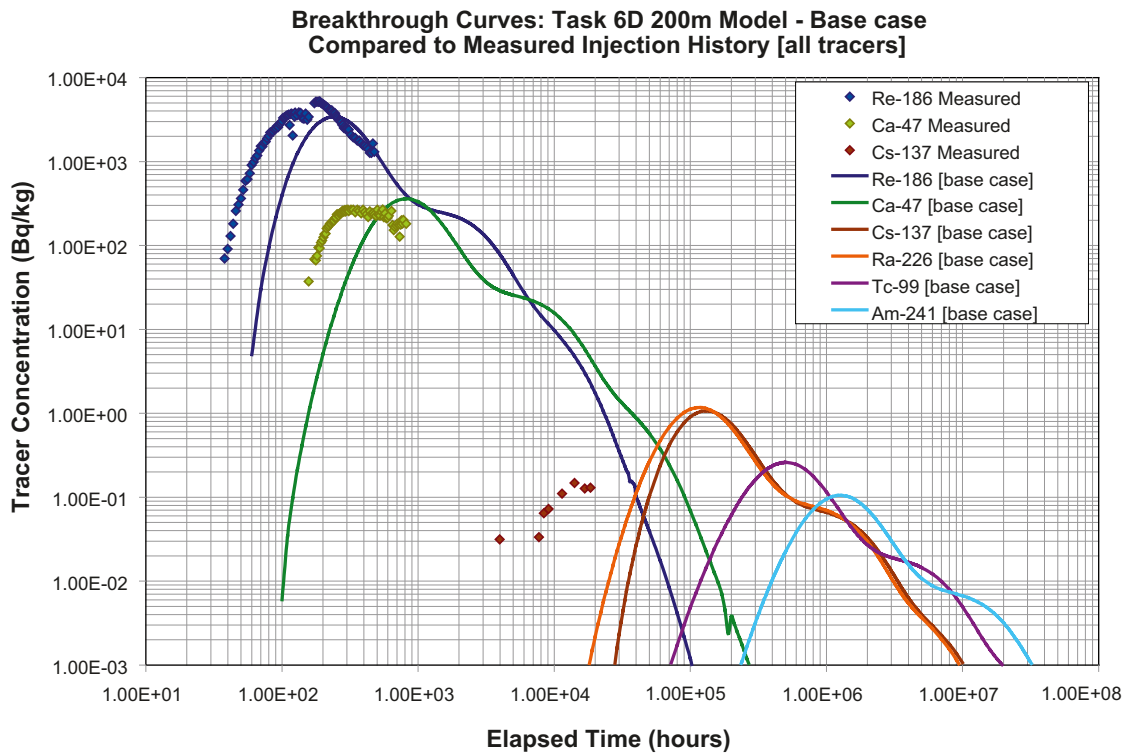


Figure 3-10. JAEA-Golder base case breakthrough curves for Task 6D /Dershowitz et al. 2006/.

The base case simulations were run with all structures having a complexity factor of 1, implying that they just consist of a single fracture. Sensitivity studies were performed in which the reactive surface area was increased in proportion to the number of fractures for all structures being complexity factor 2, or to the complexity factors specified in the Task 6C report. Complexity was introduced by increasing the effective channel surface area in the transport calculations. The results show significantly increased retention, which makes the match to the C2 tracer test results less good.

A sensitivity case in which the distributions of the background fracture intensity, orientation and size were changed indicated that tracer breakthrough was not as dependent on these parameters as for the structure type and complexity factor.

### **3.4.2 Task 6E**

The goals of the JAEA-Golder modelling team in the Task 6E effort were two-fold /Dershowitz et al. 2006/. The first was to implement lessons learned from Task 6D to improve the level of detail of pore spaces and fracture complexity in the DFN/CN models. The second goal was to gauge the sensitivity of the immobile zone concept to various changes in material and network properties.

#### ***Approach***

The Task 6E model implementation was essentially the same as for Task 6D, with the exception of the revised long-term boundary conditions, inclusion of intact rock in the microstructural model and the use of a graph theory approach rather than particle tracking for determining flow pathways. /Dershowitz et al. 2006/ moved the tracer source section slightly laterally from the coordinates specified by /Elert and Selroos 2004b/ in order to penetrate structure 23D fully.

#### ***Results and discussion***

Calculated values of  $\beta$  generally match those produced by other modelling teams. However, the JAEA-Golder model did produce flow pathways that were generally longer and slower than the other modelling teams. This is most likely due to model assumptions as to how pipe flow and transport widths are calculated from the base DFN model.

Particle tracking results suggest general transport pathway lengths in the range of 300 to 500 meters. This suggests that the channel network possesses significant totuosity, as the Cartesian distance between the source borehole and the model boundary is approximately 270 meters. The JAEA-Golder models suggest an approximate power-law relationship between travel time and  $\beta$ .

As part of a limited sensitivity analysis, it was found that feature complexity had a significant impact on breakthrough times, especially when the complexity factors of the background fractures were increased, due to the large increase in surface area available for sorption.

The sensitivity to pipe geometry generation parameters was also examined, with the only significant parameter being fracture aperture.

### **3.4.3 Task 6F**

The goal of the JAEA-Golder team for Task 6F was to facilitate inter-comparison between the transport models used by the different Task Force modelling groups.

#### ***Approach***

The target Task 6F structures, 1S (Type I) and 4S (Type II), are both stochastic 500 m scale structures of the Task 6C model. The basis of Task 6F is to limit tracer transport to within a

single structure. However, this is incompatible with the JAEA-Golder channel network approach, where a network of background fractures is required in order to produce fracture intersection traces that are connected by pipe elements to give rise to connectivity within the plane of the structure.

Consequently, the Task 6F model specification was adapted slightly. Specifically, the JAEA-Golder team used both the 200 m scale background fracture network and the deterministic structure network in the Task 6C report /Dershowitz et al. 2003/, to design a local-scale DFN around each targeted structure. For example, the resulting DFN model for structure 1S is shown in Figure 3-11. As with Tasks 6D and 6E, this DFN was converted into a CN using the PAWorks ‘No Crossing Pipes’ algorithm with pipe width assigned based on the projected trace length of the intersecting fractures. The internal nodes of the resulting CN model for structure 1S is shown in Figure 3-12.

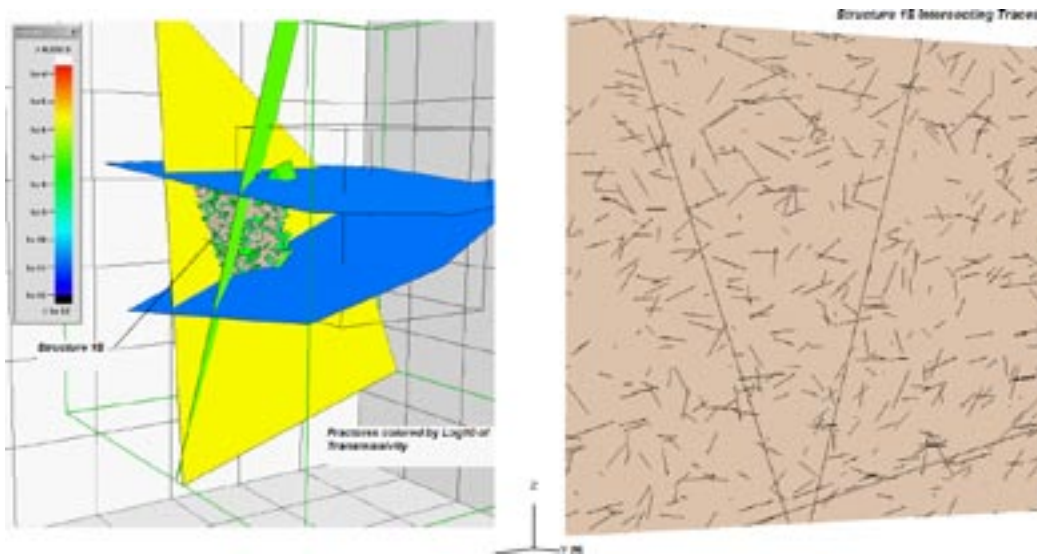


**Figure 3-11.** Task 6F Structure 1S DFN model. The figure on the right shows the fracture trace intersections with Structure 1S. Note the two long traces that cut across the entire fractures; these represent the intersection of major TRUE Block Scale deterministic structures /Dershowitz et al. 2006/.

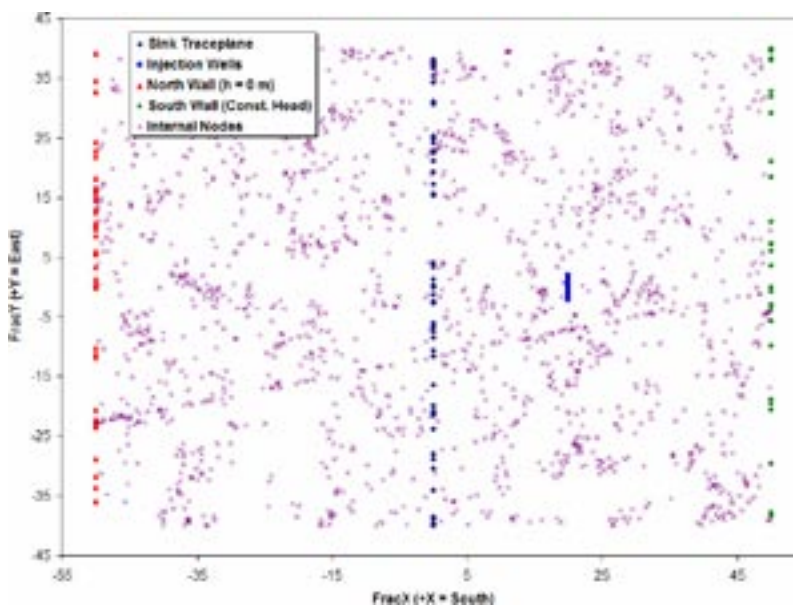


**Figure 3-12.** View of Task 6F CN model of Structure 1S. This view is looking down the +Z axis at the plane of the fracture. ‘X’s mark the locations of model nodes /Dershowitz et al. 2006/.

### 3.4.4 Task 6F2

For the Task 6F2 sensitivity studies, the JAEA-Golder team elected to study the effect of channel network geometry on the flow and transport results, specifically focussing on the discretisation of the three-dimensional discrete fracture network into a one-dimensional network of nodes and pipes.

#### **Approach**

The JAEA-Golder team addressed two specific questions in Task 6F2:

- For performance-assessment timescales, does the form and degree of the channel network discretisation affect the final flow and transport predictions?
- To what extent do factors such as node density and intersecting ('crossing') pipes affect retention in a feature of relatively limited complexity (such as Structures 1S and 4S)?

These questions were addressed through re-discretisations of the Task 6F CN models with re-runs of both the flow and transport models.

CN pipes cannot cross each other: the pipes on a given structure (such as 1S and 4S) are created so that pipes do not cross. This, in theory, should prevent the simulation of additional retention in 'intersection zones' within the plane of the test fracture. For the sensitivity study, the following options for discretising the CN pipe mesh for structure 1S were examined:

- All Pipes: This is the simplest method of pipe generation. Pipes connect every node (which is placed at the intersection of two fractures) to every other node. In addition, nodes are added where two pipes intersect. There are no geometric restrictions.
- Pipes cannot cross: A new pipe may not cut across an existing pipe. This has been the standard for all Task 6 channel networks.
- Pipes cannot cross fracture traces: Pipes may not cut across existing pipes, nor can they cut across fracture traces. This option also enforces the additional restriction that each node must have at least one pipe connected to it.
- All pipes on a given fracture must be connected: This option will generate additional nodes and pipes so that all pipes on a single fracture are connected to each other.
- Include effective pipes: This is the same as the above option, except that effective pipes are generated as per a user-specified threshold.

#### **Results and discussion**

The different pipe discretisation options had little effect on the number of nodes in the resulting 1D pipe mesh, but the number of pipes varied from about 4,000 to about 90,000. In comparison with the default 'No Crossing Pipes' option (Figure 3-13), significant dispersion of particles along the plane of structure 1S was noted for model iterations using the 'All Pipes' option as illustrated in Figure 3-14. The dense network of pipes on a Type I (fault) geologic structure produced by using the 'All Pipes' option was unsuitable for performance-assessment modelling using the current Task 6C microstructural model, as retention was drastically over-predicted such that no tracer was ever detected crossing the channel network.

/Dershowitz et al. 2006/ consider the overall conclusions of Tasks 6F and 6F2 to be:

- While solute transport in fracture networks tends to be dominated by the pattern of fracture connectivity within the network, transport in single fractures depends on the discretisation of the fracture into channels.
- The discretisation algorithms studied in Task 6F2 had a greater effect on pathway statistics than on the actual tracer transport results.



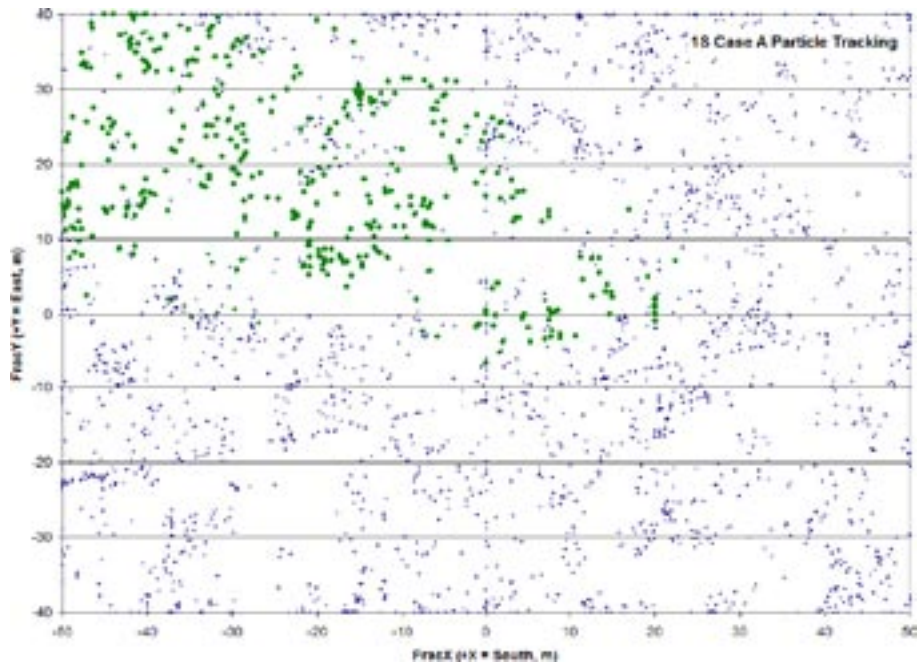


**Figure 3-13.** Particle tracking results for Case A1 in structure 1S /Dershowitz et al. 2006/.

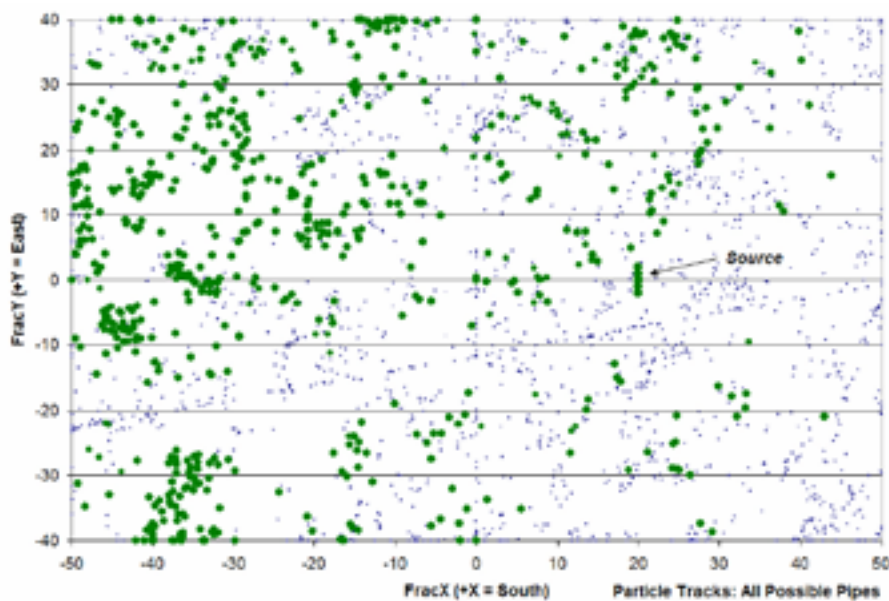


**Figure 3-14.** Pathways identified through particle tracking through structure 1S using the 'All Pipes' option /Dershowitz et al. 2006/.

- The PAWorks channel network modelling approach is optimised for evaluation of transport in complex networks, rather than for focusing on transport in single fractures as in Task 6F and 6F2. The plate element solute transport modelling used by the JAEA-Golder team for Task 6B2 and similar approaches are more suited to this application.
- Water residence time distributions for the three gradients considered in Task 6F are similar, with simple scaling by gradient.
- Sorbing solute transport behaviour, as indicated by the tau (travel time)-beta relationship, and the beta distribution are also similar between the three cases. Breakthrough curves for strongly sorbing tracers, however, do show increased retention for the slower flow rates.



### 3.4.5 Review

#### **Tasks 6D and 6E**

The DFN/CN calculations of the JAEA-Golder team for Tasks 6D and 6E provide a comprehensive study of these cases. The development of a channel network from the DFN is both computationally efficient and based on qualitative information about channelling in fracture planes. However, as revealed by the Task 6F2 study, there are some ambiguities in the way that a CN model is developed. Further information about channelling would be most welcome in this regard, especially related to fracture width, which strongly influences the degree of interaction between flowing pathways and retention by immobile zones.

The implementation of the specified microstructural model as a set of diffusive processes in parallel rather than primarily in series may over-estimate retardation. Nevertheless, the match between calculations and experiment were reasonable given that no parameters were calibrated.

It is clear that for the current purpose a discrete fracture representation is more accurate than permeable medium or PA approaches. The results are sensitive to the details of near-fracture immobile zones, and if a fundamental understanding of tracer transport experiments is required then further research should be focussed on their characteristics. However, for PA timescales, the details of near-fracture retardation are not important as retardation is dominated by diffusion into the intact rock.

It is interesting to note the JAEA-Golder conclusion that fracture geometry (orientation, size, intensity) does not have a primary influence on solute transport at site characterization and PA time scales, provided connected transport pathways exist. It follows that a key focus for future site characterisation studies should be the connectivity of fracture systems.

The complexity factor was treated in the sensitivity analyses by scaling the fracture surface area used in the transport calculations in proportion to the number of sub-parallel fractures. This was found to overestimate solute retention. The reason for this could be that the sub-fractures have unequal transmissivities in which case the highest flux pathway dominates transport, for example as demonstrated by /Poteri 2006/ and discussed in Section 3.5.4. Thus it may be correct to assume a complexity factor of 1 for complex structures, as was assumed by the JAEA-Golder team for their base cases.

#### **Tasks 6F and 6F2**

The JAEA-Golder team are to be congratulated for their heroic efforts in pursuing their channel network approach consistently to model the two stochastic 500 m scale structures from the Task 6C model. This was a very interesting exercise that brought a new perspective to the supposedly simple specifications for Tasks 6F and 6F2. The underlying concept that flow in these structures is channelled appears to be correct, based on available evidence, and the pathways (e.g. Figure 3-13 and 3-14) look more physically plausible than the homogeneous pathways in the task specification.

This work has indicated some limitations in the PAWorks tool when applied to a single structure, even though it incorporates a wide range of options for generating channel paths (pipes) from nodes. There is clearly some ambiguity as to which is the most appropriate algorithm. Further pipe generation algorithms should be considered, possibly including fracture intersection traces as pipes and possibly imposing a channel grid whose spacing takes account of whatever information on channelling is available.

For the systems and parameters considered in this study, the implications for the Task 6 objectives 1–4 (Section 1.3) include:

- 1. Assess simplifications for PA:** The details of the high diffusivity and porosity near-fracture immobile zones are not important for PA timescales, where diffusion and sorption into intact rock dominates retention. With the inexorable rise in the power of computers and the usability of simulation software, the types of tools used by the JAEA-Golder team are likely to be used for PA studies in the future.

2. **Determine constraining power of tracer and flow tests for PA:** Tracer tests do not constrain the diffusive and sorptive retardation of relevance to PA timescales. However, conservative tracers are the primary means of constraining the fracture transport porosity, and equivalent parameters.
3. **Support design of SC programmes for PA:** The JAEA-Golder DFN/CN flow and transport approach, coupled with the Task 6C hydrostructural model, represent a comprehensive SC model for the Äspö TRUE Block Scale site. Together they provide a useful set of tools for supporting the design of SC programmes of relevance to PA. Hopefully, they will continue to do so beyond Task 6.
4. **Improve understanding using SC models:** The JAEA-Golder DFN sensitivity studies provided useful insight into the behaviour of the system, and it would be worthwhile to extend these, including varying parameters of the Task 6C model, in order to ensure that the fullest understanding is gained.

## 3.5 Posiva-VTT

The Posiva modelling team from VTT Processes implemented the tasks exactly as specified with the exception that all features were assumed to have a complexity factor of 1 /Poteri 2006/. Tasks 6D, 6E, 6F and 6F2 were all modelled using the same approach, although the parameterisation differed between sub-tasks.

### 3.5.1 Task 6D

#### *Approach*

Most of the Task 6 objectives cannot be answered without both SC and PA modelling. In view of this, the following specific objectives were adopted for Task 6D.

- To test the linkage between the 3D DFN flow solution and the corresponding 1D transport of the tracers, separate models are used for the flow and transport modelling so that the hydrological control of the transport and retention provided by the flow model is passed to corresponding 1D transport paths.
- To try to apply a detailed micro-structural model of the immobile pore space to the transport problem. This objective aims to consider the scaling between the experimental and PA timescales.

The definition of the immobile pore spaces in the Task 6C model is asymmetric. The fracture coating and gouge exists only on one side of the fracture walls. Posiva-VTT modelled this by an equivalent system consisting of two successive but symmetric layers.

The flow equation was solved using the Galerkin finite-element method implemented in the code FEFTRA /VTT 2004/. All structures were modelled as two-dimensional features by two-dimensional linear and triangular elements.

The transport model included advection along the fractures, matrix diffusion and sorption in the immobile pore space. Surface sorption on the fracture walls was not modelled but the diffusion into the pore space of the fracture coating and sorption in the pore space of the coating was modelled directly.

Transport from source to the sink was described by a set of transport paths that were determined using particle tracking. Dispersion was not explicitly included, but was included implicitly through the different water transit times along the different transport paths.

Rather than model the immobile pore spaces as parallel layers, they were conceptualised as an equivalent succession of independent 1D legs, with equivalent properties, along the flow path. This is justified by the fact that the true pore structure is unknown and that the assumption of independent pores is reasonable.

With this assumption, tracer transport along a flow path can be calculated with an analytical model using a one-dimensional lattice walk where the interaction of the solute between the mobile and immobile pore spaces is described by the waiting time distribution /Cvetkovic and Haggerty 2002/. However, in the Posiva-VTT approach the waiting time distribution was calculated directly in the time domain rather than the Laplace-domain used by /Cvetkovic and Haggerty 2002/. Numerical calculations were carried out using Matlab.

Transport modelling was divided into two parts. First, the advective part of the transport and the hydrological control of the retention ( $\beta$ ) were calculated using the flow model. Results of this phase were the geometrical and transport properties of the flow paths and advective transit times for the different flow paths. The second phase of the modelling involved calculating the retention for the different flow paths and tracers. Finally, the advective delay and retention along transport paths were added together, and the results of all transport paths were combined to get the breakthrough curve at the pumping borehole for a Dirac pulse injection. The tracer breakthrough curves for the measured injection function were calculated by convoluting the breakthrough curves of the Dirac pulse injection with the measured injection curves.

The model was not calibrated against the tracer data because it was considered that the Task 6 objectives could best be met by using the same “true” model for SC (Task 6D) and PA (Task 6E) calculations.

### **Results and Discussion**

Tracking of 1,000 particles indicated five distinct pathways from the source located in structure 23D to the sink located in 21D as indicated in Table 3-2 and Figure 3-15. Most of the flow routes pass through the background fracture 1925B, with a smaller number through structure 20D.

Groundwater transit times vary from 110 to 180 hours and the corresponding lengths of the flow paths vary between about 59 m and 74 m. The  $\beta$ -factors for the five major pathways are illustrated in Figure 3-16. The solid lines show the cumulative  $\beta$  as a function of the length of the flow path. The structures are illustrated by coloured circles. From the slopes of the curves it can be concluded that strong retention (low flow rate along the flow path) takes place in structures 22D, 758C and 2403C. At the end of the flow paths in structures 20D and 21D the flow rates along the flow paths are rather large and consequently  $\beta$  is low. It is noted that the  $\beta$  associated with the only Type 1 feature (20D) is quite small indicating relatively small overall retention.

**Table 3-2. Flow paths at structure level found by particle tracking using 1,000 particles /Poteri 2006/.**

	Number of particles	Flow routes at structure level
Route 1	74	23D → 22D → 20D → 21D
Route 2	4	23D → 22D → 20D → 2403C → 21D
Route 3	100	23D → 1925B → 21D
Route 4	688	23D → 1925B → 21D → 20D → 21D
Route 5	134	23D → 1925B → 756C → 20D → 21D

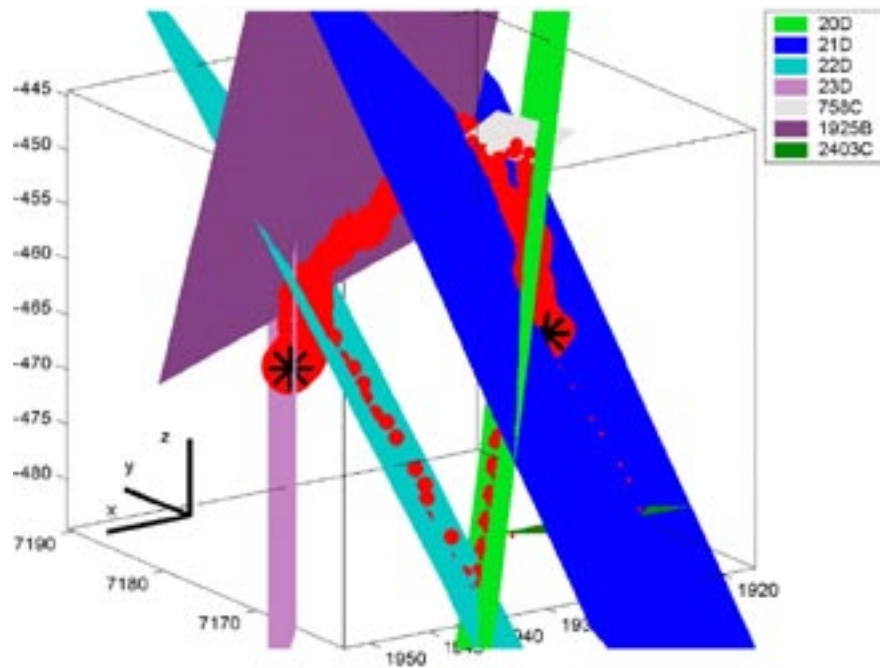


**Figure 3-15.** Flow paths from the source to the sink for the Posiva-VTT model of the C2 tracer test. The size of the red dot refers to the number of the particles that follow the route. The legend of the figure gives the colour coding of the structure numbers. The source and sink are indicated by black asterisks /Poteri 2006/.

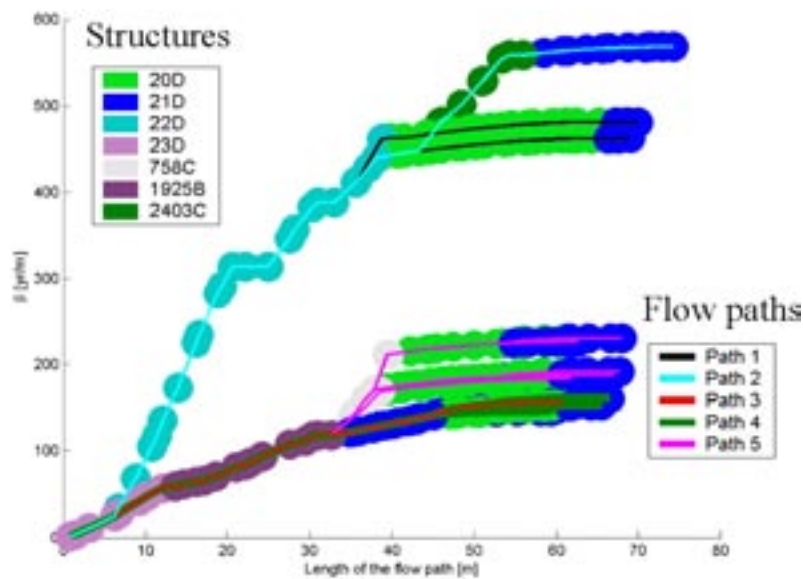


**Figure 3-16.** Hydrological control of the retention ( $\beta$ ) as a function of the path length along the flow routes. Solid lines indicate  $\beta$ , and the coloured circles behind them indicate the structures. Note, that the background circles showing the structures are only indicative. The major flow path (path number 4, green) is plotted thicker than the others /Poteri 2006/.

The Posiva-VTT modelling approach makes it possible to examine the contribution of the different geological materials to the retention and breakthrough curves. The final breakthrough curve is a convolution between the sequences of the transport pipes that represent the contributions of the different geological materials. These contributions are shown in Figure 3-17 for the non-sorbing tracer Iodine for the most dominant transport path. The fracture coating causes about half of the peak retention time. Fault gouge potentially has an important role although it exists only in the Type 1 features that only constitute about 1/10 of the total transport path.

This analysis indicates implicitly that on experimental time scales tracer breakthrough may be dominated by small amounts of materials with high porosity and diffusivity, and thus the results are very sensitive to the quantities of such materials. In particular, the fracture coating becomes saturated on the tracer test timescale and can be modelled by a simple retardation factor.

### 3.5.2 Task 6E

#### Approach

As with Task 6D, /Poteri 2006/ implemented the specification as closely as possible. In particular the model was not calibrated to the C2 tracer test. A hundred flow paths were generated, starting at random locations along the line source, and were found to go mainly through seven different structures: 23D, 1925B, 20D, 21D, 22D, 17S and 2292B.

#### Results and Discussion

It was found that  $\beta$  does not increase much after the first sampling plane, indicating that those flow paths have reached highly conducting hydraulic structures where flow rates are large and  $\beta$  is correspondingly small. The same behaviour is also apparent in Figure 3-18, where  $\beta$  is plotted as a function of flow path length, which shows that  $\beta$  tends asymptotically to a plateau. This arises because once flow paths reach well-conducting structures they tend to remain within a network of similar structures.

This general result implies that, for fracture systems with similar characteristics to the Task 6C model, the major retention takes place at the beginning of flow paths. For Task 6E it has the consequence that there is only a minor change in the peak levels of the breakthrough curves between the second and third control planes, but major changes between the first and second control planes.

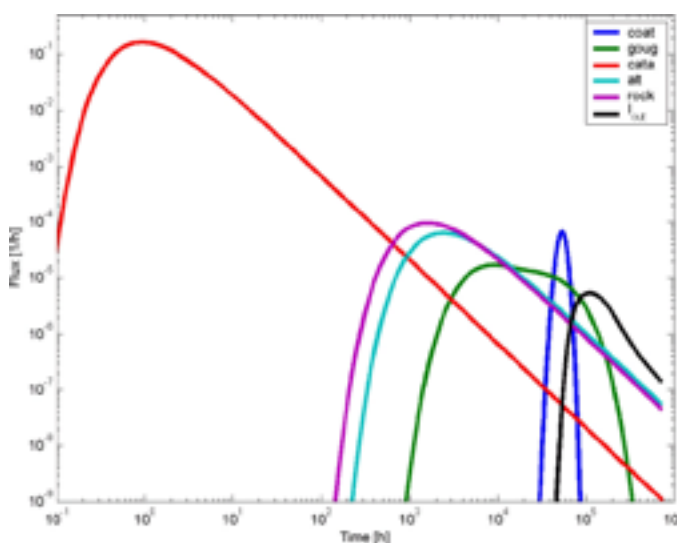


**Figure 3-17.** Breakthrough curves of the individual geological materials for Iodine through the most contributing transport path. These breakthrough curves include only the retention caused by the sorption and matrix diffusion (no advective delay). The final breakthrough curve (black line) is a convolution between the contributions of individual geological materials /Poteri 2006/.

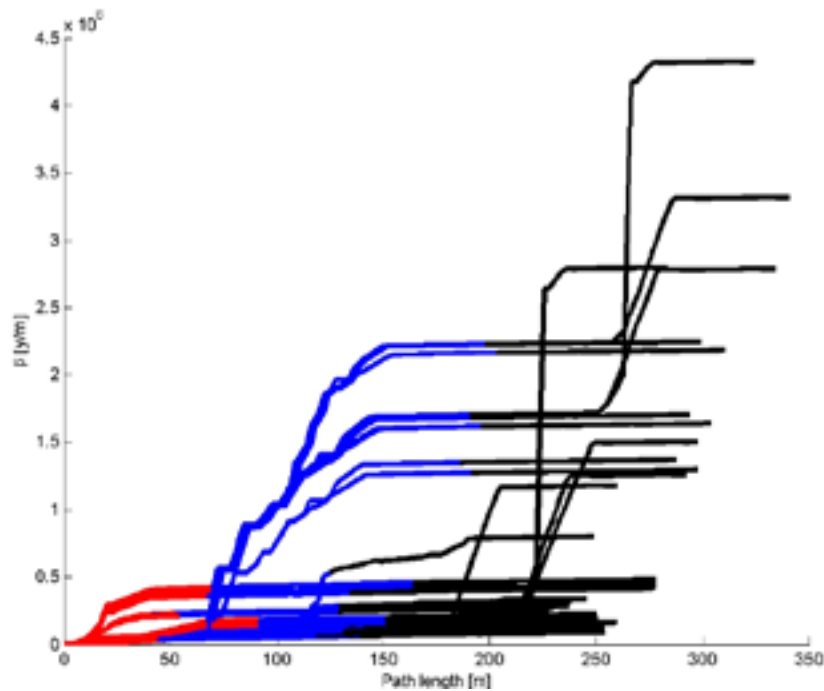


**Figure 3-18.** Accumulation of the  $\beta$  along the flow paths as a function of the path length. Red colour indicate flow paths from the source to the first sampling plane at easting=1920, red and blue colour indicate flow paths from the source to the second sampling plane at easting=1880 /Poteri 2006/.

### 3.5.3 Task 6F

#### Approach

Task 6F used the same modelling strategy as Tasks 6D and 6E although the flow paths for the Type 1 and Type 2 features in this case are very simple and given in the task specification.

#### Results and Discussion

The calculations performed for the three different flow rates clearly exemplifies the relationship between in situ tracer tests and transport on PA timescales. For short water residence times, tracers only interact with near-fracture pore spaces, while for slow flows the matrix rock dominates retention and it is therefore easier to quantify.

### 3.5.4 Task 6F2

#### Approach

The flow system investigated in Task 6F2 consisted of a Type 1 and a Type 2 fracture in parallel (Figure 3-19). The ratio of the total flow between these two fractures is varied (8:1, 4:1, 2:1 and 1:1), with the assumption that the tracer is well mixed at the inlet of the system. The study concentrated only on the retention properties and thus advective delay was omitted.

#### Results and Discussion

The results show that retention by matrix diffusion is very sensitive to the flow rate. Except for the case of equal flow rates, where a double peak is observable, the breakthrough curve is dominated by a single feature. This is a non-linear effect in that not only does one of the features have a higher flow rate, but also this higher flow rate implies a lower value of  $\beta$  and thus retention is reduced. This behaviour increases with sorption strength.



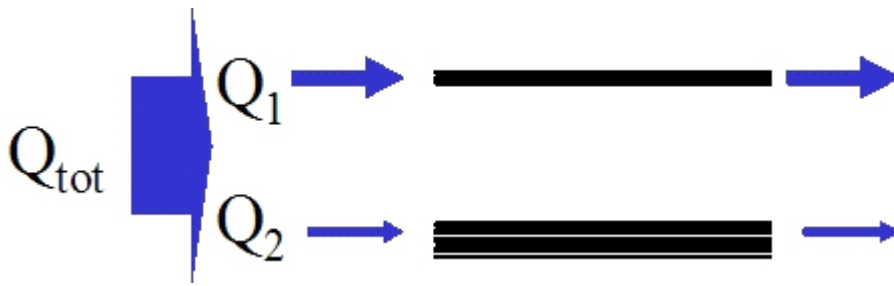


*Figure 3-19. Simplified subsystem of the complex structure that is composed of different type fractures /Poteri 2006/.*

### 3.5.5 Review

In general, /Poteri 2006/ rightly stresses that the major bridge between tracer tests and PA is not the numerical values of flow and transport parameters, but the understanding of processes to be included in assessments. For example, tracer tests clearly demonstrate that matrix diffusion should be included in PA models for fractured systems but the parameters derived from such tests are not particularly appropriate to PA. In particular, for practical reasons, tracer tests are performed in features with the highest transmissivities, whereas average transmissivity features are more relevant to PA. Also, the matrix diffusion parameters derived from tracer tests relate to high porosity zones adjacent to fractures, whereas intact rock values are most appropriate to PA.

#### **Tasks 6D and 6E**

The Posiva-VTT analysis has captured the essence of the important features and processes of relevance to the C2 tracer test. Moreover, the innovative approach to retention modelling and its inventive visual presentation facilitates insight into the nature of the controlling phenomena. In particular, Table 3-2 and Figure 3-15 give a clear indication of the controlling structures, Figure 3-16 allows contributions to the  $\beta$ -factor to be understood, and Figure 3-17 provides insight into the relative importance of the different geological materials on retardation. It would be useful for comparison purposes if other modelling teams could provide the type of flow path statistics presented in Table 3-2.

The study reinforces the conclusion that relatively small amounts of highly porous materials near the fracture surface can dominate tracer breakthroughs, and yet they are not well characterised. However, they are unlikely to play a significant role on PA time scales where the intact rock is likely to dominate retention. Thus the key extrapolation from SC to PA is process understanding rather than parameter values, and the Posiva-VTT work has made an important contribution to this understanding.

As with Task 6D, /Poteri 2006/ has made a comprehensive and innovative implementation of the Task 6E specification and has drawn insightful conclusions. In particular, the insight that  $\beta$  tends to reach an approximate plateau once the network of major flow path network is reached, could have general implications for performance assessment in sparsely fractured rocks. This arises because waste canisters will usually be sited at some distance from major flow paths. It is therefore plausible that the major contribution to  $\beta$ , and hence radionuclide retention, will come from the low transmissivity features between the canister and the major flowing features. If so, then these lower transmissivity would seem to warrant further study.

#### **Tasks 6F and 6F2**

Once again, /Poteri 2006/ made a thorough and comprehensive implementation of the task specifications, and drew useful conclusions. In the past it has been hypothesised that one fracture within a complex structure tends to dominate transport breakthrough. In Task 6F2,

/Poteri 2006/ clearly demonstrates for a simple system why this is likely to be so, in terms of the fracture with the highest flow also having the lowest  $\beta$  and hence lowest retention. This implies that structures with complexity factors greater than one may behave as if they are single fractures.

For the systems and parameters considered in this study, the implications for the Task 6 objectives 1–4 (Section 1.3) include:

- 1. Assess simplifications for PA:** On the basis of the understanding gained from this and related work, it is clear that a simplified PA model need only include diffusion into the intact rock, whose parameters can be measured directly. Also, it has been shown that it is reasonable to approximate complex structures by a single fracture pathway for the purposes of PA. Finally, the insight that  $\beta$  tends to reach an approximate plateau once the network of major flow path network is reached, could have general implications for performance assessment in sparsely fractured rocks by focussing attention on near-canister fractures and pathways through engineered barrier features.
- 2. Determine constraining power of tracer and flow tests for PA:** The primary constraining power of tracer tests lies in the understanding of important processes and features, rather than in the direct constraints on parameter values that can be derived from them. In particular, tracer tests clearly demonstrate that matrix diffusion should be included in PA.
- 3. Support design of SC programmes for PA:** An important objective for SC programmes is to demonstrate process understanding, in addition to providing quantitative information. Task 6D has the luxury of being based on a site represented by the Task 6C model where there are no uncertainties. In the real world this is far from the case, and improving the characterisation of the flow pathways remains a high priority.
- 4. Improve understanding using SC models:** The Posiva-VTT work on Task 6F2 has contributed to the understanding of transport through complex structures containing many sub-fractures. In addition, the Posiva-VTT SC modelling approach provides considerable understanding of the importance of the different features and processes through innovative visual representations of the contributions from its constituent parts, as demonstrated in Figures 3-8, 3-9 and 3-10.

### 3.6 SKB-CFE-SF

This section describes the work of the SKB modelling team from Computer-aided Fluid Engineering AB (CFE) and SF GeoLogic AB (SF). The primary objective of their work /Svensson 2006/ was to suggest and evaluate a way of including information concerning the geological structure type and complexity factor.

The models were implemented in the finite-volume DarcyTools code /Svensson et al. 2006/, which has been developed in parallel with Task 6 and whose basic assumptions are:

- The number of fractures in a certain length interval follows a power law.
- In sparsely fractured granite, flow is assumed to be distributed on relatively few flow channels, which are due to large-scale fractures and zones. It is assumed that all essential flow channels are due to fractures and zones that are larger than the grid size.

Structures are divided into two classes depending on whether they are larger or smaller than the cell size ( $\Delta$ ).

Cells intersecting the larger structures are assigned permeabilities using the GEHYCO method /Svensson 2004a/, which can be formulated as follows. A conductive element contributes to the grid value of a variable by an amount that is equal to the intersecting volume times the value of the variable in question. Contributions from all elements that intersect the control volume are added and the sum is divided by the volume of the cell.

Sub-cell structures result in micro-dispersion and are incorporated into a module FRAME /Svensson 2004b/, whose major concepts and assumptions are:

- Fractures smaller than  $\Delta$  are assumed to be filled with stagnant water (immobile volumes) and exchange matter with the flowing water (mobile volumes) by diffusion only.
- Sub-grid fractures are assumed to follow a power-law (same as for resolved fractures).
- All immobile volumes can be represented by a set of boxes (or storage volumes), each with its own length scale, volume and effective diffusion coefficient.

Computational cells within DarcyTools are characterised by the volume of mobile and immobile zones, and by flow-wetted surface. Retention is attributed to exchange with immobile volumes and the model focuses on how these should be distributed. The geological structure type and complexity factor are modelled by adjusting the immobile zone volume to account for the fact that Type 1 structures have more retention capacity than Type 2, and also that retention capacity increases with complexity factor.

The distribution of immobile zone volumes between and within structures was chosen to represent the information specified in the Task 6C report and other information relating to the heterogeneity of structures.

### 3.6.1 Task 6D

#### **Approach**

The 200 m block scale model was discretised with a 100·100·100 Cartesian non-uniform grid with a spacing of 0.5 m in the central region and expanding grid spacing outside this volume /Svensson 2006/.

Particle tracking was used to trace the possible flow paths from the injection point to the pumped borehole, which produced the two basic flow paths shown in Figure 3-20 that are at least qualitatively similar to flow paths calculated by the Posiva-VTT team (Figure 3-15) although in the Posiva-VTT case background fracture 45 was found to be important.

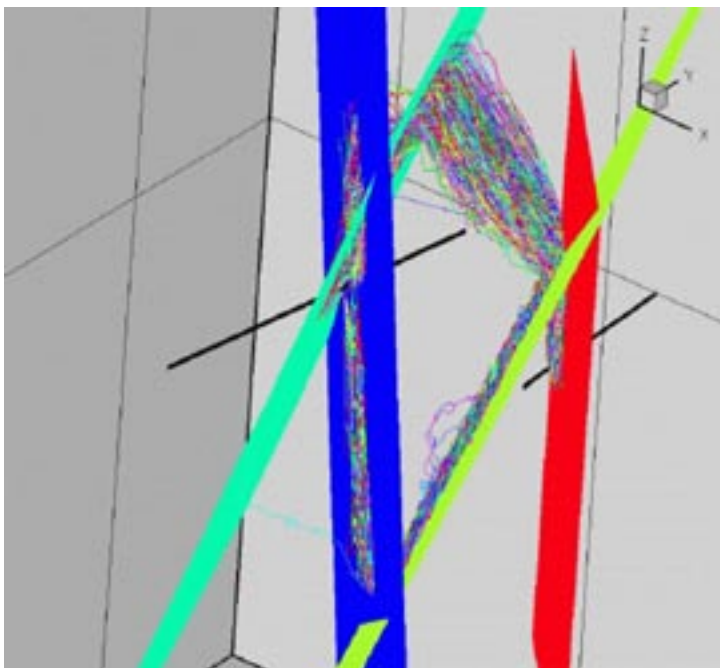


**Figure 3-20.** Flow paths for the C2 tracer test using the deterministic and synthetic fractures of the Task 6C model /Svensson 2006/.

## Results and Discussion

The computed breakthrough curves for a Dirac pulse are shown in Figure 3-21, and the curves using the measured injection are very similar. The main achievements of this work are demonstrating the feasibility of accounting for geological structure type and complexity factor within the novel DarcyTools framework. In particular, parameters required for the FRAME sub-grid model /Svensson 2004b/ have been related to measurable quantities, in particular the porosity distribution.

### 3.6.2 Task 6E

#### Approach

Particle tracking was used to define the pathways from the Task 6E source point for natural flow boundary conditions. Task 6E tracer breakthrough curves at the domain boundary, and on planes 10 m and 50 m from the source, were calculated for the same modelling assumptions as used in Task 6D, but for the specified boundary conditions. No calibration was performed. Figure 3-22 shows the pathways for the case in which all deterministic and synthetic structures were included. Particles move through a combination of deterministic and synthetic structures from the source point in structure 23 towards the western boundary.

#### Results and Discussion

There appears to be two main flow paths, one with an advective time of about 2 years and the other 5 years. The tentative conclusion of the study is that deterministic PA time scale simulations in high-resolution grids (150·150·150 cells) are feasible for a range of sorbing and non-sorbing tracers, although the realism of the results remains to be evaluated.

### 3.6.3 Task 6F

#### Approach

/Svensson 2006/ used a one-dimensional DarcyTools model to calculate the specified Task 6F cases, with sub-grid parameters dependent on geological structure type and complexity factor.

#### Results and discussion

Breakthrough curves have been calculated and the specified performance measures tabulated.

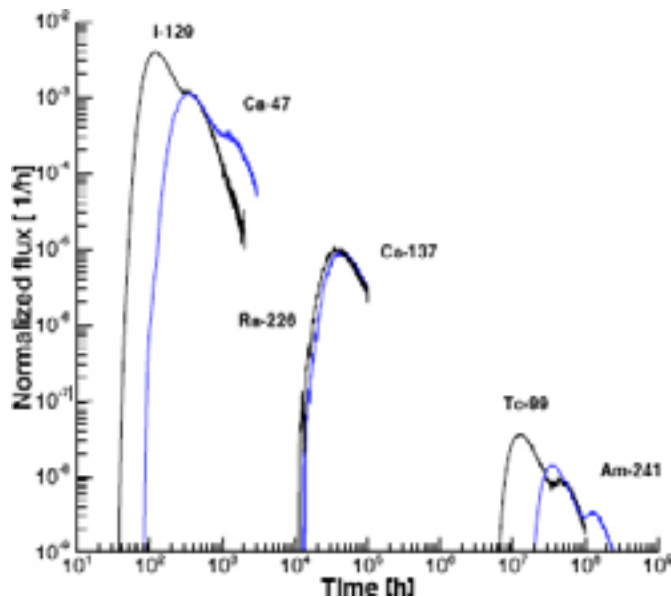
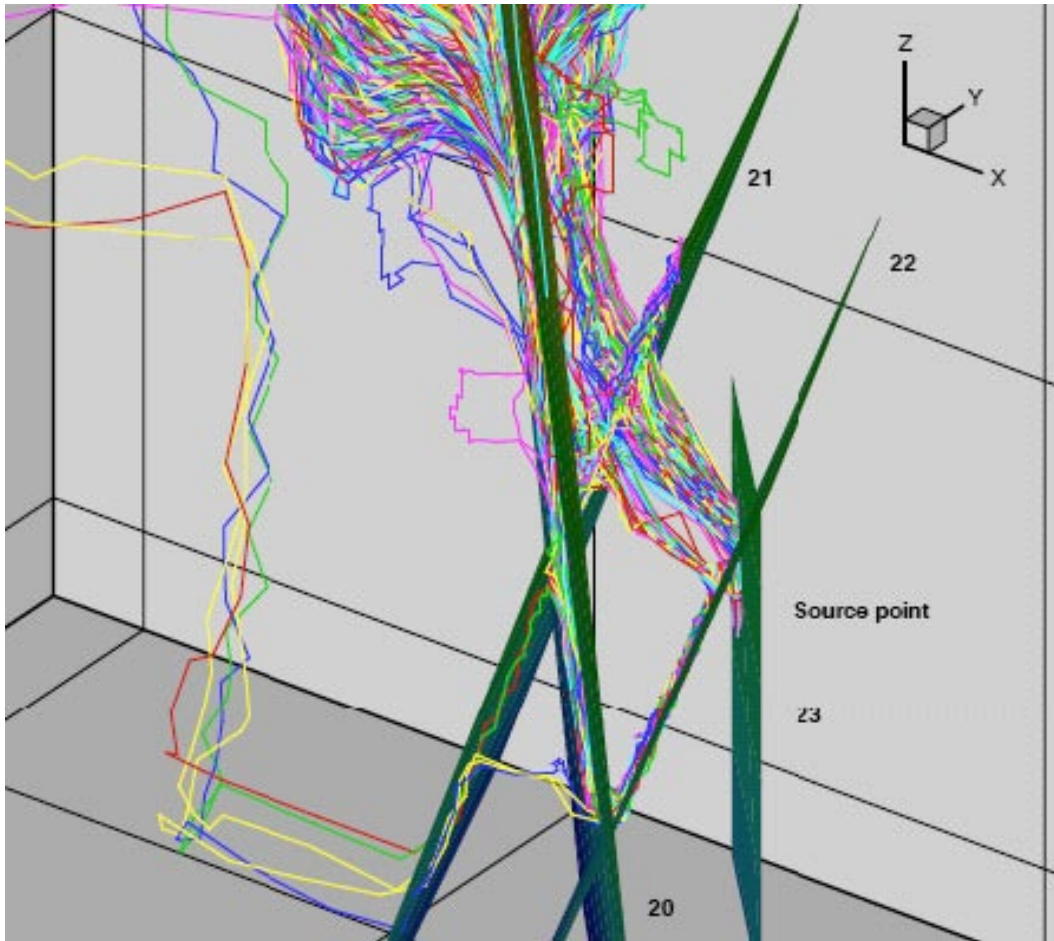


Figure 3-21. SKB-SF Task 6D breakthrough curves for a Dirac pulse /Svensson 2006/.



*Figure 3-22. Close up view of Task 6E flow paths calculated for the full Task 6C network /Svensson 2006/.*

### 3.6.4 Task 6F2

#### **Approach**

For Task 6F2 /Svensson 2006/ addressed the important question of how best to specify input parameters for a fracture network model in order to fulfil as many performance measures as possible.

#### **Results and discussion**

/Svensson 2006/ suggested a methodology based on the following two principles:

- In order to eliminate interdependencies, network characteristics should be specified one at a time.
- Priorities should be formulated based on physical arguments taking account of the relevant scales and parameters.

A structured approach specific to the DarcyTools/FRACTION model was proposed but given time limitations it was only possible to make a preliminary application. Taking account of the first principle above, the methodology starts by specifying the power law fracture length distribution independently of the transmissivity distribution. The next second of the methodology is to specify the transmissivity distribution, which in accordance with the second principle above focuses on the large scale features because they carry most of the water. This is followed by the simulation of a steady-state drawdown experiment.



A striking conclusion of this work is that the specification of the fracture network is very uncertain and the results are very sensitive to the chosen parameters. For example for two parameter sets that are both consistent with the field data, the number of fractures larger than 2 m in the TRUE Block Scale volume could be 25,000 or 300,000.

### 3.6.5 Review

DarcyTools has developed and matured throughout the course of Task 6. It is a novel approach to groundwater flow and transport modelling as regards the treatment of sub-grid processes. This new approach is to be welcomed, given the well-known problems of treating hydrodynamic dispersion as a diffusion-like process using the advection dispersion equation. This work has shown that it is feasible to implement complex discrete fracture networks in DarcyTools, and to account for sub-grid transport processes using a multi-rate diffusion model into a distribution of immobile zone volumes. In particular, it has proved possible to relate the distribution of immobile zone characteristics to measurable quantities including the geological structure type, complexity factor and porosity.

It is noted that for Task 6D the flow paths appear to be visually similar to those calculated by the Posiva-VTT and SKB-KTH-ChE groups. However, the most important background fracture was identified to be 45, whereas the Posiva-VTT and SKB-KTH-ChE groups identified 1925B as the most important. From the information available, the Posiva-VTT result seems most likely to be correct as a discrete fracture representation was used. Thus it appears that the use of a continuum representation for the flow, at a resolution of 0.5 m, may not fully capture sufficient detail of the Task 6C model. It would have been useful to have defined an additional performance measure relating to flow path geometry in order to clarify these issues.

The work on developing a structured and transparent methodology for determining fracture network parameters carried out under Task 6F is to be welcomed. This issue has been discussed by /Black and Hodgkinson 2005/ who viewed the non-uniqueness of the fracture network specification as a particular concern.

For the systems and parameters considered in this study, the implications for the Task 6 objectives 1–4 (Section 1.3) include:

- 1. Assess simplifications for PA:** The SKB-CHE-SF transport model is flexible enough to cover the requirements of both SC and PA simulation.
- 2. Determine constraining power of tracer and flow tests for PA:** Not considered in this work.
- 3. Support design of SC programmes for PA:** Not considered in this work.
- 4. Improve understanding using SC models:** The model was applied progressively to understand the impact on the performance measures of different features including the presence or absence of background fractures, and heterogeneity within structure planes.

## 3.7 SKB-KTH-ChE

For Tasks 6D, 6E, 6F and 6F2 the SKB modelling team from the Department of Chemical Engineering and Technology (ChE) at the Royal Institute of Technology (KTH) in Stockholm have used a channel network model /Crawford and Moreno 2006/, implemented in the CHAN3D code /Moreno and Neretnieks 1993, Gylling 1997/, which assumes that fluid flow and solute transport take place in a three-dimensional network of channels /Crawford and Moreno 2006/.



### 3.7.1 Task 6D

#### **Approach**

It was found that much of the Task 6C 200 m rock volume was computationally superfluous and thus a smaller 75 m rock volume was employed with 418 out of the original 5,678 structures contained fully or partly within the 75 m block. The CHAN3D model consisted of a rectangular grid of channels each with a length of 1 m, giving a channel network containing  $76^3$  nodes.

The CHAN3D grid was fitted to the defined structures as follows. Channels lying within the zone of influence (taken to be one channel length) of particular structures were assigned appropriate conductances depending upon the transmissivity of the fracture. In order to allow the possibility of flow channelling within individual structures, channel conductances were assigned randomly from a log-normal distribution with a standard deviation of unity ( $\log_{10}$  units). The conductance of channels at fracture intersections was calculated on the basis of the mean transmissivity of the fractures involved. The head boundary conditions for the 75 m block were calculated from the average of 20 realisations using the 200 m block with specified head boundary conditions.

Solute transport was simulated using a particle following technique /Robinson 1984, Moreno et al. 1988/. Particles arriving at an intersection are distributed in the outlet channel members with a probability proportional to their flow rates, which is equivalent to assuming total mixing at the intersections. The residence time for solutes was obtained from an analytical solution for solute transport where infinite matrix diffusion and sorption are considered. The channel volume was estimated by assuming that the conductance of a channel is proportional to the cube of the channel aperture.

Channels resident in fault-type fractures (Type 1) were assigned properties for cataclasite, and non-fault type channels (Type 2) were assigned material properties for unaltered rock. Surface sorption parameters were identically assumed to be the same for fracture coating material in both fault and non-fault fracture types. For channels identified as belonging to multiple fractures, the fault-type geological class was given precedence over the non-fault geological class when assigning material properties. Similarly, the highest complexity factor was assumed to take precedence where there were conflicting fracture complexity definitions for channels shared between multiple fractures. The flow-wetted surface of channels was normalised to give a total flow wetted surface corresponding to twice the DFN polygon surface area resident within the simulation volume, as would be the case for a parallel-plate fracture. The flow-wetted surface of individual channels was then multiplied by a scaling factor dependent upon the specified complexity.

In the hydraulic simulations for the C2 tracer test, flow injection and pumping were performed at single nodes in conductive fractures closest to the specified injection and recovery points. The flowing porosity was determined by fitting to the  $\text{ReO}_4^-$  breakthrough curve giving a value of  $7.3\text{E}-5$ .

#### **Results and Discussion**

Tracer transport was found to occur along two principal flow paths in the channel network (Figure 3-23) with on average 46% flowing along the upper path. The tracer particles were observed to travel predominantly in deterministic structures 20D, 21D, 22D, and 23D as well as a number of minor background fractures associated with these larger features. Flow along the upper flow path was entirely contingent upon the existence of background fracture 1925B as can be seen in Figure 3-23.

The results for non-sorbing and weakly sorbing tracers show that the dispersion in the actual fracture system is greater than in the model. This could be due to a combination of fast channelling with little matrix interaction for the early tracer breakthrough, combined with slower transport flow paths with greater matrix retention for late tracer arrival, or to additional pathways not included in the model.

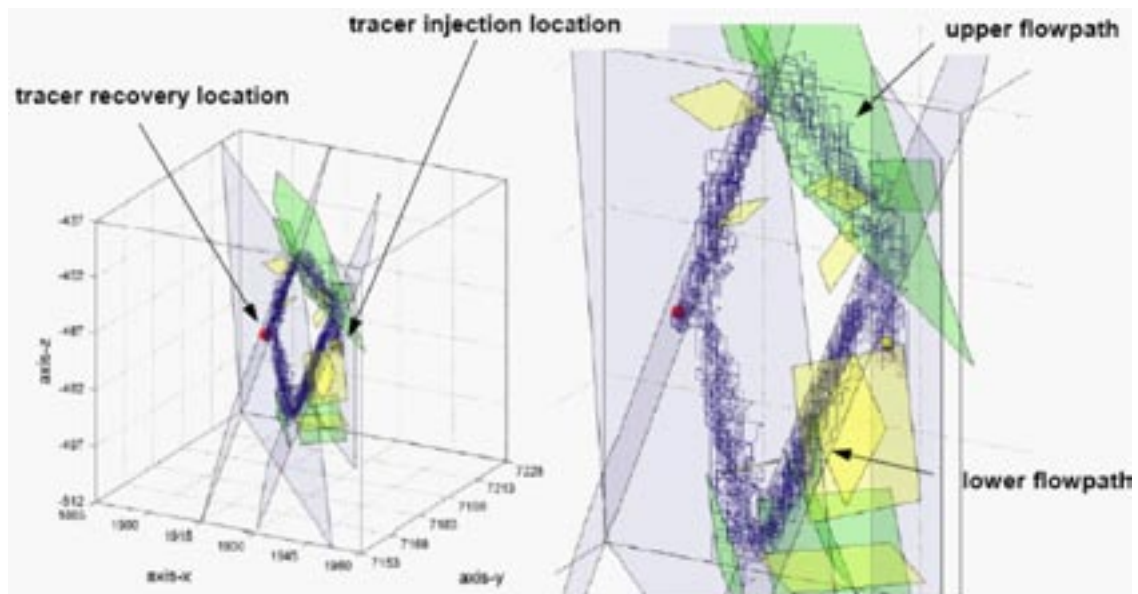


**Figure 3-23.** Visualisation of tracer flow paths for a typical CHAN3D C2 tracer test realisation. Particle tracks are shown in the context of DFN fracture planes within which tracer transport occurs. The data represents the trajectory of 100 particles randomly chosen from 10,000 actually used in the transport simulation. Background fracture 1925B is the large green shaded polygon in the top right hand section of the upper flow path /Crawford and Moreno 2006/.

Aside from the apparently broad peak of the experimental breakthrough of  $^{186}\text{Re}$  that is suggestive of strong channelling, the SKB-KTH-ChE team considers that there is very little constraining power in the experimental data for the tracer tests. Considering the short timescale of the tracer experiment C2, the impact of matrix porosity is also very small and largely dominated by the sorption properties of the fracture coating for the moderately- and strongly-sorbing tracers.

The tracer recovery data supplied to the modelling groups consisted of “decay-corrected” activity-time curves for the radiotracers. The SKB-KTH-ChE team considers that the tracer cut-off at 500 hours for  $^{186}\text{Re}$  relates to the limit of detection of the  $\gamma$ -spectrometric analysis combined with the short half-life of the tracer (90 h) rather than a true cut off for tracer recovery. It would therefore seem that  $^{186}\text{Re}$  is a less than ideal choice of tracer for recovery times extending beyond about 500 hours. The  $^{47}\text{Ca}$  radiotracer also has a relatively short half-life (108 h) and it is likely that the poor recovery of 29% for this tracer relates as well to the fact that the late arriving tracer has had sufficient time to decay to levels below the limit of detection.

The non-sorbing and poorly sorbing tracer breakthrough curves approximately match the experimental data, although this is purely an artefact of the calibration procedure as matrix diffusion effects are largely absent from these data sets. There is not sufficient data available from the  $^{137}\text{Cs}$  data set to draw any specific conclusions, as there are only a few experimental data points available. The first appearance of the tracer at 4,000 h, however, is broadly consistent with the first simulated breakthrough and is significantly delayed relative to the first breakthrough of the non-sorbing and poorly sorbing tracers.

The SKB-KTH-ChE team questioned the usefulness of using the full model containing 5,648 features to simulate the tracer test C2, owing to the fact that the bulk of these features are “synthetic” in nature and represent only one stochastic realisation of a DFN.

### 3.7.2 Task 6E

#### Approach

For the Task 6E simulations the entire 200 m rock volume as described in the Task 6C hydrostructural model was employed with a channel length of 2 m, thereby giving a channel network containing  $101^3$  nodes. In Task 6E the flow occurs due to a hydraulic head gradient of 0.5% from East to West. Tracer injection was performed passively at three adjacent locations (i.e. a so-called “line source”) resident in deterministic feature 23D, located near the centre of the TRUE Block Scale volume. Apart from these factors, the model was the same as used for Task 6D.

#### Results and discussion

Tracer transport to the western boundary was found primarily to converge along a single principal flow path after the first few tens of metres, with small numbers of particles taking alternate routes (Figure 3-24). The tracer particles were observed to travel predominantly in features 20D-23D and 17S. Also, background structures 1925B and 2292B were found to be crucial for tracer transport as these structures link the aforementioned D and S features into a contiguous pathway from the injection location to the western boundary plane.

For tracer recovery at the western boundary plane there is no discernable difference in shape or breakthrough time for the extended pulse and Dirac pulse in the case of the moderately sorbing and strongly sorbing tracers. However, for the non-sorbing tracers, the shape of the breakthrough curve is smeared out into a triangular peak for the extended pulse, although with a central moment translated about 500 years forward in time as compared to the Dirac pulse.

Owing to fast channelling effects, the predictions made by CHAN3D give a faster peak breakthrough with smaller dispersion than what would be estimated purely from the average properties of the Block Scale volume as it has been conceptualised in these simulations.

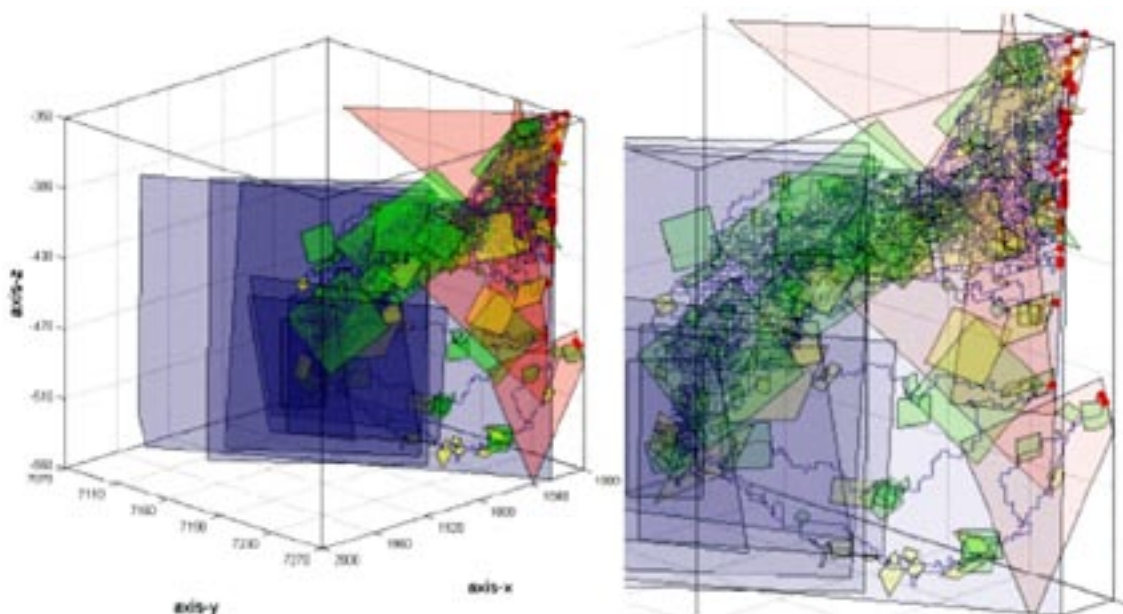


**Figure 3-24.** Visualisation of tracer flow paths for a typical CHAN3D Task 6E transport realisation simulating tracer transport from the release location to the recovery plane at the Western simulation boundary. Particle tracks are shown in the context of DFN fracture planes within which tracer transport occurs. Tracer recovery locations are shown with red markers /Crawford and Moreno 2006/.

A potential problem relates to the scaling of flow-wetted surface, which was carried over from Task 6D. At the Task 6E performance assessment timescales it appears that the scaling of flow-wetted surface is too generous and may overestimate matrix retention by as much as a factor of 4. It may be appropriate to neglect the increased flow-wetted surface of sub-parallel fractures at PA-timescales, as their spacing is likely to be less than the radionuclide penetration depth.

### **3.7.3 Task 6F**

#### ***Approach***

For Task 6F, /Crawford and Moreno 2006/ represented the structures by two-dimensional grids with 225 nodes in each direction, implying a channel grid length of 0.5 m, with processes and material parameters as for Task 6E.

#### ***Results and Discussion***

Breakthrough curves were calculated for five realisations, but no large differences were found between realisations.

### **3.7.4 Task 6F2**

#### ***Approach***

In Task 6F2, the channel network model was improved to handle diffusion into a matrix composed of several layers and a semi-infinite matrix. The differential equation for the fracture, the layers, and the semi-infinite matrix are solved using Laplace Transforms. The breakthrough curves in the time-domain are then obtained by numerical inversion of the solution in the Laplace-domain. A study was made of how the different components of the residence time vary with the water flow rate and the sorption coefficient.

#### ***Results and Discussion***

A conclusion from Task 6F2 is that the residence time is determined by different mechanisms in SC and PA. Also if the solute transport is modelled assuming instantaneous equilibrium with the material in the fracture (coating, gouge, cataclasite) the resulting residence time may be not conservative.

### **3.7.5 Review**

The CHAN3D model appears to capture the essential flow features of the Task 6C fracture system in a computationally efficient manner. Surprisingly for a channel network model, it does not appear to include the full effects of channelling in Task 6D, in particular early tracer arrivals and post-peak dispersion. Possibly one reason for this is that the variability of channel conductance was not large enough.

Channel network models are an important part of the portfolio of models considered in the Äspö Task Force, because they offer the possibility of reproducing the sparsity of water inflow points observed, for example in the system of tunnels. Thus they should continue to be applied and further developed. For example, it would be interesting to develop methods for aligning the channels more closely to the fracture system than can be achieved by imposing a rectangular lattice. This might possibly be achieved by distorting the 3D rectangular lattice used in CHAN3D. However, a preferable approach would be to impose suitable 2D lattices on the identified structures together with the imposition of a suitable degree of connectivity along the structure intersections. In this way the conductances in the structure planes and along the structure intersections could be assigned different distributions, which is more physically realistic than the single distribution used in the current application of CHAN3D.

Sensitivity studies have confirmed that the interpretation of the C2 tracer test is not unique, for example an equally plausible calibration can be made if there are no stochastic background fractures.

The extension of CHAN3D to include multi-layered matrix zones, applied in Task 6F2, is a welcome development that improves the realism of the code.

For the systems and parameters considered in this study, the implications for the Task 6 objectives 1–4 (Section 1.3) include:

- 1. Assess simplifications for PA:** On PA timescales, it is not appropriate to model the structure complexity by scaling the flow-wetted surface in proportion to the number of near-parallel fractures because the separation between these fractures is likely to be less than the penetration depth and thus there would be double counting.
- 2. Determine constraining power of tracer and flow tests for PA:** Short-term SC tracer tests do not significantly constrain the matrix interaction parameters required for long-term PA modelling. The concept of penetration depth can be used to understand and quantify this lack of constraint.
- 3. Support design of SC programmes for PA:** The use of complex representations of fracture geometry, as in the Task 6C model, may not be the best way to proceed in supporting the design of SC programmes. A more non-representational approach focussing on the understanding of the statistics of flow-wetted surface proportioning and flow channelling may be more appropriate. For example, different assumptions of flow geometry made during the construction of conceptual models of the fracture system may give rise to strongly biased SC models. Parameters derived from these SC models could potentially have far-reaching consequences when subsequently used in PA-modelling.
- 4. Improve understanding using SC models:** Channel network models have the potential to improve understanding of the relatively sparse connectivity found at Äspö and other sites. However, to fully realise this promise it would be useful if their geometry could be aligned more closely to that of the fracture system.

## 3.8 SKB-KTH-WRE

The SKB modelling team from the Department of Water Resources Engineering of the Royal Institute of Technology (KTH) in Stockholm used the LaSAR modelling approach /Cvetkovic et al. 1999/ coupled with permeable medium flow modelling for Tasks 6D, 6E, 6F and 6F2 /Cheng and Cvetkovic 2006/.

The Task 6C model was implemented with structures represented by parallel plates with transmissivities related to the square of the aperture according to Tom-Doe's law /Outters and Shuttle 2000/ with the largest transmissivity being assigned at the intersection of structures.

The flow simulations were performed with the finite-difference code MODFLOW 2000 /Harbaugh et al. 2000/ with structures represented by a number of staggered elements. Permeabilities were assigned based on the transmissivities of the transecting structures.

### 3.8.1 Task 6D

#### **Approach**

The first step for Task 6D /Cheng and Cvetkovic 2006/ was to simulate flow in the 200 m block with 2 m cubic elements. Using the output heads from this model as boundary conditions, flow was then simulated in an inner 100 m cubic domain with 1 m cubic elements.

Flow paths for the C2 tracer test were calculated in the 100 m block using particle tracking, and the residence time ( $\tau$ ) and the  $\beta$  parameter of the LaSAR model /Cvetkovic et al. 1999, 2000/



were computed at the pumping section for all injected particles. This established an approximately linear relationship between  $\tau$  and  $\beta$ , and this distribution was used to obtain the ensemble mean and variance of  $\tau$ . In the transport calculation the distribution of  $\tau$  was assumed to be inverse Gaussian.

The following mass transfer processes were included:

- dispersion of tracers in the fracture due to velocity variation based on the  $\tau$ - $\beta$  distribution;
- unlimited diffusion into a uniform rock matrix and linear equilibrium sorption inside the rock matrix; and
- equilibrium sorption on fracture surfaces.

Effective mass transfer parameters relevant to the C2 tracer test were derived from the Task 6C data set as follows. The surface sorption coefficients were calculated from the distribution coefficient and depth of the fracture coating. The matrix porosity was calibrated to the non-sorbing breakthrough curve for the C2 tracer test, and the distribution coefficients for calcium and caesium were calibrated to their respective C2 breakthrough curves.

### **Results and Discussion**

Two main flow paths were identified from the particle tracking, with 69% of particles traversing the four deterministic structures (23D – 22D – 20D – 21D) and the remainder passing through some background fractures (Figure 3-25), which appears to be in qualitative agreement with the results of other groups.

The determination of  $\tau$  and  $\beta$  from particle tracking, and calibration to the non-sorbing tracer breakthrough curve resulted in a reasonable match between calculation and experiment for I-129 as shown in Figure 3-26. However, despite the calibration of rock matrix distribution coefficients to the breakthrough curves, the Ca-47 and Cs-137 calculations were more retarded than the measurements. This may be due to over-estimation of the retention coefficients.

The sensitivity to the discretisation was investigated by repeating the calculations for the 200 m block flow model. The coarser discretisation had a lower mean residence time and higher variance leading to earlier arrival and broader breakthrough curves.

The effect of the background fractures was studied by only including the deterministic structures in the calculations. This reduced the mean water residence time, yielding earlier tracer arrivals, but the variance did not change significantly.

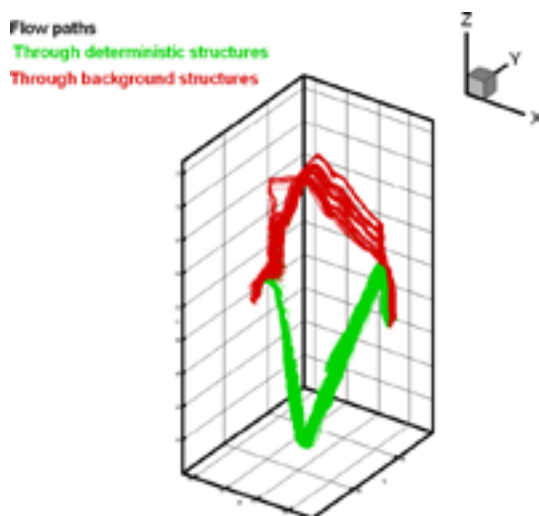


**Figure 3-25.** Flow paths through the deterministic (green) and background (red) fractures /Cheng and Cvetkovic 2006/.



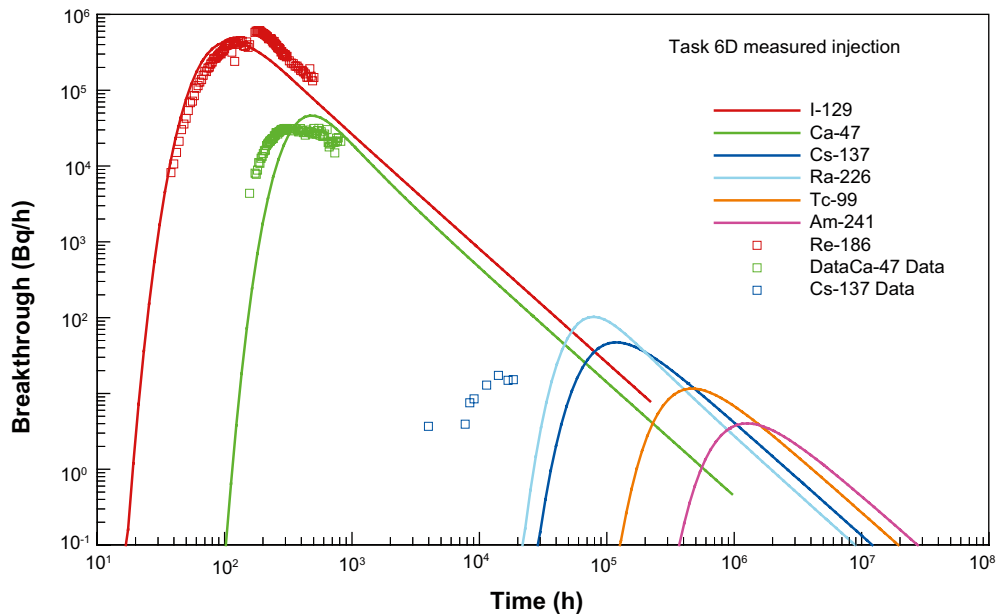


**Figure 3-26.** Calculated breakthrough curves for measured injection for Task 6D compared to C2 tracer test results /Cheng and Cvetkovic 2005/.

### 3.8.2 Task 6E

#### Approach

The approach to Task 6E was similar to that described above for Task 6D with the exception that all flow simulations used the 200 m cubic block of rock with 1 m cubic elements. The particle tracking was performed from the injection section in structure 23 to the three control planes:  $x = 1,920$  m,  $x = 1,880$  m and  $x = 1,800$  m (the west boundary) to give distributions for the water residence time and the  $\beta$  parameter at the three control planes.

Effective values for matrix porosity and distribution coefficients for the Type 1 and Type 2 structures were obtained by calculating the penetration depths for the time at which 85% of the tracer had been recovered in a scoping calculation. Average values were then derived from the immobile zone properties given in the Task 6C report. complexity factors were accounted for by calculating the average percentage of each structure type along a flow path or several flow paths.

#### Results and Discussion

Close to the release point the particles follow two main trajectories passing through structures 23D – 1925B – 21D – 20D and 23D – 22D – 20D. Between the 1,920 m and 1,880 m control planes, these paths first converge and then fan out towards the western boundary (Figure 3-27).

Effective retention parameters (porosity and sorption coefficient) for the entire immobile zone, which are dependent on penetration depth, are required by the SKB-KTH-WRE approach. In this work the penetration depth chosen was at the time when the somewhat arbitrary value of 85% of the mass has been recovered, and the average retention properties for this depth were used.

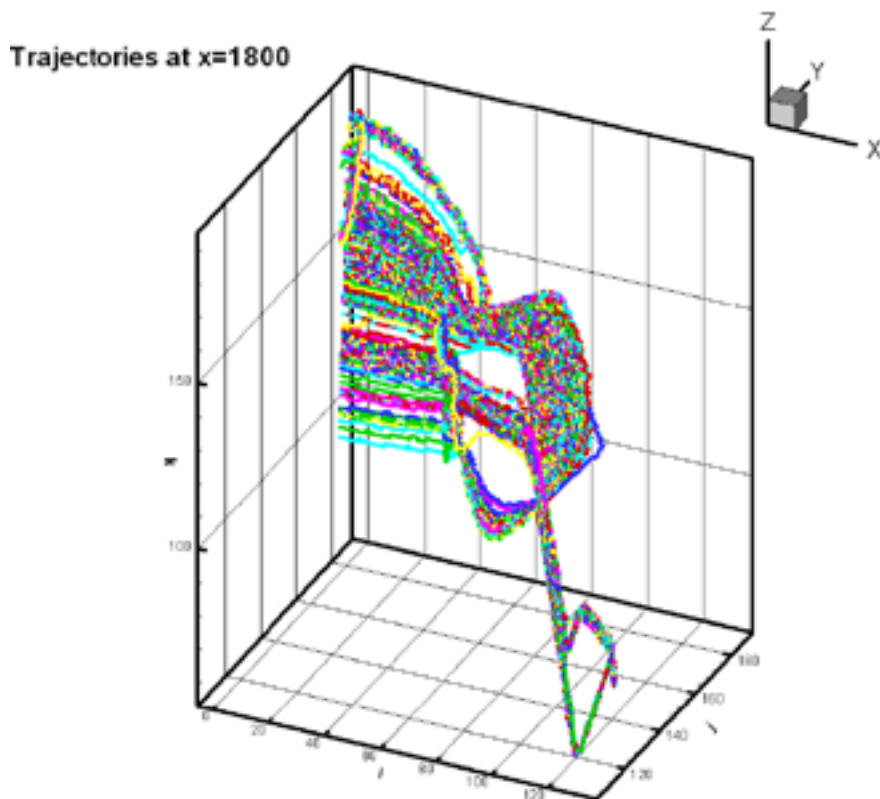


*Figure 3-27. Flow paths for Task 6E at  $x = 1,800$  m /Cheng and Cvetkovic 2006/.*

### 3.8.3 Task 6F

#### **Approach**

For Task 6F /Cheng and Cvetkovic 2006/ followed a similar procedure to Task 6E. The two structures were modelled as homogeneous 2D fractures for which  $\beta$  is strictly linearly related to travel time.

#### **Results and discussion**

The breakthrough curves for the specified cases were calculated and the performance measures tabulated.

### 3.8.4 Task 6F2

#### **Approach**

For Task 6F2 /Cheng and Cvetkovic 2006/ considered a series of three planar fractures of equal lengths and width but with different heterogeneous aperture (or transmissivity) distributions (Figure 3-28). There are two degrees of variability. The first is the variability in the geometric mean of the  $i$ th realisation, which represents the variability between fractures (global heterogeneity). The second is the spatial variability within a given fracture (internal heterogeneity).

#### **Results and discussion**

Simulations were performed for a wide range of the two degrees of heterogeneity in order to understand their impact on the relationship between  $\beta$  and travel time, and  $\beta$  and water flux in the compound fracture.

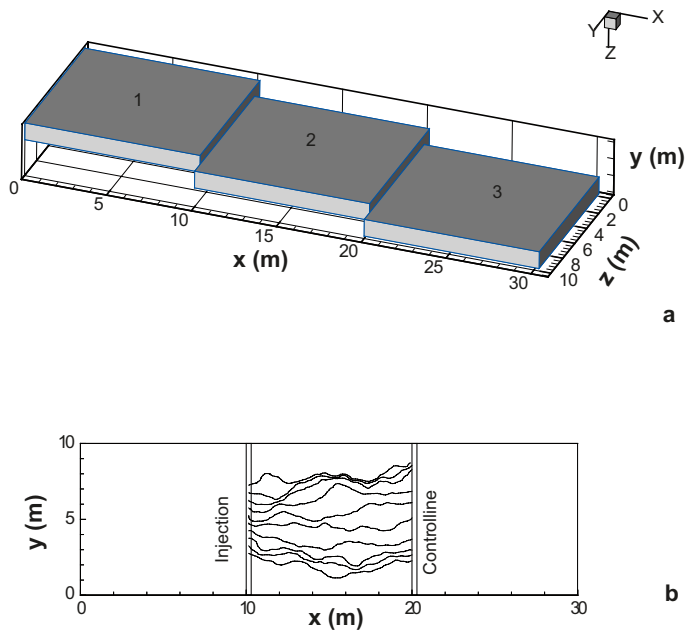


**Figure 3-28.** (a) Configuration of three connected fractures; (b) a typical realization of trajectories with  $W = 5.0$  m /Cheng and Cvetkovic 2006/.

### 3.8.5 Review

The Task 6D sensitivity analysis illustrated that flow paths and transport modelling are sensitive to the degree of discretisation. While the flow paths for the smallest grid size (1 m) in Figure 3-25 appear to be similar to those found by other groups using discrete fracture modelling, it has not been proved that this is precisely the case. It would be interesting to repeat the procedure using a 0.5 m grid in the region around the tracer test, as was used by the SKB-CFE-SF team, in order to settle this matter. Also it would be useful if the structures involved in the particle tracking were documented to facilitate comparison with the other groups.

It is somewhat surprising that despite the extensive calibration of the 6D transport model, the sorbing tracer data is not well reproduced. Also, in Task 6E the SKB-KTH-WRE team tend to predict earlier breakthroughs than other modelling teams. Possibly this is due to the evaluation of retention parameters a late time (85% recovery).

The current implementation of the LaSAR technique only allows for one immobile zone layer, and thus the application to a multi-layered diffusive zone was not straightforward and involved approximations dependant on penetration depth that cannot easily be tested. It would be interesting to know whether the technique is capable of being extended to multi-layered diffusive zones.

In general the correlation between  $\beta$  and  $\tau$  is nonlinear and follows a power law. However, in this and related work a linear relationship has been assumed. It would be interesting to extend the LaSAR approach to incorporate this power law behaviour.

For the systems and parameters considered in this study, the implications for the Task 6 objectives 1–4 (Section 1.3) include:

1. **Assess simplifications for PA:** From the results presented it is difficult to determine the accuracy of the simplifications made in the PA modelling.
2. **Determine constraining power of tracer and flow tests for PA:** The water residence time distribution for the pathway involved in the C2 tracer test has been reasonably well constrained, but this is not expected to have a major impact on PA studies. PA modelling indicates that retention in the unaltered rock is the most important, whereas on SC time scales near-fracture immobile zones are dominant.

- 3. Support design of SC programmes for PA:** The SKB-KTH-WRE team have collaborated closely with the TRUE Block Scale site characterisation team, and this interplay of expertise has undoubtedly benefited the site characterisation programme and helped to provide a bridge between SC and PA.
- 4. Improve understanding using SC models:** The current tasks have highlighted the fact that the analysis of tracer experiments using SC models should primarily be aimed at understanding the relevant processes rather than determining parameters for use in PA modelling. Of course, the variation of retention parameters over times of interest for PA cannot be determined by SC experiments, but must rely on natural evidence.

## 4 Inter-comparison of modelling results

The following section presents an inter-comparison based on modelling team results that have been provided to the secretariat in numerical form.

### 4.1 Task 6D

Figures 4-1 to 4-3 present inter-comparisons of the available modelling team breakthrough curves for I-129, Ca-47 and Cs-137, and comparisons with the measured decay-corrected breakthroughs for the C2 tracer test.

From the perspective of consistency with the experimental measurements, the results of the ANDRA-CEA team provide the overall closest match. This is consistent with the aim of the ANDRA-CEA team, which was to identify an optimal data set of flow and transport parameters for the major structures. To achieve this, they calibrated 4 transport apertures, near-fracture matrix zone diffusivity and porosity, and sorption coefficients.

However, the Task 6D specification /Elert and Selroos 2002, 2004a/ did not advocate calibration but rather considered Task 6D to be a forward modelling exercise. From this perspective it is most appropriate to compare the uncalibrated modelling results and try to understand differences between these and the experimental results.

The POSIVA-VTT, SKB-CFE-SF and JAEA-Golder results shown in Figures 4-1 to 4-3 were not calibrated. Given this, their results are reasonably consistent with the C2 tracer experiment. The major discrepancy is that the calculated results for Ca-47 and Cs-137 are too retarded, possibly reflecting an overestimation of sorption. The lack of an explicit hydrodynamical dispersion term in the POSIVA-VTT analysis is evident at early times in the I-129 results. With the exception of this short-term behaviour it is notable that the POSIVA-VTT and JAEA-Golder results are close, implying a fair degree of cross-verification. It should be noted that the angular appearance of the SKB-CFE-SF breakthrough curves is due to the limited number of output points provided; the true curves (shown in Figure 3-21) have a more natural dispersion-like appearance.

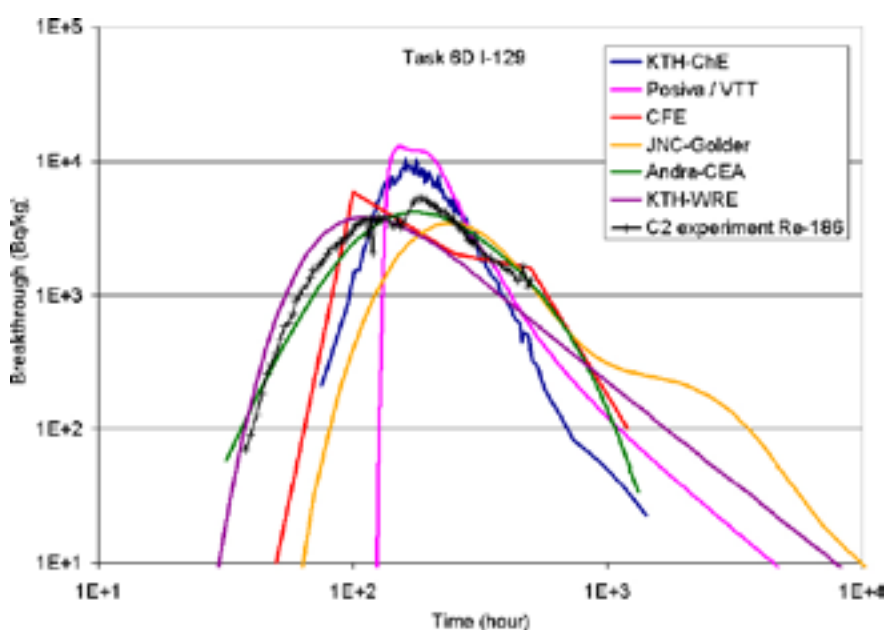


**Figure 4-1.** Inter-comparison of calculated breakthrough curves for I-129 in Task 6D together with the C2 tracer test results.

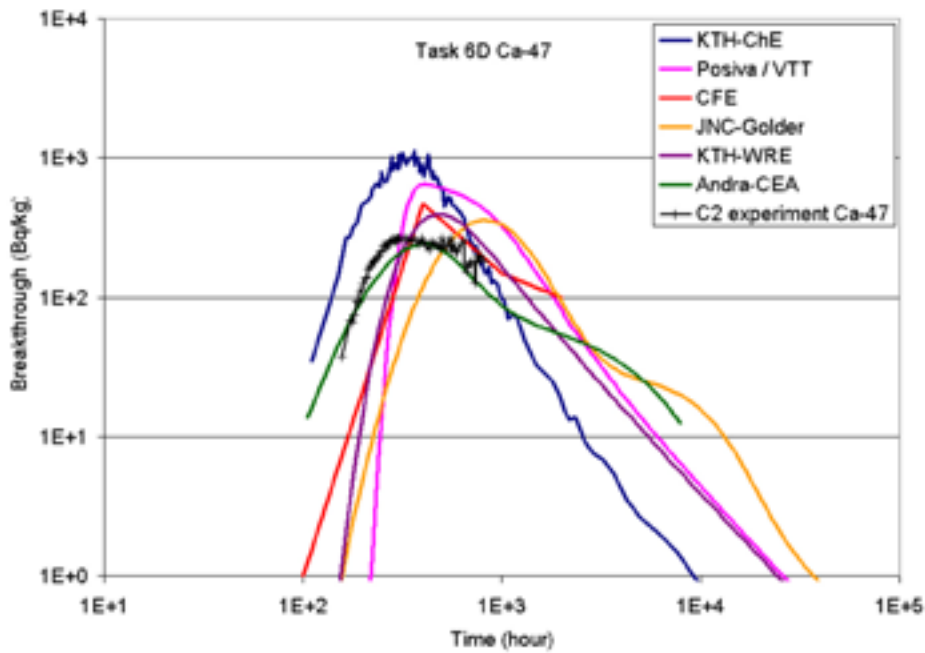


**Figure 4-2.** Inter-comparison of calculated breakthrough curves for Ca-47 in Task 6D together with the C2 tracer test results.

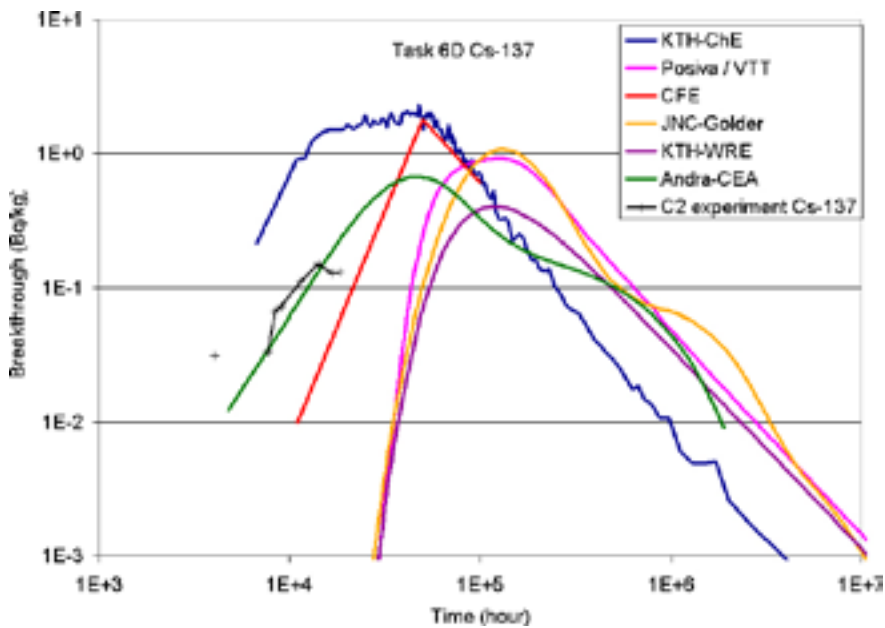


**Figure 4-3.** Inter-comparison of calculated breakthrough curves for Cs-137 in Task 6D together with the C2 tracer test results.

Figures 4-4 and 4-5 show the modelling team results for Task 6D in terms of maximum release rate and the time to 50% breakthrough for a Dirac pulse. It is seen that the results agree to within an order of magnitude for I-129, Ca-47, Cs-137 and Ra-226, and to within two order of magnitude for Tc-99 and Am-241. Even for these latter nuclides the POSIVA-VTT and JAEA-Golder results are similar confirming the cross-verification.



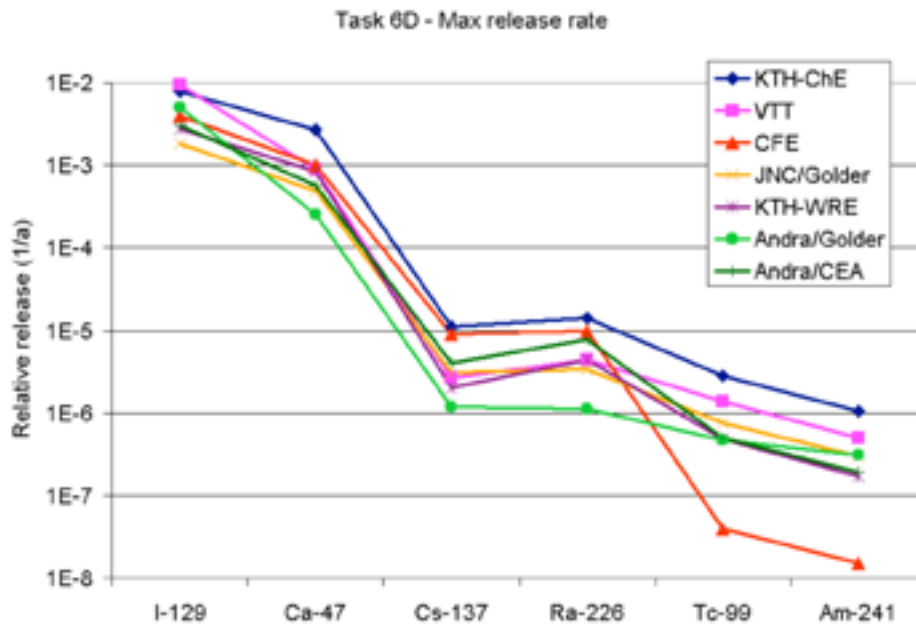


Figure 4-4. Calculated maximum release rates for Task 6D Dirac release.

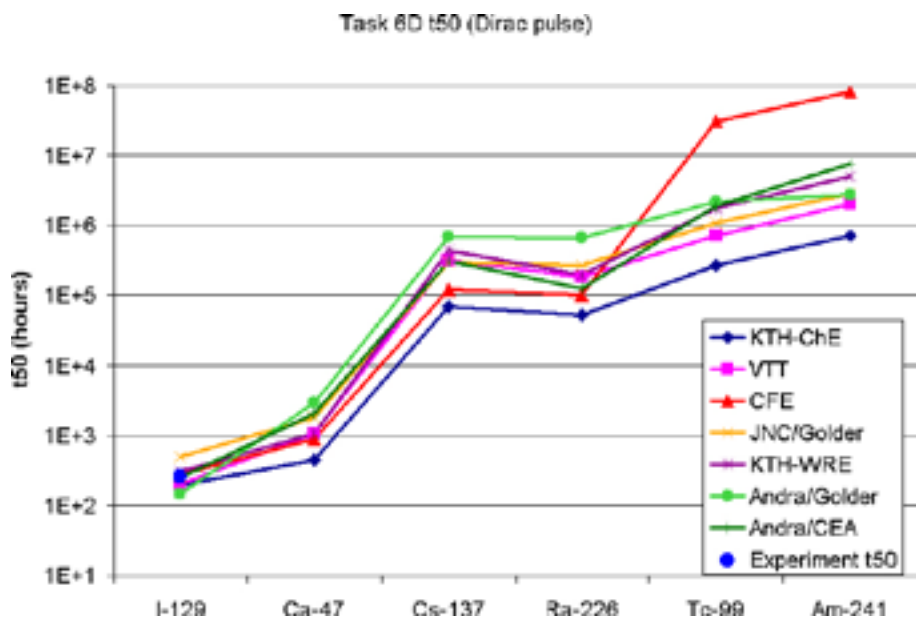


Figure 4-5. Calculated times for 50% breakthrough for Task 6D Dirac release.

The water residence time distributions are shown in Figure 4-6.

Finally, Figure 4-7 presents an inter-comparison of the reported ranges for the  $\beta$  factor. There appears to be a reasonable consensus around about 100 years/m, with the ANDRA-Golder result as an outlier arising from their permeable medium approach.

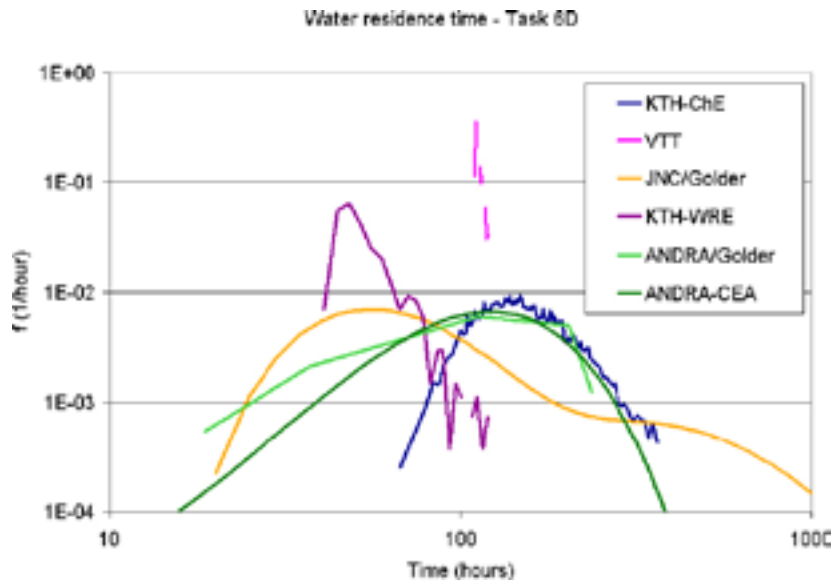


Figure 4-6. Task 6D water residence time distribution.

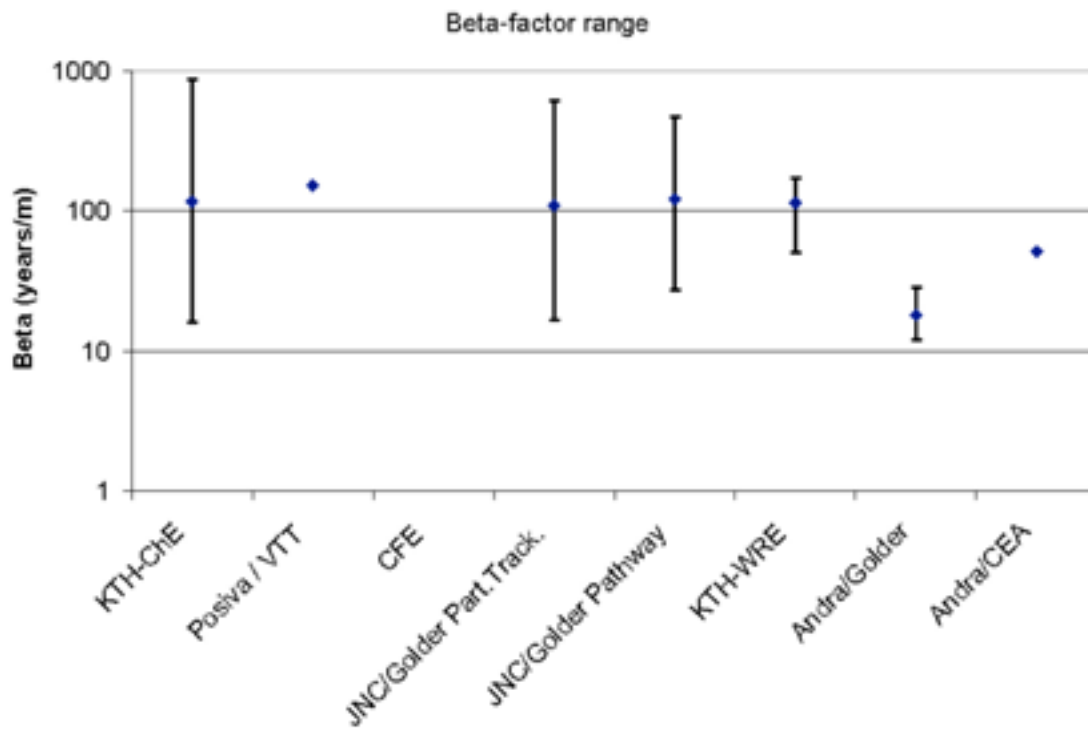


Figure 4-7. Reported ranges of  $\beta$  factor for Task 6D.

## 4.2 Task 6E

Figures 4-8 and 4-9 show a comparison of Task 6E I-129 and Am-241 breakthrough curves for a Dirac pulse at the western boundary.

The maximum release rates and times to 50% breakthrough at the western boundary for all calculated radionuclides corresponding to a Dirac pulse are shown in Figures 4-10 and 4-11.

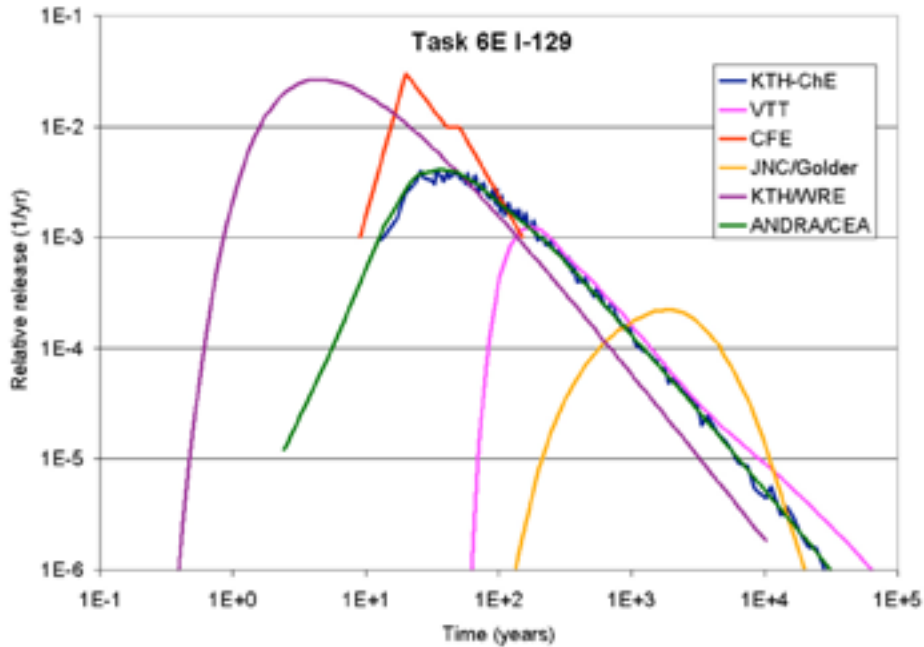


Figure 4-8. Task 6E I-129 breakthrough curves for a Dirac pulse at the western boundary.

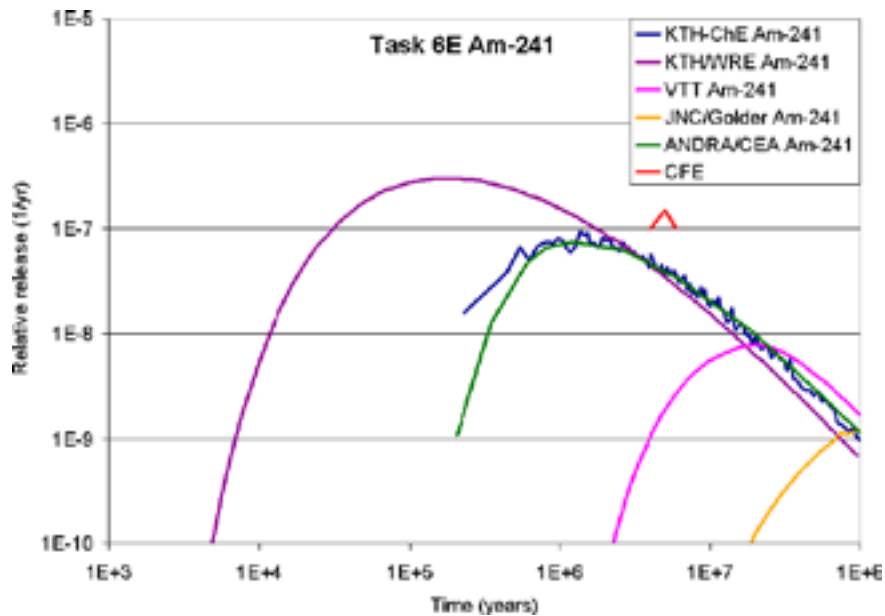


Figure 4-9. Task 6E Am-241 breakthrough curves for a Dirac pulse at the western boundary.

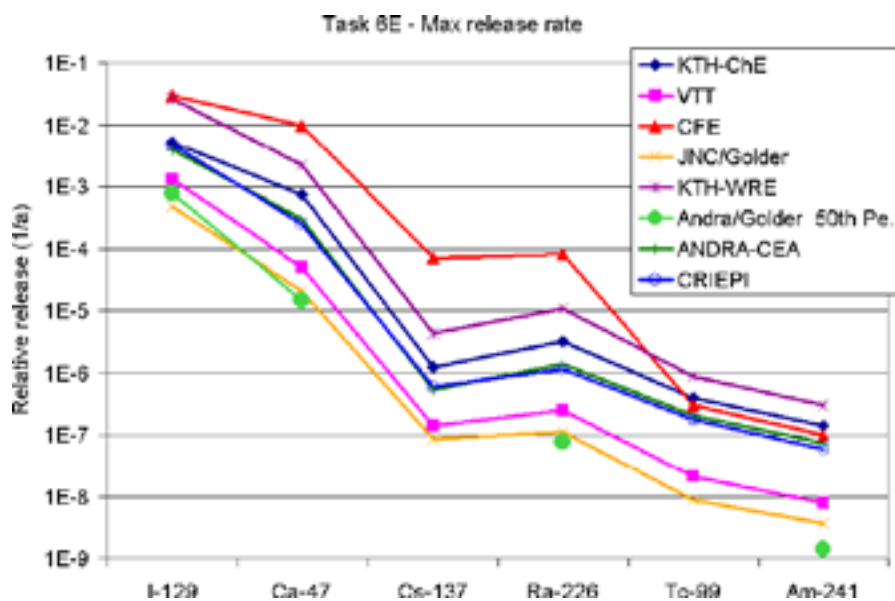


Figure 4-10. Task 6E maximum release rates at the western boundary for all calculated radionuclides corresponding to a Dirac pulse.

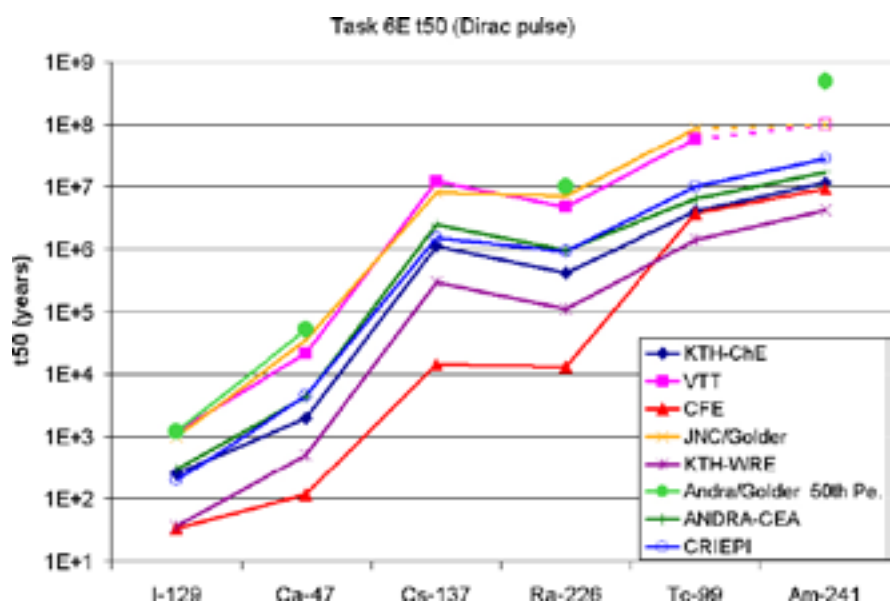


Figure 4-11. Task 6E times to 50% breakthrough at the western boundary for all calculated radionuclides corresponding to a Dirac pulse.

The initial reaction to Figures 4-8 to 4-11 is that the spread of results is rather large for such a tightly defined system. To investigate this, the water residence time distribution and ranges of  $\beta$  factors are shown in Figures 4-12 and 4-13. An important contribution to this diversity appears to be due to the order of magnitude differences in the  $\beta$  factors (Figure 4-13) since, when matrix diffusion and sorption dominates, the time for peak release is proportional to  $\beta^2$  and the maximum release to  $\beta^{-2}$  /European Commission 2005/. Also, differences are expected because of the wide range of modelling approaches used (Section 3).

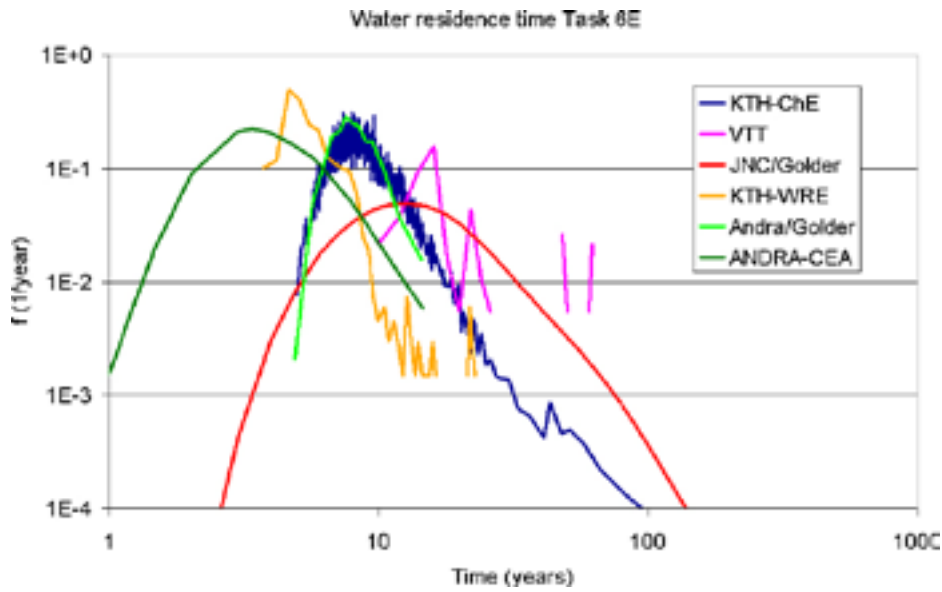


Figure 4-12. Task 6E water residence time distributions for the western boundary.

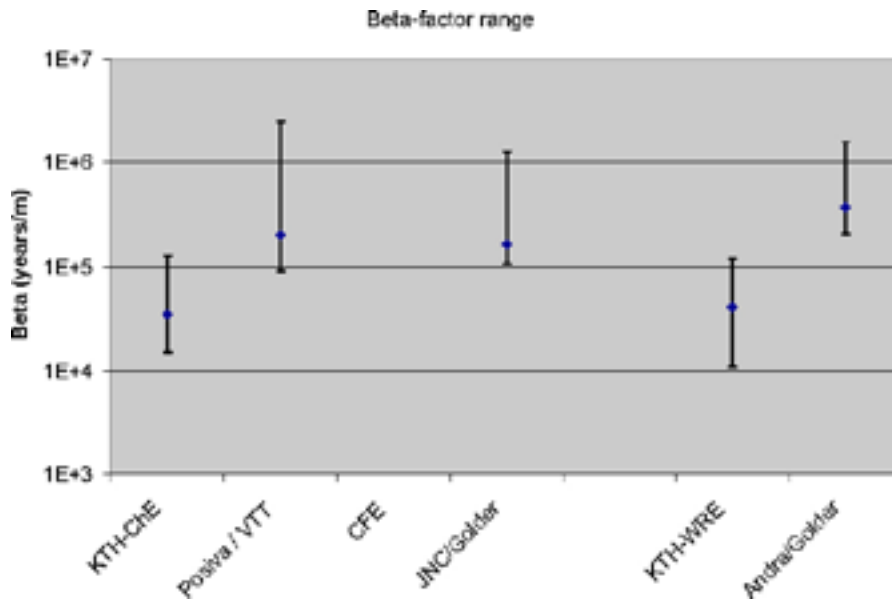


Figure 4-13. Task 6E  $\beta$  factors for the western boundary.

### 4.3 Task 6F

As discussed in Section 2.5, Task 6F consists of a series of “benchmark” studies on single features from the Task 6C hydrostructural model in order to improve the understanding of differences between the participating models.

As an example of the results, a compilation of I-129 breakthrough curves for Case A1 (travel time 0.1 y, Feature 1S) is shown in Figure 4-14. Somewhat surprisingly for such a simple and well-posed problem, the breakthrough curves have some differences.

Four of the modelling teams reported values for the  $\beta$  factor and these are shown in Table 4-1.

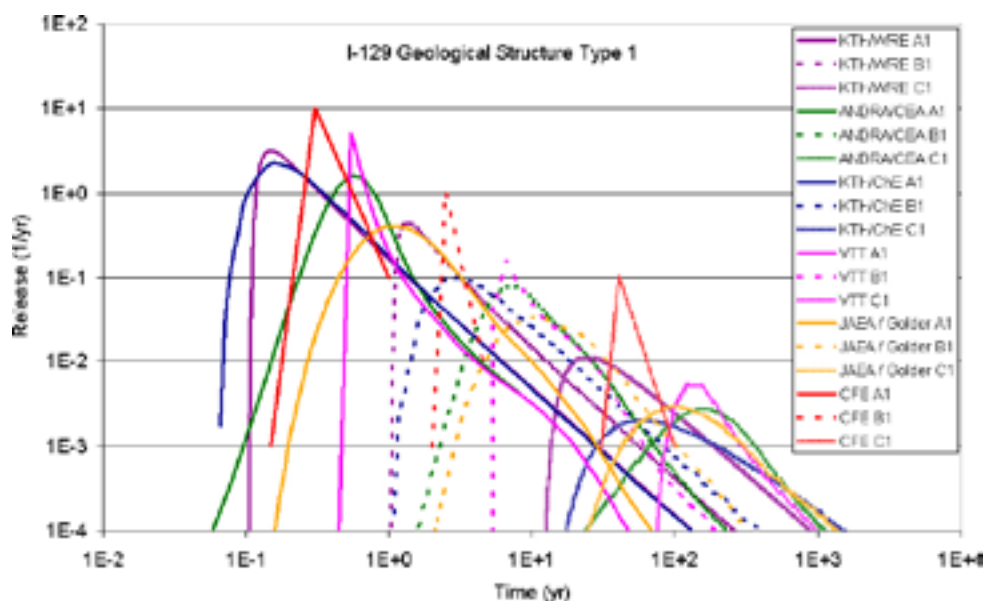


**Figure 4-14.** Task 6F breakthrough curves for I-129 migration in the Type 1 feature for a travel time of 0.1 years (Case A1).

**Table 4-1. Reported  $\beta$  factors for Task 6F Case A1 (Feature 1S, travel time 0.1 y).**

Modelling team	$\beta$ factor (y/m)
SKB-KTH-ChE	704
POSIVA-VTT	388
JAEA-GOLDER	648
SKB-KTH-WRE	775
ANDRA-CEA	388

For the simple geometry and flow specified in Task 6F  $\beta = 2 \tau/\varepsilon_i$  where  $\tau$  is the water travel time and  $\varepsilon_i$  is the transport aperture. As discussed in Section 2.7.6 for the purposes of this comparison it is assumed that the hydraulic and transport apertures are equal, whence for Case A1  $\beta = 775.2$ , which is close to three of the values in Table 4-1. It is presumed that the POSIVA-VTT and ANDRA-CEA teams defined  $\beta$  for a single fracture surface so that their value is reduced by a factor of two.

Based on the above reasoning it appears that  $\beta$  is not the primary cause of the differences among the breakthrough curves in Figure 4-14, but that it arises because of the different approaches used by the modelling teams.

Results for maximum release rate and time to 50% breakthrough for a Dirac pulse have been submitted by a number of groups, and these are shown in Figures 4-15 and 4-16 respectively. The spread of results arises from the wide range of modelling assumptions made by the modelling teams, as discussed in Section 3. Clearly there are significant modelling differences, which are also a component of the spread of results seen in Task 6E. This has implications for the Task 6 objectives in that modelling uncertainty can be seen to be an important element of the bridge between SC and PA modelling.



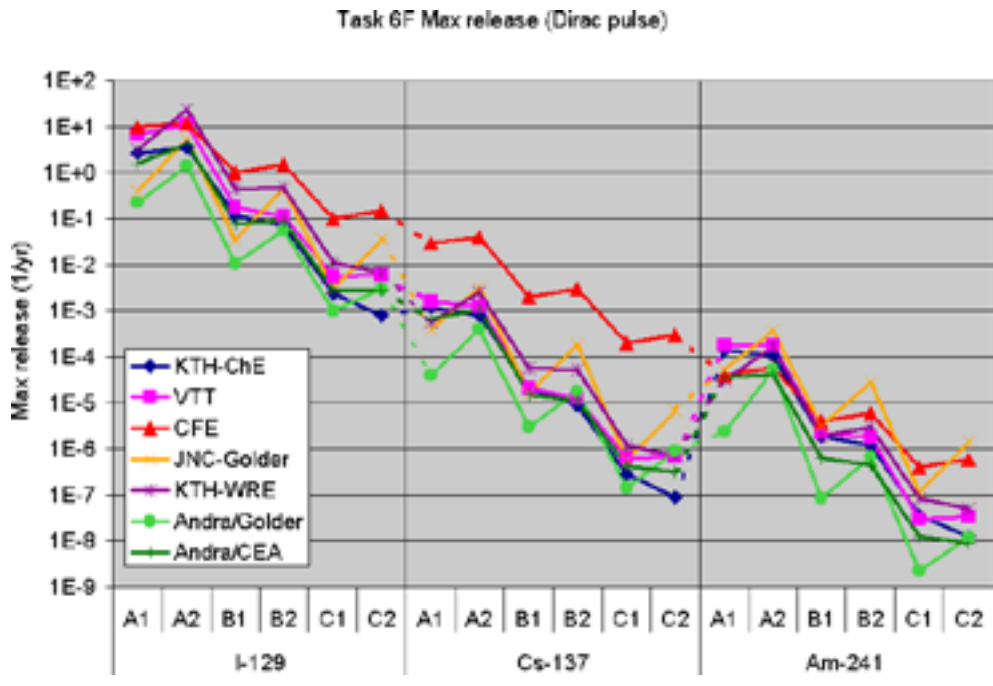


Figure 4-15. Task 6F maximum release rate for a Dirac pulse.

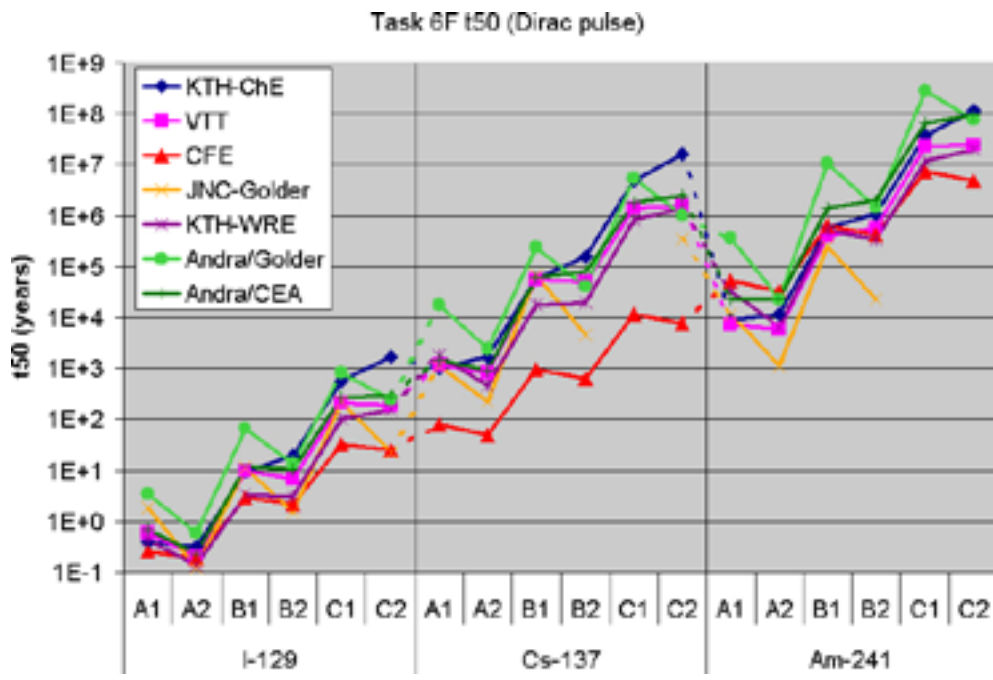


Figure 4-16. Task 6F 50% breakthrough time for a Dirac pulse.

## 5 Issues

This section draws upon discussions at the interactive sessions at the 20<sup>th</sup> and 21<sup>st</sup> Task Force meetings. The overall questions it addresses is:

- What have we learnt since the start of Task 6?
- What are the important outstanding issues?

A number of related issues about flow and transport in fractured rock were considered in the Task 6ABB2 review /Hodgkinson and Black 2005/ and are not repeated here.

This section is structured as follows. Sub-section 5.1 discusses issues related to the specification and implementation of Tasks 6D, 6E, 6F and 6F2. This is followed by four sub-sections (5.2 to 5.5) addressing the Task 6 objectives (see Subsection 1.3) in turn, followed by reflections on the Äspö Task Force experience (5.6) and the outlook for the future (5.7).

### 5.1 Task specification and implementation

#### 5.1.1 Philosophy of basing Tasks 6D and 6E on a hydrostructural model

The Task specifications assume that the Task 6C model is a true representation of the TRUE Block Scale site in order to act as a test bed so that Tasks 6D and 6E can explore a range of issues over and above the uncertainties related to the hydrostructural model. The reason for using the Task 6C model was to eliminate SC uncertainty, and thereby investigate how well PA can be carried out if the hydrostructural model is known. Thus Task 6D was intended to be a forward modelling exercise rather than an inverse modelling exercise. By modifying the Task 6C model, groups reinstated SC uncertainties. However, the JAEA-Golder team used the Task 6C model as specified and compared the Task 6D tracer modelling results with the C2 measurements, without trying to fit any of the parameters. In fact the comparison was reasonably good. However, this ground rule was not followed by all of the modelling teams.

It was argued by some teams that the synthetic structures including the background fractures should not be included in Task 6D because they were just one realisation of a statistical distribution, and it is therefore not appropriate to include them when comparing with the result of a specific experiment.

In practice this was not too much of a problem as the location of the C2 tracer test was selected to be such that the flow was mainly along highly transmissive and connected structures, and this was confirmed by sensitivity analyses in which simulations were made with and without the background fractures.

A number of teams chose to calibrate the Task 6C model, primarily the transport apertures of the deterministic structures, to the C2 test results. This was possibly partly due to the confusion in the aperture specifications (see 4.1.2). As a consequence, the models used in Task 6E differed between the groups.

It was argued by the SKB-KTH-ChE team that the use of complex representations of fracture geometry, as in the Task 6C model, might not be the best way to proceed in future. A more non-representational approach focussing on the understanding of the statistics of flow-wetted surface proportioning and flow channelling may be more appropriate. For example, different assumptions of flow geometry made during the construction of conceptual models of the fracture system may give rise to strongly biased SC models. Parameters derived from these SC models could potentially have important consequences when subsequently used in PA-modelling.

### 5.1.2 Apertures

It appears from this review that in general the Task specifications were sufficiently clear and detailed that they could be implemented by all of the modelling teams.

One exception to this rule was a potential ambiguity regarding the aperture values supplied in the task specifications. For Task 6D and Task 6E, based on the Task 6C model, these were hydraulic apertures, and the ratio of the transport aperture to the hydraulic aperture was specified to be 0.125. For Task 6F most modelling teams assumed that the hydraulic and transport apertures were equal, even though the features were taken from the Task 6C model. Thus the de facto specification for Task 6F was that the hydraulic and transport apertures were equal, and the JAEA-Golder team re-ran their calculations to fit in with this.

The apertures used in the task specifications were derived using Tom Doe's law, which assumes that they are proportional to the square root of the transmissivity. This was in keeping with the philosophy of the Task 6C specification, which was to define a deterministic hydrostructural model. It would be interesting to examine the sensitivity of this assumption, for example by considering a cubic law.

### 5.1.3 Additional performance measures and report structure

It is relevant to consider whether the additional performance measures and the recommended report structure proved useful, and whether any further performance measures might have been beneficial for understanding and inter-comparison purposes.

In particular, since the flow path geometries are the basis of the transport modelling it would be useful to be able to compare these. While it is possible to make a qualitative visual comparison of the flow paths calculated by some of the different groups, it would have been useful to have a more quantitative comparison, for example using Table 5-1 of flow path statistics (adapted from /Poteri 2006/). For example, this would help to clarify the approximations made by teams modelling the system using continuum codes.

It would have been a more stringent test of the models if concentration had been included as a performance measure in Task 6D, which takes account of the dilution in the pumped borehole.

Also, for Task 6E it would have been useful to have included a sensitivity study in which the source region is located in background fractures, in order to draw inferences about the extent of retention in the background fractures from the waste canisters to the major flowing features.

From the perspective of the Task Force secretariat, the recommended report structure was based on previous experience and proved very useful.

**Table 5-1. Table of flow path statistics.**

Path	Probability (%)	Flow paths at structure level	Path length range
Path 1	7.4	23D → 22D → 20D → 21D	
Path 2	0.4	23D → 22D → 20D → 2403C → 21D	
Path 3	10.0	23D → 1925B → 21D	
Path 4	68.8	23D → 1925B → 21D → 20D → 21D	
Path 5	13.4	23D → 1925B → 756C → 20D → 21D	

#### 5.1.4 Was the C2 test sufficiently representative?

The locations and flow rates for the ‘C’ tracer tests were chosen in order to maximise the tracer recovery. It is relevant to consider whether this biases our understanding. For example, waste canisters are likely to be placed in averagely fractured rock, rather than in the higher transmissivity features involved in the C2 tracer test. We need to be careful about drawing conclusions about average transmissivity features without appropriate evidence. Also, it is interesting to consider whether we could learn something useful about the connectivity of the fracture system from tracer tests where there was little or no recovery /Dershowitz et al. 2001/.

For philosophical reasons related to producing a robust performance assessment based on pessimistic assumptions, some organisations are only interested in the most transmissive features. However, there is an increasing trend to complement this approach with more realistic PA, for example in the EC NF-PRO project ([www.nf-pro.org](http://www.nf-pro.org)). This is related to the need to be able to present a Safety Case explaining the likely evolution of the system and its associated uncertainties. If this more realistic approach were to be followed then, in addition to studying the most highly transmissive features, it would be appropriate to examine flow and transport in background fractures that are expected to provide the major barrier between waste canisters and highly conducting features. Once radionuclides reach high transmissivity features they are likely to migrate relatively rapidly because of the high flow rate and low  $\beta$ . It is understood that an experiment in an average fracture is currently underway at Äspö.

On the other hand, the primary aim of the TRUE programme is to understand retention processes, rather than to determine specific parameter values. From this perspective it is the understanding of interactions with the immobile zones that is the most important aspect, which it is more practical to examine on shorter time scales in high transmissivity features.

Of course, site investigations produce a lot of data on the transmissivity of tight fractures, and this can be used in PA on the assumption that the retention processes are the same as for more transmissive features. It is interesting to speculate what kind of experiments might be done that would be of most use to PA.

A final characteristic of the C2 tracer test relevant to this discussion is that it was performed with forced injection at the source location, which could have created additional connected pathways and led to additional dispersion.

#### 5.1.5 Flow modelling

It is pertinent to consider how well the Task 6C hydrostructural model can be implemented in non-DFN codes such as continuum and channel network codes.

As discussed in Section 5.1.3 above, the calculated flow path lengths between source and sink for the C2 tracer test can be used as a performance measure for the accuracy of the flow modelling. From the information available, it appears that the flow pathways derived from different DFN codes are similar.

For continuum flow modelling the Task 6D flow path length indicates that the accuracy of flow modelling depends on the discretisation length scale. For example the ANDRA-Golder Task 6D flow simulations with a 2 m discretisation gave a path length of 25.3 m, which is to be compared flow paths varying between about 59 m and 74 m in the discrete fracture modelling performed by the Posiva-VTT team. In contrast, the SKB-CFE-SF team using continuum modelling with a 0.5 m grid spacing in the vicinity of the C2 test, produced paths which visually resemble the Posiva-VTT discrete fracture results.

The tentative conclusion from this is that either discrete fracture flow modelling should be used for the Task 6D and Task 6E cases, or continuum modelling with a grid size of 0.5 m or less.

In fact it is not just a matter of cell size, but also how discrete features are implemented in continuum models. For example the ANDRA-Golder and SKB-KTH-WRE teams used the Oda tensor method and the SKB-CFE-SF team used the GEHYCO method. Also, finite-element, and finite-volume approaches resolve the space between fractures in different ways.

Similar questions arise in connection with the representation of a discrete fracture network with channel network models. The SKB-KTH-ChE team found that it was possible but difficult to implement the Task 6C model in CHAN3D and that this exercise resulted in ideas as to how the code could be developed further.

Overall, it is preferable to implement the discrete fracture hydrostructural model in a DFN code (preferably also including channels within features) rather than continuum and channel network codes.

### **5.1.6 Geological Structure Type**

The definition and specification of a geological structure type (GST) for each structure has been a major innovation of the present exercise. It has allowed the effects of geologically realistic features to be studied. It is useful to reflect on how this was implemented by the modelling teams, and its impact on radionuclide transport.

Structure type is important on the experimental timescale because of the importance of immobile zones with the highest porosity and diffusivity (fault gouge and cataclasite), which only occur for Type 1 structures. For example, sensitivity studies carried out by the JAEA-Golder team confirm for Task 6D that if Type 2 structures are dominant then tracer retention is reduced.

In general, on PA timescales diffusion and sorption are expected to be dominated by intact rock away from the fracture surface and thus GST is less important. However, there are some situations where gouge can be important on PA timescales. For example the non-uniform distribution of gouge can lead to channelling, which is important on PA timescales and thus the GST concept can be applied in PA as an indicator of channelling.

### **5.1.7 Channelling**

Three teams, SKB-KTH-ChE, JAEA-Golder and SKB-CFESF, included the effect of channelling within structure planes. There is extensive evidence that this is an important phenomenon at Äspö and similar sites. However, efforts to include it are hampered by a dearth of relevant information. It remains an important issue for future research.

A key issue is whether flow-wetted surface can be derived from SC experiments and used directly in PA. Further data is required to fully resolve this issue but there are a number of difficulties including the fact that it is experimentally difficult to separate the effect of the matrix parameter group and beta, and that SC and PA flow fields are usually very different. The most relevant SC data for flow-wetted surface appears to be that becoming available from resin injection experiments.

Moreover, it is often assumed that only a fraction of the fracture surface area is active. However, consider a channel within the gouge of a fracture. On SC timescales flow takes place within the channel and diffusion occurs approximately perpendicular to the fracture from the channel into the immobile zones. However, on PA timescales, there is time for tracers to diffuse through the gouge in the remainder of the fracture and also in two dimensions through high-porosity near-fracture zones. Thus on PA timescales, for sufficiently low flows, the entire immobile pore space could be accessible to diffusion even though flow only takes place in channels covering a fraction of the fracture surface.

### 5.1.8 Complexity Factor

The second innovation of the Tasks 6C hydrostructural model was the specification of a complexity factor for each structure. While in principle this concept could be implemented in a number of ways, it appears that to date the modelling teams have included the complexity factor by increasing the flow wetted surface area of structures.

This implementation may be appropriate for experimental timescales when the diffusion penetration depth is less than the separation between individual fractures of the complex structures. However, for PA timescales this implementation leads to non-conservative double counting. Provided that penetration depths are considerably greater than sub-fracture separations it is expected that the complexity factor would have less impact at PA timescales assuming that the total transmissivity of the structure is accounted for.

A further issue is that it appears that most modelling teams have implicitly assumed that the sub-fractures are of equal transmissivity and the flow and transport is thereby shared equally. In fact it is far more likely that there is a distribution of sub-fracture transmissivities, for example a log-normal fracture distribution is assumed in related contexts. As shown in the Task 6F2 sensitivity study by /Poteri 2006/ and discussed in Section 3.5.4, if the transmissivity of one parallel fracture is more than twice the others it will dominate the transport. This is a non-linear effect in that not only does one of the fractures have a higher flow rate, but this higher flow rate also implies a lower value of  $\beta$  and thus less retention. Consequently in most circumstances where there are sub-parallel fractures with a distribution of transmissivities, a single fracture pathway will be expected to dominate the breakthrough curve.

In the Task 6C model, the complexity of features was not included in the flow model, but the complexity factor was added as a characteristic to be accounted for in transport modelling. It is clear that this is not a fully consistent approach. The most appropriate experimental and theoretical approaches to complexity remain a topic for future research.

### 5.1.9 Visual presentation

The modelling team reports demonstrate the power of visual presentation of quantitative information. A number of teams have presented visualisations of the fracture system and in some cases these have been augmented by superimposed head and flow fields. Moreover, the Posiva-VTT team have developed new visual representations to throw light on the variation of  $\beta$  as a function of path length and the contribution of different geological materials to the overall breakthrough curve.

All these visualisations considerably enhance the understanding of the system and the modelling results, and it is hoped that the best practice used by the modelling teams will be widely adopted in the future.

## 5.2 Simplifications for PA modelling

The following conclusions regarding simplifications for PA modelling can be drawn from a range of studies conducted as part of Task 6.

- Diffusion and sorption into intact rock are the primary retention processes on PA timescales.
- Diffusion and sorption into higher porosity near-fracture immobile zones provide secondary retention and can be approximated by a retardation factor on PA timescales.
- Geological Structure Type is a useful concept for classifying features, but does not have a first-order influence on PA.

The above points have been taken forward within the SKB programme.



Important outstanding issues regarding simplifications for PA modelling include:

- Appropriate ways of representing flow path geometry based on SC information, and how to extrapolate and simplify this for PA.
- Quantification of the  $\beta$  factor under PA conditions. While there is considerable uncertainty in the value of  $\beta$  under PA conditions, it should be possible to derive robust bounds on its magnitude.
- The degree of connectivity between flow paths in different features that it is reasonable to assume for PA. For example, a single connected flow path from the repository to the surface could be viewed as a rather an extreme assumption, especially when there is evidence for compartmentalisation.
- The relative importance of background fractures, for example in the vicinity of waste canisters, in providing retardation on a PA timescale.
- The PA impact of not assuming linear reversible sorption.
- The weight of evidence, e.g. from natural analogues, for the assumption that diffusion occurs for an unlimited distance into the intact rock.

Underlying all these issues, the development and use of micro-structural models has provided a useful bridge between SC and PA modelling, which has improved our understanding of what is important for PA timescales.

### **5.3 Tracer test constraints on PA parameters**

The following conclusions regarding tracer test constraints on PA parameters can be drawn from a range of studies conducted as part of Task 6.

- Immobile zone parameters from tracer tests are not first-order contributors to PA retardation.
- However, tracer tests are invaluable for confirming our understanding of the dominant transport processes for PA.
- Tracer tests provide useful information for quantifying transport aperture and flow wetted surface.
- All (even null) tracer test results, and also hydraulic (especially cross-hole) test results, can provide useful constraints on hydrostructural models.

Important outstanding issues regarding tracer test constraints on PA parameters include:

- Current hydrostructural models tend to be over-connected. For example, the Task 6C model could not explain the lack of conductivity in some parts of the block. This should be addressed in future work, for example by constraining the model using null signals from cross-hole tests.
- In the Task 6C model it is assumed that the background fractures and fracture zones belong to separate distributions. It is an open question as to whether they are both essentially part of a universal distribution.
- Similarly, an important unresolved issue is the transmissivity – length correlation.

### **5.4 Support to the design of SC programmes for PA**

The following conclusions regarding supporting the design of SC programmes for PA have emerged from a number of studies during Task 6.

- Hydrostructural models are an essential link between SC and PA modelling.

- The Task 6C hydrostructural model is a more comprehensive approach to quantitatively describing a volume of fractured rock than has been achieved hitherto. Work on hydrostructural modelling should continue, especially regarding connectivity and eventually the inclusion of channelling.
- PA requires direct measurements of diffusion and sorption parameters on intact rock samples, and also hydraulic tests on background fractures.

Important outstanding issues regarding supporting the design of SC programmes for PA include:

- A key issue is how to improve the experimental characterisation of the flow and diffusion of solutes within structures. Resin injection experiments can throw light on these processes, for example around tracer injection and withdrawal boreholes. However, resin injection results should be regarded as conceptual support rather than numerical input into models. An alternative perspective is to focus directly on the dynamical behaviour of water along transport paths rather than investigating flow geometries.
- Channelling within fractures remains a key issue but there is a dearth of quantitative information. A promising technique /Bourke 1987/ is to drill injection and withdrawal boreholes in the plane of a feature in order to give better control of the boundary conditions through having line sources and sinks. In this way, all channels can be activated.
- There are arguments against carrying out tracer tests in URLs, because it is desirable to perform them under natural conditions without large gradients. Thus alternative approaches should be considered, for example carrying out tracer tests from boreholes drilled from the surface.
- It is relevant to consider alternative tracer test designs. For example a useful experiment would be the measurement of passive tracer dilution in a borehole while pumping other boreholes (multiple reciprocal tracer dilution test). Also, as considered during Task 5 /Rhén and Smellie 2003/, a natural geochemical end member could be used to investigate larger-scale flow rates and dynamical behaviour.
- There are some additional issues that need to be considered in support of the safety case, which would benefit from SC experiments. These include scenarios involving the penetration of oxygenated water into a repository, and phenomena that can block matrix diffusion.

## 5.5 Improving understanding using SC models

The following conclusions regarding improving understanding using SC models have emerged from studies during Task 6.

- Task 6 has advanced the understanding of the impact of near-fracture-surface immobile zones on retention. For example, gouge is important for retention on SC timescales.
- In general the Task 6 experience has emphasised the importance of geological information, for example in understanding transport pathways and integrating understanding into a hydrostructural model.
- Three-dimensional hydraulic models of complex features, such as the JAEA-LBNL SC model used in Task 6A /Doughty and Uchida 2004/, are useful for enhancing confidence and understanding, and for the development of equivalent PA parameters.
- In general, the approach of using parameter groups, such as  $\beta$ , has proved a useful aid to understanding.
- $\beta$  tends to reach a plateau when major flow paths are reached, demonstrating the importance of near-source low-flow features /Poteri 2006/.
- Transport through high complexity factor features is mainly through a single path with the highest water flux /Poteri 2006/.

- Two-dimensional diffusion from channels through gouge and other stagnant zones could effectively increase the surface area between mobile and immobile zones on PA timescales.
- Task 6 has provided a good starting point for new thinking on understanding the dynamics of water flow and tracer transport in fractured rocks, which is being taken forward in Task 7.

## 5.6 The Äspö Task Force experience

Task 6 of the Äspö Task Force has been a valuable learning experience for all concerned, in particular:

- It has been an excellent forum for exchange of ideas and for the training of researchers entering the field.
- Through participating in Task Force meetings, modellers have come to appreciate the strengths and weaknesses of alternative approaches. It has proved useful to augment presentations of results with interactive discussion sessions.
- There has been a surprisingly wide range of models and approaches, but they have all been based on the same underlying physics and the same data.
- In previous tasks the emphasis was on the use of in-house models and there was unspoken competition among modelling teams. In Task 6 there has been a greater sharing of ideas, openness and transparency.
- The involvement of external review guards against ‘group think’. For Task 6, the reviewers started earlier than for previous tasks, and were more proactive.
- It has proved difficult for the modelling teams to produce reports by the agreed dates. The report format has proved useful in improving the clarity of the modelling team reports.
- There is a need to publish more in the open literature. This has been recognised by the secretariat, and there are plans to submit a suite of articles on Task 6 to a peer-reviewed journal.
- The Task Force is a civilised forum with respect for alternative views, reflecting the character of its Chairman, Gunnar Gustafson.

## 5.7 Outlook

The overall objective of Task 6 is to provide a bridge between site characterization (SC) and performance assessment (PA) approaches to solute transport in fractured rock. One reason that a bridge is needed is that SC and PA view the problem from different perspectives. For SC it is natural to focus on where most of the water flows, and thus most effort is placed on characterising structures with the highest transmissivity. In contrast to this, PA is concerned with assessing barriers to flow and transport, for example the averagely fractured rock around waste canisters which constrains the influx of corrosive species and the out flux of radionuclides.

In this situation, some SC data, for example from tracer tests, will not be directly applicable to PA. However, this does not diminish their value for PA, which lies in their contribution to confirming our understanding of the important flow and transport processes. From this perspective, a key element of the bridge between SC and PA is the understanding of processes. Once processes are understood, it is possible to measure or estimate the relevant parameter ranges required for PA.

For example, Task 6 has improved our understanding of the importance of diffusion into near-fracture immobile zones during tracer experiments. Armed with this knowledge, we can obtain the diffusion and sorption parameters required for PA by direct measurements on intact rock.

A second example is the understanding of the importance of the  $\beta$  factor for transport in fractured rock. This insight tells us that fractures with the lowest flows provide sufficient time for the largest retention to occur. Consequently low transmissivity fractures between waste canisters and major flowing zones should provide a significant retardation barrier whose PA impact can be estimated from hydraulic measurements on background fractures coupled with the diffusion and sorption characteristics of intact rock.

An intrinsic theme of Task 6 has been that growing computer power brings SC and PA modelling closer together, and thus in future performance assessments can use of more complex representations of the system, although the realism is constrained by the availability of sufficient data.

For example, Task 6, in common with most other radionuclide transport modelling exercises, has assumed instantaneously linear reversible sorption. In the past this assumption has been necessitated by the lack of availability of suitable models, data and computer power together with a desire for simplicity. Advances are being made in reactive-transport modelling, which in the future offers the opportunity of treating retention processes from a more fundamental perspective. Combined experimental and reactive transport modelling studies for key radionuclide-rock systems would help to increase confidence in the Safety Case.

Task 6 has stimulated a debate about what investigations should be done at URLs and what should be done from the surface. There are valid arguments for performing tracer experiments in boreholes drilled from the surface; in particular the hydraulic distortion of tunnels is avoided. However, they are more difficult to perform, for example to drill boreholes with specified separations. A related issue is to distinguish between issues that are generic and those that need to be performed at potential repository sites, in order to avoid too many penetrations. Finally, there is a need to design experiments with a consistent philosophy, for example recognising the different zones of influence of different techniques.

There are still areas where there are significant uncertainties in our understanding. One of these concerns the infrastructure of features, in particular channelling and flow wetted surface. However experiments and modelling have the power to reduce these uncertainties, for example by building on resin injection experiments at Äspö and the analysis of cross-hole responses in Task 7 /Ahokas and Koskinen 2005/. Indeed, Task 7 could be regarded as the start of a paradigm shift, where increased focus is placed on understanding details of the flow field at relevant scales.

An important challenge for radioactive waste disposal organisations is to move from scientific understanding to engineering. For example this is happening at SKB. This transition recognises that we will never know everything about a disposal system and that to take things forward there is a need to take decisions despite the uncertainties.

### ***Acknowledgements***

I would like to thank the Task Force secretariat for their help and support in conducting this review, and the Task Force participants for their openness and forbearance during the review process. In particular I would like to thank Mark Elert for providing the inter-comparison figures shown in Section 4.

## References

- Ahokas H, Koskinen L, 2005.** Äspö Task Force on Modelling of Groundwater Flow and Transport of Solutes: Task 7: Modelling the KR24 long-term pumping test at Olkiluoto.
- Andersson P, Byegård J, Holmqvist M, Skålberg M, Wass E, Widestrand H, 2001.** Äspö Hard Rock Laboratory. True Block Scale Project. Tracer test stage. Tracer tests, Phase C. SKB IPR-01-33. Svensk Kärnbränslehantering AB.
- Andersson P, Dershowitz W, Hermanson J, Meier P, Tullborg E-L, Winberg A, 2002a.** Final report of the TRUE Block Scale project, 1. Characterisation and model development. SKB TR-02-13. Svensk Kärnbränslehantering AB.
- Andersson P, Byegård J, Winberg A, 2002b.** Final report of the TRUE Block Scale project, 2. Tracer tests in the block scale. SKB TR-02-14. Svensk Kärnbränslehantering AB.
- Bäckblom G, Olsson O, 1994.** Program for Tracer Retention Understanding Experiments. PR 25-94-24. Svensk Kärnbränslehantering AB.
- Benabderrahmane H, Dershowitz W, Selroos J O, Uchida M, Winberg A, 2000.** Task 6: Performance Assessment Modelling Using Site Characterisation Data (PASC), November 28, 2000.
- Black J H, Hodgkinson D P, 2005.** Äspö Task Force on Modelling of Groundwater Flow and Transport of Solutes: Review of Task 6C. SKB R-05-33. Svensk Kärnbränslehantering AB.
- Bourke P J, 1987.** Channelling of flow through fractures in rock, Ed: A Larsson, Proceedings of the SKI/NEA GEOVAL-1987 Symposium, 167–177.
- Byegård J, Albinsson Y, Skarnemark G, Shalberg M, 1992.** Field and laboratory studies of the reduction and sorption of technetium VII. *Radiochim. Acta* 58/59, 239–244.
- Cheng H, Cvetkovic V, 2006.** Äspö Task Force on Modelling of Groundwater Flow and Transport of Solutes: Modelling of Task 6D, 6E and 6F, flow and transport simulations in fracture networks. SKB IPR-06-20. Svensk Kärnbränslehantering AB.
- Crawford J, Moreno L, 2006.** Äspö Task Force on Modelling of Groundwater Flow and Transport of Solutes: Modelling of Task 6D, 6E and 6F, using CHAN3D. SKB IPR-06-19. Svensk Kärnbränslehantering AB.
- Cvetkovic V, Selroos J O, Cheng H, 1999.** Transport of reactive tracers in rock fractures, *J. Fluid Mech.*, 378, 335–356, 1999.
- Cvetkovic V, Cheng H, Selroos J O, 2000.** Evaluation of Tracer Retention Understanding Experiments (first stage) at Äspö, SKB ICR-00-01. Svensk Kärnbränslehantering AB.
- Cvetkovic V, Haggerty R, 2002.** Transport with multiple-rate exchange in disordered media. May 2002, *Phys. Rev. E*, Vol. 65, 051308.
- Dershowitz W, Foxford T, Sudicky E, Shuttle D, Eiben T, 1999.** PAWorks: Pathway Analysis for Discrete Fracture Networks with LTG Solute Transport. User Documentation. Version 1.5. Golder Associates Inc., Seattle.
- Dershowitz W, Doe T, Fox A, Uchida M, Cladouhos T, 2001.** Learning from recovery: Thoughts on Feature A transport experiments, *in* First TRUE Stage – Transport of solutes in an interpreted single fracture: Proceedings from the 4<sup>th</sup> International Seminar Äspö, September 9–11, 2000, SKB TR-01-24. Svensk Kärnbränslehantering AB.



**Dershowitz W, Winberg A, Hermansson J, Byegård J, Tullborg E L, Andersson P, Mazurek M, 2003.** Äspö Hard Rock Laboratory, Äspö Task Force on modelling of groundwater flow and transport of solutes, Task 6C, A semi-synthetic model of block scale conductive structures at the Äspö Hard Rock Laboratory. SKB IPR-03-13. Svensk Kärnbränslehantering AB.

**Dershowitz W, Shuttle D, Uchida M, 2004.** Task 6A, 6B and 6B2. GoldSim and FracMan/LTG Modeling: Performance Assessment Modeling Using Site Characterisation Data (PASC). SKB IPR-04-32. Svensk Kärnbränslehantering AB.

**Dershowitz W, Uchida M, Fox A, Lee G, Van Fossen M, 2006.** Äspö Task Force on Modelling of Groundwater Flow and Transport of Solutes: Discrete Fracture Network Flow and Transport Modeling at the Rock Block Scale: Äspö Modelling Task Force – Task 6D, 6E, 6F and 6F2. SKB IPR-06-22. Svensk Kärnbränslehantering AB.

**Doughty C, Uchida M, 2004.** PA Calculations for Feature A with Third-dimension Structure Based on Tracer Test Calibration. SKB IPR-04-33. Svensk Kärnbränslehantering AB.

**Elert M, Selroos J O, 2002.** Task 6D Modelling task specification. Version 1.0. Äspö Task Force Technical Note, 29 November 2002.

**Elert M, Selroos J O, 2004a.** Task 6D Specification of additional performance measures. Version 1.0. Äspö Task Force Technical Note, 6 February 2004.

**Elert M, Selroos J O, 2004b.** Task 6E Modelling task specification. Version 3.0. Äspö Task Force Technical Note, 20 January 2004.

**Elert M, Selroos J O, 2004c.** Task 6F Sensitivity analysis: Modelling task specification: Simplified ‘Test Bench’ transport calculations. Version 3.0. Äspö Task Force Technical Note, 15 December 2004.

**Elert M, Selroos J O, 2004d.** Task 6F2 Sensitivity analysis: Modelling task specification: Additional tasks. Version 1.0. Äspö Task Force Technical Note, 15 December 2004.

**European Commission, 2005.** Treatment of radioactive transport in geosphere within safety assessments (RETROCK): Final Report. European Commission Nuclear Science and Technology report EUR 21230 EN.

**Fournio A, Grenier C, Mouche E, Benabderrahmane H, 2003.** Qualification and Validity of a Smeared Fracture Modelling Approach for Transfers in Fractured Media. Priceeding of: Groundwater in Fractured Rocks, 15–19 September 2003, Prag (Czech Republic). IHP-VI, Series on Groundwater, No. 7.

**Goldsim, 2004.** Goldsim Contaminant Transport Module. See [www.GoldSim.com](http://www.GoldSim.com).

**Grenier C, Bernard-Michel G, 2006.** Äspö Task Force on Modelling of Groundwater Flow and Transport of Solutes: Modelling of Task 6D, 6E, 6F and 6F2, using Cast3M code. SKB IPR-06-18. Svensk Kärnbränslehantering AB.

**Grenier C, 2004.** Modelling Transfers in a Single Fracture System: From Site Characterisation to Performance Assessment Models. Contribution to Task 6A and 6B from the Äspö Modelling Task Force Exercise. SKB IPR-04-37. Svensk Kärnbränslehantering AB.

**Gylling B, 1997.** Development and Applications of the Channel Network Model for Simulation of Flow and Solute Transport in Fractured Rock. Ph.D. Thesis, Department of Chemical Engineering and Technology, Royal Institute of Technology.

**Harbaugh A W, Edward R B, Marry C H, Mcdonald M G, 2000.** MODFLOW-2000, The U.S. Geological Survey Modular Ground-water Model – user guide to modularization concepts and the ground-water flow process. U.S Geological Survey, OFR 00-92, 2000.



- Hodgkinson D P, Black J H, 2005.** Äspö Task Force on Modelling of Groundwater Flow and Transport of Solutes: Review of Tasks 6A, 6B and 6B2. SKB TR-05-14. Svensk Kärnbränslehantering AB.
- Holmén J G, 1992.** A three-dimensional finite difference model for calculation of flow in the saturated zone. Department of quaternary geology, Uppsala University, Uppsala, Sweden, ISBN 91-7376-119-2, ISSN 0348-2979.
- Holmén J G, 1997.** On the flow of groundwater in closed tunnels. Generic hydrogeological modelling of nuclear waste repository, SFL 3-5. SKB TR-97-10. Svensk Kärnbränslehantering AB.
- Holmén J G, Forsman J, 2005a.** Äspö Modelling Task Force: Modelling of Tasks 6D and 6E: Draft Golder Associates Report for ANDRA, GRP 0 GOL 04 – 21-3101/A, Version 25.
- Holmén J G, Forsman J, 2005b.** Äspö Modelling Task Force: Modelling of Tasks 6F: Draft Golder Associates Report for ANDRA, G RP 0 GOL 04 – 21-3101 /A.
- Holmqvist M, Andersson P, Trick T, Fierz T, Eichinger L, Scholtis A, 2000.** Test of new possible non-reactive tracers – experimental description and evaluation. Äspö Hard Rock Laboratory, ITD-00-14.
- Jacob A, 2004.** Matrix Diffusion for Performance Assessment - Experimental Evidence, Modelling Assumptions and Open Issues. Paul Scherrer Institut report 04-08, ISSN 1019-0643.
- Miller, M, Alexander, R, Chapman N, McKinley I, Smellie J, 2000.** Geological Disposal of Radioactive Wastes and Natural Analogues: Lessons from Nature and Archaeology. Waste Management Series, Volume 2. Pergamon, Elsevier Science.
- Moreno L, Tsang Y W, Tsang C F, Hale F V, Neretnieks I, 1988.** Flow and tracer transport in a single fracture. A stochastic model and its relation to some field observations, Water Resources Research, 24, pp. 20033-3048.
- Moreno L, Neretnieks I, 1993.** Fluid flow and solute transport in a network of channels, Journal of Contaminant Hydrology, 14, 163–192.
- Oda M, 1985.** Permeability Tensor for Discontinuous Rock Mass. Geotechnique, 35:483–495, 1985.
- Outters N, Shuttle D, 2000.** Sensitivity analysis of a discrete fracture network model for performance assessment of Aberg. SKB R-00-48. Svensk Kärnbränslehantering AB.
- Poteri A, 2006.** Äspö Task Force on Modelling of Groundwater Flow and Transport of Solutes: Modelling of Task 6D, 6E, 6F and 6F2 using the Posiva streamtube approach. SKB IPR-06-17. Svensk Kärnbränslehantering AB.
- Poteri A, Billaux D, Dershowitz W, Gómez-Hernández J J, Cvetkovic V, Hautjärvi A, Holton D, Medina A, Winberg A, 2002.** Final report of the TRUE Block Scale project, 3. Modelling of flow and transport, SKB TR-02-15. Svensk Kärnbränslehantering AB.
- Rhén I, Smellie J, 2003.** Task force on modelling of groundwater flow and transport of solutes: Task 5 Summary Report. SKB TR-03-01. Svensk Kärnbränslehantering AB.
- Robinson P C, 1984.** Connectivity, Flow and Transport in Network Models of fractured media, Ph.D. Thesis, St. Catherine's College, Oxford University, UKAEA Report TP 1072.
- SKB, 2004.** Äspö Hard Rock Laboratory: Annual Report 2003. SKB TR-04-10, Svensk Kärnbränslehantering AB.
- Svensson U, 2004a.** Modelling flow and transport in a sparsely fractured granite: Some working concepts and assumptions. Proceedings of the fourth IMA conference on modelling permeable rocks: Integrating geology and mathematics for groundwater, environmental and petroleum applications. 30<sup>th</sup> March–1<sup>st</sup> April 2004, University of Southampton, UK.

**Svensson U, 2004b.** Modelling Subgrid dispersion and Retention Processes: Äspö Task Force: Task 6F. Draft report 09-11-2004.

**Svensson U, 2006.** Äspö Task Force on Modelling of Groundwater Flow and Transport of Solutes: Modelling of Task 6D, 6E, 6F and 6F2. Flow, transport and retention in a sparsely fractured granite. SKB IPR-06-21. Svensk Kärnbränslehantering AB.

**Svensson U, Kuylenstierna H O, Ferry M, 2006.** DarcyTools-Concepts, Method, Equations and Tests.

**Tanaka Y, 2003.** Preliminary results of application of FEGM to Task 6D. Presentation at the 17<sup>th</sup> meeting of the Äspö Task Force.

**Tanaka Y, 2004.** Preliminary results of application of FEGM to Task 6E. Presentation at the 19<sup>th</sup> meeting of the Äspö Task Force.

**Tanaka Y, 2005.** Preliminary results of application of FEGM to Task 6F. Presentation at the 20<sup>th</sup> meeting of the Äspö Task Force.

**VTT, 2004.** FEFTRA: The finite-element program package for modelling of groundwater flow, solute transport and heat transfer. VTT Processes. <http://www.vtt.fi/pro/pro1/feftra>.

**Walker D, Gylling B, 1998.** Site-scale groundwater flow modelling of Aberg. SKB TR-98-23. Svensk Kärnbränslehantering AB.

**Winberg A, 1997.** Test plan for the TRUE Block Scale Experiment. Swedish Nuclear Fuel and Waste Management Company. Äspö Hard Rock Laboratory. International Cooperation Report ICR 97-02.

**Winberg A, Andersson P, Poteri A, Cvetkovic V, Dershowitz W, Hermanson J, Gómez-Hernández J J, Hautojärvi A, Billaux D, Tullborg E L, Holton D, Meier P, Medina A, 2003.** Final report of the TRUE Block Scale project, 4. Synthesis of flow, transport and retention in the block scale. SKB TR-02-16. Svensk Kärnbränslehantering AB.

ISSN 1404-0344

CM Digitaltryck AB, Bromma, 2007